Aus dem Institut für Immunologie der Ludwig-Maximilians-Universität München

Direktor: Prof. Dr. Thomas Brocker

Macroautophagy Substrates are loaded onto MHC Class II of Medullary Thymic Epithelial Cells for Central Tolerance

Dissertation
zum Erwerb des Doktorgrades der Naturwissenschaften
an der Medizinischen Fakultät
der Ludwig-Maximilians-Universität München

vorgelegt von

Chunyan Wu

aus

Lanzhou, Gansu, China

2014

Gedruckt mit Genehmigung der Medizinischen Fakultät der Ludwig-Maximilians-Universität München

Betreuer: **Prof. Dr. Ludger Klein**

Zweitgutachterin: **Prof. Dr. Elfriede Nößner**

Dekan: **Prof. Dr. med. Dr. h. c. M. Reiser, FACR, FRCR**

Tag der mündlichen Prüfung: **15.01.2014**

Table of Contents

Summary

The immune system is highly organized and multifunctional; it protects the organism against invading pathogens (immune response), while at the same time being tolerant to 'self' (immune tolerance). Central tolerance is achieved during T-cell development by negative selection via self-peptide-MHC complexes (pMHC) presented by thymic dendritic cells (tDCs) and medullary thymic epithelial cells (mTECs). However, how self-antigens are processed into peptides that further are shuttled onto major histocompatibility complex (MHC) class II in thymic epithelial cells (TECs) is not fully understood. One candidate pathway involved in this process is macroautophagy (referred to as autophagy hereafter), originally thought to solely be involved cellular housekeeping, has previously been implicated to contribute to MHC class II endogenous antigen presentation by TECs.

This research project investigates the role of autophagy in negative selection by TECs. A model antigen was targeted specifically to the autophagosome in autoimmune regulator $(Aire)^+$ mTECs. Transgenic mice expressing this antigen were generated. Experimental data indicated that the efficient direct presentation of this endogenous antigen by mTECs observed *in vitro* was sufficient to induce negative selection *in vivo*. By contrast, interference with autophagosomal processing of this antigen through exchange of one amino acid or disruption of an essential autophagy gene abolished endogenous antigen presentation by mTECs and impaired negative selection, which resulted in the escape of autoreactive CD4 T-cells. Moreover, further investigation showed that if the level of antigen expression was limited, autophagy-dependent direct presentation by mTECs was essential for T-cell deletion, while with sufficient amounts of antigen provided by mTECs, direct presentation by mTECs and indirect presentation by tDCs co-operated to induce central CD4 T-cell tolerance.

These findings strongly suggest that the autophagy pathway contributes to CD4 T-cell tolerance induction by facilitating the loading of intracellular antigens onto MHC class II in mTECs.

Zusammenfassung

Das Immunsystem ist sehr strukturiert aufgebaut und hat vielseitige Funktionen, es schützt den Organismus vor eindringenden Krankheitserregern (Immunreaktion), während es gleichzeitig 'Selbsttoleranz' (Immuntoleranz) aufweist. Die zentrale Toleranz wird während der Entwicklung von T-Zellen durch negative Selektion über Eigenpeptid-MHC-Komplexe (pMHC) von dendritischen Zellen im Thymus (tDCs) und medullären Thymusepithelzellen (mTECs) erreicht. Wie allerdings Selbstantigene in Peptide prozessiert werden, die weiter auf Haupthistokompatibilitätskomplex- (MHC-Komplex)-Klasse-II Moleküle von Thymusepithelzellen (TECs) gelangen, ist nicht hinreichend verstanden. Ein potenziell involvierter Kandidat ist Makroautophagie (im Folgenden als Autophagie bezeichnet), von der man ursprünglich annahm, dass es sich lediglich um einen zellulären Homöostase-Prozess handelt, wurde zuvor mit der endogenen MHC-Klasse-II vermittelten Antigenpräsentation in TECs in Verbindung gebracht.

Dieses Forschungsprojekt untersucht die Rolle der Autophagie bei der negativen Selektion von T-Zellen. Die Expression von einem Modell-Antigen wurde gezielt auf Autophagosome in autoimmune regulator $(Aire)^+$ medullären Thymus-Epithelzellen gerichtet. Transgene Mäuse, die dieses Modell-Antigen tragen, sind wurden generiert. Experimentelle Daten zeigten, dass die effiziente Direktdarstellung dieses endogenen Antigens, die durch medulläre Thymus-Epithelzellen *in vitro* beobachtet wurde, ausreichend war, um die negative Selektion *in vivo* zu induzieren. Im Gegensatz dazu, hat die Interferenz mit der autophagosomalen Verarbeitung dieses Antigens, durch den Austausch einer Aminosäure oder Störung eines wesentlichen Autophagiegens, die durch medulläre Thymus-Epithelzellen herbeigeführte endogene Antigen-Präsentation beseitigt und eine negative Selektion zur Folge gehabt, die zur Freisetzung von autoreaktiven CD4 T-Zellen geführt hat. Darüber hinaus, zeigten weitere Untersuchungen, dass wenn die Antigen-Merkmale begrenzt waren, eine Autophagieabhängige Direktpräsentation von medullären Thymus-Epithelzellen für die Zerstörung von T-Zell von wesentlicher Bedeutung war, während bei ausreichenden Mengen von Antigenen, die durch medulläre Thymus-Epithelzellen zur Verfügung gestellt wurden, bei der direkten Präsentation von medullären Thymus-Epithelzellen und

der indirekten Präsentation von tDCs Kooperation betrieben wurde, um eine zentrale CD4 T-Zell-Toleranz herbeizuführen.

Diese Ergebnisse weisen deutlich darauf hin, dass der Weg der Autophagie zur CD4 T-Zell-Toleranz-Induktion beiträgt, indem die Belastung von intrazellulären Antigenen bei MHC-Klasse-II in medullären Thymus-Epithelzellen ermöglicht wird.

1. Introduction

1.1. Overview

The immune system contains a variety of exquisitely adapted structures and biological processes. Its major function is to recognize and eliminate harmful invaders and foreign antigens, as well as maintain tolerance to the host's own proteins, cells, and healthy tissues. To eliminate invaders such as microorganisms, parasites, and viruses, two major components of the immune system have evolved: innate and adaptive immunity.

Innate immunity functions at the initial stage of infection. The skin and mucosa are physical barriers that act as the first line of defense to prevent pathogenic microorganisms from entering the host. Furthermore, antimicrobial peptides and enzymes secreted by mucosa also deter the establishment of infection. Once these barriers are breached, innate immune cells such as macrophages and neutrophils provide an immediate, but non-specific response against those invaders as the secondary line of defense, mediated by accessory molecules that activate signaling pathways. Together, these innate protective mechanisms are generally sufficient to prevent infection by many microorganisms. However, initiation of the innate immune response is restricted as it relies on cellular pattern recognition receptors (PRRs) to recognize microbe-specific molecules that are commonly expressed by microorganisms[1]. As microorganisms continually evolve strategies to avoid detection by the host's innate immunity, so the host immune response has co-evolved. The adaptive immune system developed as an improved defense strategy to eliminate pathogens that escape the innate immune response[2].

The adaptive immune system is believed to have evolved first in jawed vertebrates and is activated by the innate immune response. It provides the vertebrate immune system with the ability to recognize and target pathogens in a more specific manner. Furthermore, this improved response is maintained as immunological memory, which results in a faster and stronger immune response when the pathogens are re-encountered.

The adaptive immune system is highly adaptive due to the diversity and specificity of antigen receptors expressed by lymphocytes. The specificity of these receptors is determined by a genetic mechanism known as variable (diversity) joining (V(D)J) recombination, which occurs during lymphocyte development in the bone marrow and the thymus. It leads to a rearrangement of the gene segments coding for the antigen receptor, which results in a unique antigen receptor expressed on an individual lymphocyte. Consequently, a highly diverse lymphocyte receptor repertoire with the ability to recognize a myriad of antigens or pathogens is generated.

1.2 T-cell development

T-cells initially arise from hematopoietic progenitors, and then migrate to the thymus for further differentiation. The thymus as the primary T-lymphoid organ provides essential niches and constant signals for supporting to development of thymocytes into mature T-cells. As thymocytes go through the thymus, they continually receive signals via interactions with cortical thymic epithelial cells (cTECs), medullary thymic epithelial cells (mTECs), and thymic dendritic cells (tDCs). After a series of selection processes, a highly diverse repertoire is generated with thymocytes expressing functional, self-major histocompatibility complex (MHC)-restricted T-cell receptors (TCRs). Eventually, these mature T-cells migrate to peripheral lymphoid tissues.

1.2.1 Early T-cell differentiation in the thymus

The colonization of the thymus with hematopoietic progenitors of myeloid, lymphoid, or mixed myeloid/lymphoid potential[3, 4] occurs as early as embryonic day 11.5 (E11.5) in mice and in the eighth week of gestation in humans[5, 6]. During the initial phase, hematopoietic progenitor cells enter the thymus via the cortico-medullary junction[7]. Although the mechanism that mediates homing to the thymus is not fully understood, several chemokine receptors, such as C-X-C chemokine receptor type 4 (CXCR4)[8], C-C chemokine receptor type (CCR)7[9], CCR9[10], and P-selectin glycoprotein ligand-1 (PSGL1)[11] have been implicated to contribute to the migration of immature thymocytes.

Based on the temporally coordinated expression profiles of CD44, CD25, and CD127 on the surface of thymocytes, early T-cell differentiation can be further subdivided into four sequential phenotypic stages (DN1 to DN4). The earliest T-cell progenitors have the most immature phenotype, and are characterized as double negative (DN)1 thymocytes without expression of CD4 or CD8 surface markers[12, 13]. At the initial stage, DN1 thymocytes are $CD44^{+}CD127^{+}CD25^{-}$. They leave from the cortico-medullary junction of the thymus and move towards and into the inner cortex as they commit to the DN2 stage with the upregulation of CD25. This progress relies on signals mediated by thymocyte progenitor-derived NOTCH1, which is activated upon interaction with its ligand, delta-like ligand 4 (DLL4) expressed by TECs[14, 15], and is supported by signals from interactions between cTEC-derived interleukin-7 (IL-7) and IL-7R in T lineage progenitors[16, 17].

As DN1 cells commit to the DN2 stage, they proliferate extensively, with increasing in number about 100-fold[18, 19]. DN2 thymocytes undergo further maturation as they migrate to the subcapsular region of the thymic cortex and downregulate the expression of CD44 and CD127. This indicates entry into the DN3 differentiation stage. At the DN3 stage, proliferation is halted and marks the first developmental checkpoint for committing thymocytes, at which proper TCR gene rearrangement is verified, a process known as β-selection[20].

Somatic rearrangement of the TCR genes occurs as DN thymocytes make their way to the subcapsular region of the thymus and initiates at the TCRβ locus. The TCRβ locus is composed of numerous variable (Vβ), diversity (Dβ), and joining (Jβ) gene segments, and a constant (Cβ) gene. Rearrangement occurs at the V, D, and J gene coding region. After DJ recombination, randomly selected DJ segments are then rearranged with a V segment to generate the VDJ complex that subsequently combines with the constant region gene. The translated product of this transcript pairs with pre-TCRα (pTα) chain and CD3 to form the pre-TCR complex on the cell surface[21]. A survival signal will be given to the cells for further proliferation and differentiation through using intracellular intermediates triggered by the pre-TCR complex, possibly via oligomerization, in the absence of ligand for the pre-TCR complex[22]. Additionally, signaling via at least two

other molecules contributes to β selection: CXCR4, a receptor for stromal-derived-factor-1 (SDF-1)[23, 24], and NOTCH1[25]. Concomitantly, pre-TCR signals lead to the cessation of TCRβ chain rearrangement and result in allelic exclusion, which ensures each individual T-cell only expresses one TCRβ chain[26]. The existence of β selection, a key step in the development of the T-cell lineage, suggests that only those thymocytes that successfully rearrange their TCRβ gene and harbor a functional pre-TCR complex on their surface are able to survive and undergo further differentiation into the DN4 stage[27].

As the thymocytes commit to the DN4 stage, CD25 expression is downregulated. DN4 thymocytes then proliferate extensively to yield abundant progeny cells with co-expression of both CD4 and CD8 receptors and differentiate to double positive (DP) thymocytes. At the DP stage, thymocyte proliferation is again halted, which allows the initiation of somatic rearrangement at the TCRα locus. Unlike the TCRβ locus, the TCRα locus consists of numerous Vα and Jα gene segments but lacks a D segment. The rearranged TCRα chain pairs with TCRβ to form the TCRαβ complex as an intact TCR on the cell surface. During the whole expansion phase, the recombination activation genes (RAG) are turned off to prevent any premature rearrangement of the TCRα locus. During the formation of TCRαβ complexes, expression of receptors in response to cytokine signals is ceased and the thymocytes become unresponsive. Specifically for interleukin-7 receptor (IL-7R) that is dramatically downregulated to weaken the interaction with thymic stromal cells. In addition, high expression of suppressor of cytokine signaling 1 (SOCS1), an intracellular inhibitor of cytokine signaling, also occurs[28]. As the αβTCR is generated from random and flexible juxtaposition of TCR loci, positive and negative selections are conducted to test whether those TCRs are MHC-restricted and not autoreactive.

1.2.2 Selection processes at the late T-cell differentiation stage

Selection processes in the thymus ensure that fully differentiated thymocytes fulfill two essential prerequisites: that they recognize and respond to foreign peptide-MHC complexes, and are tolerant to the self-peptide-MHC complexes (pMHC). Three key

events mark the developmental progression of these cells[29]: (i) positive selection; (ii) CD4-CD8 lineage differentiation; (iii) negative selection.

1.2.2.1 Positive selection

Positive selection is a process for rescuing DP thymocytes from apoptosis and creating a pool of thymocytes expressing self-restricted TCRs. As a requirement for positive selection, DP thymocytes possess a newly generated and unselected TCR repertoire expressing low levels of TCRαβ complex[30]. The DP thymocytes migrate further towards the deep cortex of the thymus and interact with pMHC expressed by thymic stromal cells that are mainly cTECs. Experiments using two-photon laser scanning microscopy to track influenza antigen F5-TCR-specific DP cells within the well-characterized reaggregate thymic organ culture (RTOC) system revealed a large fraction of F5 DP thymocytes in contact with MHC-bearing stromal cells, which are known to provide the signals required for positive selection. Two distinct patterns of thymocyte-stromal cell contact were identified: 50% of the F5 DP thymocytes maintained a very stable interaction with stromal cells during the entire observation period, while the remainder displayed a high dynamic contact. This raises the possibility that two modes of TCR signaling may occur during positive selection[31].

In contrast to β selection, positive selection is strictly dependent on TCR-pMHC interaction between T-cells and cTECs. The frequency of generation of a MHC-restricted TCR is very low; hence, to avoid the fate of apoptosis resulting from failure to be positively selected, DP thymocytes have to rearrange their TCRα locus continuously until a productive and appropriate TCRαβ complex is finally generated. However, evidence suggests that the average life span of DP cells is only 3–4 days, indicating that DP cells need to receive survival signals to be able to proceed with development. Several factors, including RAR-related orphan receptor gamma (RORγ) and T-cell-specific transcription factor 1 (TCF1), are thought to contribute to upregulation of the anti-apoptotic molecule, B-cell lymphoma 2 (Bcl2) on DP thymocytes and regulate cell survival during positive selection[32-34]. Despite receiving survival signals, most cortical

DP thymocytes still fail to be positively selected and commit to apoptosis at this stage. Consequently, only 3–5% of developing thymocytes survive beyond this checkpoint[35].

DP thymocytes must tune their TCR sensitivity to enable better response to low-affinity ligands. CD5, a negative regulator of TCR signaling, is involved in tuning the sensitivity of DP cells to low affinity for positively selected pMHC ligands[36]. Recent studies have highlighted the potential roles of the calcineurin/nuclear factor of activated T-cells (NFAT) pathway[37] and of microRNA (miR) 181a[38] in DP thymocyte selection. Crabtree's group showed that the extracellular-signal-regulated kinases (ERKs, including ERK1 and ERK2) signaling pathway activated by calcineurin is necessary for increasing the sensitivity of DP thymocytes to low-affinity ligands to promote positive selection. In calcineurin-deficient mice, they demonstrated that pre-selected DP thymocytes depend on calcineurin to reach a transient and hypersensitive stage for ERK, which is essential to allow responses to low affinity, but positive-selecting ligands[37]. In addition, miR181a, which is highly expressed in the immature thymocyte population and decreases rapidly from DN4 to the single positive (SP) stage, was found to increase thymocyte sensitivity for TCR engagement by directly downregulating the expression of several phosphatases (SH2-containing tyrosine-specific protein phosphatase (SHP2), protein tyrosine phosphatase non-receptor type 22 (PTPN22), and dual specificity protein phosphatase 5/6 (DUSP5/6)) that inhibit TCR signals[38].

1.2.2.2 CD4-CD8 lineage differentiation

Following successful TCR recognition of pMHC ligands at low affinity, DP thymocytes receive signals for survival and further differentiate to either CD4 or CD8 SP thymocytes, which is determined by their restriction to MHC class II or I, respectively. The choice of CD4 or CD8 lineage is the key to T-cell functional differentiation. However, the decision-making process is still not fully understood. Several theory models have been proposed to explain how the CD4 *vs*. CD8 lineage differential decision is made. In these models, positive selection and CD4/CD8-lineage commitment occur simultaneously and both events are induced by the same TCR signals. TCR signaling during positive selection can selectively terminate either *CD4* or *CD8* gene expression, and the major difference

between the proposed models is whether termination of co-receptor transcriptional expression is random or instructed. The stochastic selection model suggests that CD4 or CD8 termination during positive selection occurs randomly. A second TCR-dependent rescue signal is required for thymocyte survival only if the cells harbor matched TCR and co-receptor; otherwise, the cells die[39, 40]. The instructive model infers that MHC class I- and MHC class II-restricted TCR signals are distinct from each other and the CD4/CD8-lineage commitment is determined by the strength (strength-of-signal instructional model)[41] and/or the duration (duration-of-signal instructional model)[42] of the signals transduced by co-engagement of TCR and co-receptor during positive selection. While these three models are experimentally contradicted, the concept that TCR signal duration is a major CD4/CD8-lineage determinant remains to be accepted.

Based on the most recent experimental data, CD4/CD8 lineage choice seems to be best explained by the kinetic signaling model[43]. In this model, positive selection and lineage choice are sequential, but not simultaneous. According to observations both *in vitro* and *in vivo*, it is proposed that TCR-mediated positive selection signals first terminate *CD8* gene transcription, which converts TCR-signaled DP thymocytes into a $CD4^{+}CD8^{low}$ intermediate phase that is still lineage-uncommitted but has the potential to differentiate into either CD4 or CD8 SP thymocytes[43-45]. Then the CD4/CD8 lineage commitment is based on whether signaling from TCR persists or ceases after CD8 downregulation. It means that persistence of TCR signaling in $CD4^{+}CD8^{low}$ thymocytes induces the deviation into the CD4 SP lineage. Conversely, cessation of TCR signaling in $CD4^{+}CD8^{low}$ thymocytes results in differentiation into the CD8 lineage. The initiation of CD4/CD8 lineage commitment in this model is determined by cytokines that use receptors belonging to the common cytokine receptor γ-chain (γc) family, such as IL-7, as well as several other transcription factors. IL-7 has been shown to promote co-receptor reversal. Blockage of IL-7R signaling enhances *CD4* gene silencing and induces the re-initiation of *CD8* gene transcription[46]. Other relevant transcription factors in lineage commitment are T-helper-inducing POZ/Krüppel-like factor (ThPOK)[47, 48] and runt-related transcription factor (RUNX3)[49], together with thymocyte selection-associated high mobility group box protein (TOX)[50] and GATA-binding protein 3

(GATA3)[51]. ThPOK, TOX, and GATA3 are responsible for CD4 lineage differentiation[52-54], while only RUNX3 is known to be important in mediating CD8 lineage differentiation[49]. TOX is important for generation of $CD4^{+}CD8^{low}$ intermediate thymocytes after *CD8* termination[52]. GATA3 promotes ThPOK expression by binding to a region of the ThPOK locus required for its expression. ThPOK enhancement of CD4 lineage commitment is GATA3-dependent, while inhibition of differentiation into CD8 lineage is independent of GATA3 and further prevents RUNX3 from silencing the CD4 locus[55]. By contrast, IL-7R signaling upregulates the expression of RUNX3, which can bind to the *CD4* silencer element, silencing CD4 expression and inhibiting the expression of ThPOK[56].

1.2.2.3 An overview of central tolerance mechanisms

Up to the point in their development described so far, positively selected SP thymocytes possess a variety of TCRs comprising a T-cell repertoire of millions of T-cells with the potential to recognize all pathogenic entities. However, among these thymocytes, there is still a group of T-cell clones bearing TCRs that can recognize self-antigens. If these self-reactive thymocytes proceed through the terminal maturation stage and migrate to the periphery, they may recognize and respond to self-antigens and consequently lead to autoimmunity. However, autoimmune symptoms are not generally observed in the normal body. Burnet, in his 'clonal selection hypothesis' published in 1959, proposed that the clones that are potentially self-reactive will be removed from the T-cell repertoire to prevent autoimmunity[57]. There is strong experimental evidence for the 'clonal deletion model' of immune tolerance demonstrating that autoreactive T-cells are indeed purged from the repertoire in the thymus. For example, in mice expressing a superantigen (SAg) derived from the mouse mammary tumor virus, SAg-specific Vβ17a TCR-expressing T-cells were efficiently eliminated, while Vβ17a T-cells escaped from clonal deletion in mice lacking the Sag expression[58]. Furthermore, several TCR transgenic mouse strains that express a self-antigen recognized by a specific TCR have been widely used as models to investigate negative selection. Most of these systems are designed to express the antigens from transgenes, but in some cases, such as H-Y, the antigen is naturally expressed (see review[29]).

About 20 years later, Le Dourain and colleagues tested whether there were other mechanisms regulating central tolerance. They found that transplantation of embryonic limb buds from quail into age-matched chicken embryos led to rejection of grafted tissues soon after birth. Interestingly, if limb buds with embryonic thymi were simultaneously transplanted into recipients, the grafted limb buds were accepted[59, 60]. This unexpected finding revealed the importance of the thymic epithelium (TE) for induction of central tolerance because the embryonic thymi were grafted before they had been colonized by hematopoietic cells. More importantly, it demonstrated that the recessive tolerance induction mechanism (clonal deletion) could not explain why the transplanted limb buds were accepted.

Although in certain transgenic models the clonal deletion of antigen-specific T-cells is efficient, the deletion of polyclonal T-cells is incomplete because autoreactive T-cells with downregulated TCR can be found in the periphery[61]. This observation raises the question of whether there could be an additional mechanism for tolerance induction. Modigliani and colleagues found that reconstitution of athymic mice with grafted 10-day-old embryonic thymi led to normal numbers of T-cells generated. When transferring of these $CD4^+$ T-cells from such TE chimeras into athymic recipients, it exhibited life-long tolerance to syngeneic skin grafts. Importantly, hematopoietic cell colonization still does not switch on in 10-day-old embryonic thymi. These data imply that a special type of TE-selected CD4 T-cell may be generated in the thymus and acquires the capacity to inhibit graft-reactive T cells[62]. However, the existence of such T-cell was still a puzzle. In the same year, a subset of T-cells with regulatory function (regulatory T-cell; Treg) had been finally identified by Sakaguchi's group. The cells were of the CD4 T-cell lineage constitutively expressing the IL-2R α chain (CD25)[63] and had the capacity to suppress those effector T cells that are activated upon exposure to their cognate antigen. The transcription factor forkhead box protein P3 (FOXP3) has been proposed to be the key regulator[64, 65] involved in Treg development. This comes from the finding that severe autoimmune manifestations result from impaired Treg induction in the 'scurfy' mouse and in humans with the genetically equivalent IPEX syndrome, because of a frame-shift mutation in the *FOXP3* gene that affects the forkhead/winged-helix domain of the

FOXP3/scurfin protein[66-68]. Hence, a new mechanism of tolerance induction, termed 'dominant tolerance', had been discovered and it is now generally accepted that recessive and dominant mechanisms co-operate to establish immune tolerance. Negative selection and induction of Tregs will be discussed separately in the following sections.

1.2.2.3.1 Recessive tolerance – negative selection

As immature DP thymocytes develop into mature SP thymocytes, cortical DP cells show an increased expression of the chemokine receptor CCR7 and transit from the cortex to the medulla[31]. CCR7 ligands, C-C motif chemokine (CCL)19 and CCL21, are predominantly produced by mTECs in the postnatal thymus[69, 70]. Therefore, thymocytes that receive TCR-mediated signals are attracted to the medulla through CCR7-mediated chemotaxis. Indeed, positively selected mature thymocytes are found in the cortex and central tolerance breaks down if the thymocyte homing pathway is blocked in CCR7- and CCR7 ligand-deficient mice[69]. Subsequent studies have shown that the thymic medulla has an indispensable role in negative selection. Intuitively, the medulla is the likely site for conducting negative selection, as it provides the most complex ligandome. To achieve successful negative selection, the thymus needs to present self-antigens that are expressed ubiquitously or are tissue-restricted. The medulla is heavily colonized by thymus-homing hematopoietic antigen presenting cells (APCs) capable of bringing ubiquitous antigens from the peripheral blood[71]. In addition, the main stromal cell subset residing in the medulla, mTECs, are capable of expressing a wide range of tissue restricted self-antigens (TRAs), which is termed as 'promiscuous gene expression'. It has been estimated that around 2000–3000 TRAs are expressed by human and murine mTECs[72-74].

Kyewski's group demonstrated that a individual TRA is expressed by only 1–3% of total mTECs[73, 75]. Most TRA-expressing mTECs have a mature phenotype, with high expression of MHC class II and the co-stimulatory molecule CD80 ($mTEC^{hi}$)[73]. The mTEC subset in general is rapidly replaced, and the terminally differentiated $mTEC^{hi}$ has an even higher turnover rate[76, 77]. Therefore, TRA expression by mTECs is a

dynamic process. The topology of mTECs constantly changes and provides a source of extracellular antigens for neighboring tDCs to mediate cross-presentation. Meanwhile, it has been found that the medulla contains a substantial fraction of semi-mature, HSA^{hi} CD4 SP T-cells that are still sensitive to tolerance induction[78]. SP thymocytes are assumed to spend 4–5 days in the medulla before export from the thymus[79]. During this period, the SP thymocytes go through a maturation process that can be differentiated according to expression of CD62 ligand (CD62L) and CD69; from $CD62L^{lo}CD69^{hi}$ semi-mature SP cells convert to $CD62L^{hi}CD69^{lo}$ mature SP thymocytes[80, 81].

The importance of thymic TRA expression has been emphasized by the study of the rare human immune disorder autoimmune polyendocrine syndrome type 1 (APS-1), which is characterized by a spectrum of autoimmune diseases caused by mutations in the autoimmune regulator (AIRE) gene[82, 83]. Expression of AIRE is highest in mature mTECs, while tDCs express a much lower level[73]. Studies have shown that mTECs of AIRE-deficient mice have a significant reduction in TRA expression. As a consequence, these animals have multi-organ autoimmunity accompanied by inflammatory infiltrates and autoantibody production[84]. Analysis of AIRE-deficient mTECs reveals that expression of some (approximately 500) but not all TRAs, including the archetypal autoantigen insulin and salivary protein 1, is regulated by AIRE[73, 84]. Although the molecular mechanism of how AIRE regulates the transcription of TRAs is not well understood, its functional domains and several interacting partners have been identified. One important domain, caspase-recruitment domain (CARD), implicates the homo-oligomerization of AIRE[85]. Interaction between the CARD of AIRE with protein inhibitor of activated STAT1 (PIAS1) is important for the formation of AIRE-associated nuclear structures[86]. A second important domain in AIRE is a SAND (SP100, AIRE1, NucP41/P75, and DEAF1) domain, the presence of which suggests that AIRE participates in DNA binding. A third one, a plant homeodomain (PHD) zinc finger domain, interacts with the DNA-dependent protein kinase (DNA-PK) complex, and the residues Thr68 and Ser156 of AIRE protein are DNA-PK phosphorylation sites. By introducing mutations into these sites, transcription activated by AIRE is markedly decreased[87]. The presence of these functional domains in the *AIRE* gene and the

known interactions suggest that AIRE mediates transcriptional regulation of target genes. Furthermore, it has been reported that the first PHD zinc finger of AIRE preferentially binds to the non-methylated histone H3 lysine 4 (H3K4me0)[88], indicating that AIRE could function as a transcriptional activator to initiate expression of target genes. Additionally, the interaction of AIRE with the transcriptional co-activator CREB-binding protein (CBP)[89] and the positive transcription elongation factor b (P-TEFb)[90] also imply enhancement of gene expression mediated by AIRE. Nevertheless, the full picture of AIRE-mediated gene activation is still incomplete. A recent study by Abramson *et al*. integrates these scattered pieces into a framework to rationalize how AIRE affects those particular genes[91]. By combining mass spectrometry-based screening with co-immunoprecipitation and RNA interference, four groups of AIRE-interacting partners were identified and classified, from which a model was proposed integrating the complexes formed by these partners with AIRE, as well as the distinct processes in which they participate (including alteration of chromatin structure, incitation of DNA-damage response, gene transcription initiation or repression, regulation of RNA processing, and enhancement of nuclear transport).

According to the 'clonal selection theory', an innocuous T-cell repertoire requires the elimination of those thymocytes that express TCRs with a high affinity (that is, above a certain quantifiable threshold) for self-antigens. Since the same upstream TCR signaling pathways are used in both positive and negative selection, how a TCR makes the distinction remains elusive. Several signaling molecules regulating negative selection have been identified. c-CbI is thought to negatively regulate TCR signaling in thymocytes. A mutation in the *c-CbI* RING finger domain abolishes its function as an E3 ubiquitin ligase. Knock-in mice bearing this RING finger domain mutation (c-CBI C379A) exhibited a nearly complete thymic deletion with much less proportion of mature CD4 and CD8 SP thymocytes, and this mutation increased sensitivity to TCR-mediated apoptosis. Meanwhile, TCR signaling could be promoted, as reflected by the enhanced activation of ZAP70, JNK, and p38 MARK[92]. Another factor with a potential crucial role in negative selection is misshapen/Nck interacting kinase (NIK)-related kinase (MINK)[93], which is expressed at high levels in DP thymocytes[94]. Knocking down the expression of

MINK in bone marrow cells by siRNA prior to reconstitution confers a specific defect on negative selection in several models, including HY-TCR and ovalbumin (OVA)-specific TCR (OT-II) transgenic mice, but has no effect on positive selection. Furthermore, consistent with the role of MINK in negative selection, phosphorylation of JNK, but not ERK, is affected by downregulation of MINK expression and it also causes impaired BIM expression[93]. In short, these data suggest that MINK can specifically regulate the JNK pathway, and thereby decide the fate of thymocytes.

Clonal deletion generally eliminates cells by apoptosis, and the key initiator proteins in this process are the pro-apoptotic BCL2 family members BIM, BAX, and BAK[95, 96]. Experimental data show that deficiency of BIM or combined deficiency of BAX and BAK cripple negative selection[97]. In fact, in a number of different model systems, BIM is the dominant protein for inducing apoptosis in thymocytes[96]. However, Baldwin's group observed that BIM-mediated apoptosis was not required for negative selection in mice transgenic for a TCR specific for a ubiquitously expressed self-antigen[98, 99]. Another crucial effector during clonal deletion is the orphan nuclear receptor Nur77 (also known as nerve Growth factor IB (NGFIB)). Evidence for its role in negative selection comes from transgenic mice overexpressing a dominant negative version of Nur77, which had a defective thymocyte deletion[100]. Furthermore, Winoto's group reported that Nur77 could translocate from the nucleus to the mitochondria. By directly interacting with BCL2, it converted BCL2 from an anti-apoptotic protein into a pro-apoptotic protein[101]. The same conformational change in BCL2 was noted in DP thymocytes undergoing negative selection in two TCR transgenic mouse models[101].

1.2.2.3.2 Dominant tolerance – Treg generation

The random rearrangement of TCR gene segments generates not only a functional T-cell repertoire, but also a group of potentially dangerous T lymphocytes. Clonal deletion and anergy are the mechanisms that mediate elimination of autoreactive T-cells bearing high affinity TCRs for pMHC. However, even in healthy individuals negative selection is inevitably incomplete, leading to the appearance of T lymphocytes that harbor the potential to recognize 'self'. It is proposed that tolerance is maintained in this

circumstance by the contribution of Tregs. Direct evidence for this comes from experiments showing that depletion of Tregs from 3-day-old mice caused development of autoimmune disease, which could be relieved by the re-introduction of Tregs[63].

Treg differentiation is thought to occur mainly in the thymic medulla. This notion is supported by experiments with neonatal bone marrow chimeras, which revealed that the first wave of $FOXP3^{+}$ Treg generation is initiated from thymocytes of the semi-mature, HSA^{hi} CD4 SP stage, which reside in the medulla[102]. It indicates that Treg differentiation can be spatially and temporally separated from positive selection occurring in the thymic cortex. Neonatal thymectomy in mice leads to severe autoimmunity[63] and a Treg subset, so-called natural Treg (nTreg), is identified in the thymus, which indicates that Treg differentiation is an important branch deviating from mainstream T-cell development during intrathymic maturation.

This raises the question of how these autoreactive thymocytes avoid being deleted and deviate into the Treg lineage when self-antigens are encountered. TCR stimulation is regarded as the essential driving force for thymocyte development. However, the intrinsic properties of TCR specificities are clearly unlikely to be involved in the fate decisions in thymocytes. Several investigations have shown that some transgenic TCR-bearing (e.g., with hemagglutinin (HA)-specific TCR) T-cells undergo differentiation into the Treg lineage after encountering self-antigen[103-105], while others report a massive loss of T cells by clonal deletion upon the same intrathymic antigen encounter[106, 107].Taken together, the data imply that some co-stimulatory or cytokine signaling is provided by a combination of extrinsic and intrinsic factors that are crucial for Treg differentiation in the thymic medulla. CD28-B7 signaling has emerged as important in Treg differentiation because of the finding that the proportion and numbers of thymic Tregs were severely reduced in mice with genetic ablation of either CD28 or its ligands[108-110]. In addition, CTLA4 signaling shows a reciprocal effect on Treg differentiation. Overexpression of full-length CTLA4 resulted in an impaired efficacy of SAg-specific thymocyte deletion[111]. The ‘two-step model’ supports Treg development is segregated into a TCR-driven ‘instructive’ phase and a cytokine-driven ‘consolidation’ phase[112, 113], thus, the importance of another candidate signaling pathway, such as via

IL-2 and other γc-dependent cytokines, which co-operates with a TCR stimulus and skews development towards Tregs, is also plausible. It is supported by evidence that in IL-2/IL-7/IL-15-deficient or STAT5-deficient mice, interference with cytokine signaling via γc led to a greater reduction in Tregs[114-116]. Furthermore, it has been reported that transforming growth factor β (TGFβ) is required for thymic Treg generation. With the ablation of TGFβRI or TGFβRII[117, 118], the first wave of thymic Treg generation is diminished. It is feasible that the loss of Tregs could be compensated by an IL-2-dependent expansion of residual Tregs. And in fact, a complete depletion of thymic Tregs is observed in mice with deficiencies in both TGFβ- and IL-2-signaling pathways[118].

Collectively, both recessive tolerance and dominant tolerance are essential for developing a normal immune system and preventing autoimmunity. That both are required is highlighted by the observation of even more severe autoimmune manifestations in mice dually deficient in Aire and Foxp3, compared with mice with each sole deficiency[119].

1.2.3 Cell-interactions in the thymic microenvironment

The scope of central tolerance is determined by developing thymocytes recognition of self-antigens presented by various APCs in the thymus. A central element in this process is the promiscuous expression of TRAs by mTECs. Since a given TRA can only be detected in 1–3% of mTECs, the mechanism by which a restricted TRA expression pattern in mTECs engages complete tolerance is still debated. Two hypotheses have recently been proposed. The first one provided by Le Borgne's groups proposed that after reaching the medulla, thymocytes were highly motile, randomly 'walking' at a rate of >10 μm/min, and this movement was restricted in a limited globular volume. However, they observed that when the negatively selecting self-antigen (OVA) was present, OT-I cells demonstrated a more confined motion pattern with a lower velocity and prolonged contact with APCs[120]. Consequently, it is feasible that thymocytes scan the medullary region efficiently through serial interactions with APCs to achieve negative selection in their 4–5 day residence time. The second one came from the study of Millet and

colleagues proposed that intact membrane domains of pMHC at the surface of mTECs and/or intracellular antigens expressed by mTECs could spread to neighboring cells, including DCs. Evidence for intercellular transfer of membrane components comes from experiments in which membrane dye (green fluorescent protein (GFP)) in combination with MHC molecules could be detected in GFP-negative epithelial cells when co-cultured with GFP-expressing cells. Additionally, analysis of chimeric mice confirmed that epithelial cells were indeed able to transfer MHC to DCs *in vivo* in a polarized way. Around 5% of tDCs in the recipients acquired MHC molecules[121]. Furthermore, Koble *et al.* found that the interaction between mTECs and DCs resulted in mTEC-derived antigen transferring to DCs, which consequently led to a more efficient antigen presentation when compared to endogenous antigen presentation solely mediated by DCs themselves. Meanwhile, a subset of DCs bearing a mature phenotype (high expression of CD80, CD86, CD103, and MHC II) has been identified, and this mature subset was able to acquire TEC-derived membrane receptors as well as cytoplasmic proteins[122].

In the thymus, reciprocal interactions between developing thymocytes and TECs are bidirectional. It not only commits TECs to educate thymocytes for differentiation by presenting antigens to their TCR, but also activates the necessary signaling for TEC maturation and function via production of some factors by developing T-cells. This phenomenon is termed 'thymic crosstalk'[7, 123, 124]. While cTEC development is poorly understood, two non-redundant pathways of CD4 SP thymocytes, mediated by the ligands LTα/LTβ, RANKL, and CD40L, are known to contribute to mTEC development. Independent studies from three separate groups demonstrated that RANK/RANKL and CD40/CD40L interactions between mTECs and CD4 thymocytes co-operate to generate mature mTECs for postnatal homeostasis, while the earlier stage of mTEC development is regulated by $RANKL^{+}$ lymphoid tissue inducer (LTi) cells before the emerging of mature thymocytes[125-127]. Moreover, data from Irla's group show that the provision of ligands to TCRs requires the direct interaction of autoreactive CD4 thymocytes with mTECs that are presenting self-peptide-MHC class II complexes in an antigen-specific manner[128].

1.3 Antigen processing

1.3.1 The MHC class I and class II pathways

MHC class I molecule is a heterodimer expressed on the surface of all nucleated cells in the body. It comprises a polymorphic heavy chain (consisting of a α1, α2, and α3 domain) non-covalently linked to a non-polymorphic light chain called β_2-microglobulin (β_2m). The α1 and α2 domains are folded to form the MHC peptide-binding groove, which accommodates a peptide of 8–11 amino acids in length. The α3 domain contains a transmembrane (TM) domain and interacts with CD8 co-receptor. Both chains are synthesized in the endoplasmic reticulum (ER). Prior to peptide loading, the MHC class I molecules are inherently unstable and require binding with ER-resident chaperones such as calreticulin, the ER oxidoreductase ERp57, and protein disulphide isomerase (PDI)[129]. Furthermore, the binding of calreticulin results in a more stable interaction between MHC class I molecules and TAP-associated glycoprotein (tapasin)[130], which is a transmembrane glycoprotein and plays an important role on peptide loading and further peptide transport across the ER membrane. This combination forms a large multimeric complex (consisting of transporter associated with antigen presentation (TAP), tapasin, MHC class I, calreticulin, and ERp57), called the peptide-loading complex (PLC).

MHC class I molecules present peptides, generated by proteasome-mediated degradation of cytosol-derived proteins, at the cell surface. The proteasome, which consists of a 20S core barrel with proteolytic activity[131] and two 19S caps, is responsible for the degradation of intracellular ubiquitinated proteins into small peptides, and the catalytic function is performed by three subunits, β1, β2, and β5 (in the constitutive-proteasome) or β1i, β2i, and β5i (in the immunoproteasome). Immunoproteasomes are constitutively expressed in the primary and secondary lymphoid organs. Interferon (IFN)-γ, in particular, induces the formation of immunoproteasomes during inflammation[132, 133].

Recent findings have suggested that positive selection requires unique MHC-associated peptides that are generated by the action of intracellular proteolytic enzymes exclusively

expressed by cTECs[134]. A database search revealed that a previously unrecognized catalytic subunit of proteasomes, thymus-specific β5 family member (β5t), is exclusively expressed in cTECs; β5i, however, is expressed in a broad range of immune tissues[133]. The β5t-containing proteasome, which associates with β1i and β2i subunits over β1 and β2 in cTECs, is termed the thymoproteasome and exhibits proteolytic activity to produce cytoplasmic peptides that is distinct from β5- or β5i-containing proteasomes. In β5t-overexpressing cells, the chymotrypsin-like activity of the 20S component is reduced by 60–70%; however, protein-degradation activity shows normal. In addition, in β5t-deficient mice, positive selection of MHC I-restricted transgenic TCR is impaired, along with a marked reduction in the number of CD8 SP thymocytes, while CD4 SP T-cell development is unaffected. Taken together, the thymoproteasome is proposed to increase the repertoire of cytoplasmic self-peptides specific to cTECs compared to those epitopes generated by constitutive proteasomes and immunoproteasomes[134, 135 136].

The peptides that result from proteasomal degradation are released into the cytosol. Therefore, they have to be translocated from the cytosol into the lumen of the ER by TAP to access MHC class I molecules. As tapasin recruits MHC class I molecules to TAP, the coupled peptide is translocated into the ER[137]. Before binding to MHC class I molecules, the peptide may require further trimming to generate the required length of 8–11 amino acids for MHC class I loading[138]. Trimming is performed by one ER aminopeptidase (ER aminopeptidase associated with antigen processing; ERAAP) in mice and two (ER aminopeptidase (ERAP) 1 and ERAP2) in humans[139-141]. Once a peptide with sufficient affinity is loaded onto the MHC class I molecules, the MHC class I complexes are released from the chaperones and leave the ER through the secretory pathway to be presented at the cell surface. Conversely, peptides that fail to associate with MHC class I molecules in the ER are returned to the cytosol for either degradation[142] or further trimming for a new round of TAP translocation and MHC class I loading[143] (Graphic 1).

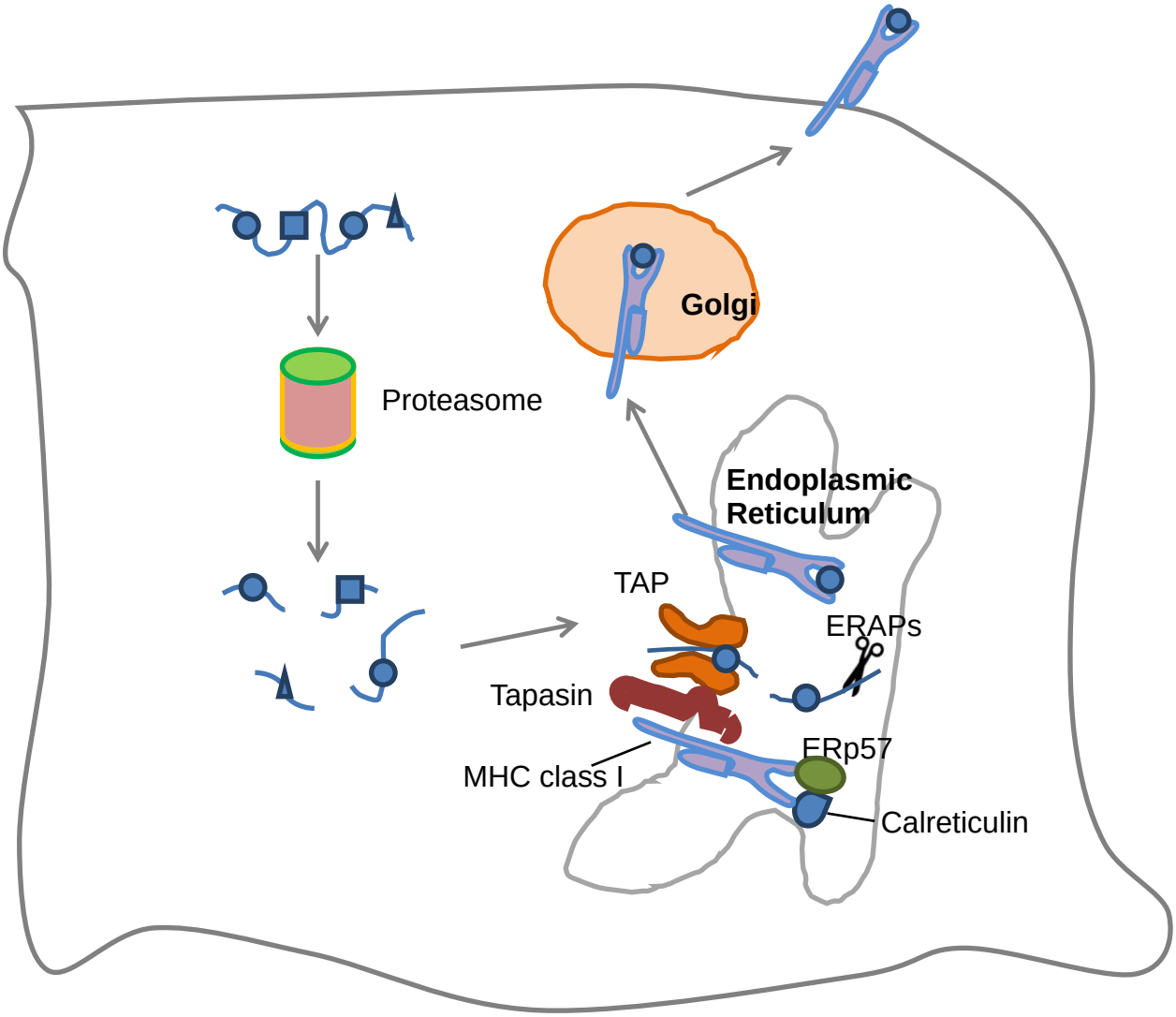

Graphic 1. The basic MHC class I antigen presentation pathway. MHC class I molecules are synthesized in the endoplasmic reticulum (ER) and stabilized by binding of calreticulin and ERp57. Intracellular antigens are degraded by proteasomes which results in peptides released into the cytosol and translocated into the lumen of the ER via TAP and tapasin. For binding to MHC class I molecules, the peptides require further trimming via ERAPs. The stable MHC class I complexes are then transported through the Golgi and presented at the cell surface.

Unlike the ubiquitously expressed MHC class I molecules, expression of MHC class II molecules is restricted to the steady-state APCs, such as DCs, macrophages, B cells and, importantly, on cTECs and mTECs. Thus, TECs are the only non-hematopoietic cell types that constitutively express MHC class II. However, MHC class II expression

can be upregulated on fibroblasts, other mesenchymal stromal cells, endothelial and epithelial cells, by IFN-γ or other inflammatory stimuli[144, 145].

Like MHC class I, MHC class II molecules are also heterodimers, and consist of two peptide chains, MHC II-α and MHC II-β. Both α- and β-chains of MHC class II are transmembrane proteins, which are synthesized in the ER and assembled with the help of ER-resident chaperone proteins such as calnexin. Compared with the smaller peptide-binding groove on MHC class I molecules, the peptide accommodated in the open-ended groove of MHC class II molecules is much longer, generally between 10 and 24 amino acid residues. To prevent premature peptide loading onto MHC class II molecules, the assembled MHC class II αβ heterodimer associates with the invariant chain (Ii) in the ER[146]. It is believed that the class II-associated Ii peptide (CLIP) region of Ii occupies the MHC class II binding groove. Indeed, the levels of endogenous antigen presentation are higher in Ii-deficient mice[147]. However, biochemical analysis suggests that it is hard for any MHC class II molecules to gain a stable peptide-loaded state in the absence of Ii during peptide loading[148, 149].The resulting Ii-MHC class II complexes are then guided via the cytoplasmic tail of Ii and transported through the Golgi to the late endosomal/lysosomal compartment[150] termed as the MHC class II containing compartments (MIICs), which contain endocytosed and degraded proteins. Ii is degraded in the MIICs by lysosomal hydrolysis and the CLIP fragment is left in the peptide-loading groove to prevent further peptide binding to MHC class II molecules. Afterwards, CLIP is released and subsequently replaced by an antigenic peptide with the help of the HLA-DM chaperone. This assistance stabilizes the ‘empty’ groove of the MHC class II dimer by preventing its aggregation or degradation prior to loading with an appropriate epitope, and further facilitates the exchange of CLIP to a specific peptide derived from proteolytic degradation of endosomal proteins.

MHC class II, HLA-DM, and cathepsins have been defined *in vitro* as the minimal requirements for MIIC formation[151]. Cathepsins are lysosomal proteases involved in Ii-mediated antigen processing[152]. Strikingly, tissue-specific expression of distinct cathepsins in the thymus has been observed: a unique cathepsin (Cat)-L is exclusively expressed in cTECs, while Cat-S is predominantly expressed in mTECs, tDCs[153]. In

Cat-L-deficient mice, an increased number of MHC II/CLIP complexes instead of normal MHC II/peptide complexes is found expressing on the surface of cTECs[153], leading to a 70% reduction in total thymic CD4 T-cells[154, 155]. Moreover, analysis of mice deficient in both Cat-L and Ii indicates that impaired CD4 T-cell selection is not solely due to the inefficient degradation of Ii[156]. The evidence suggests that Cat-L in cTECs may be directly involved in MHC class II presentation by determining the positively selecting peptide repertoire. In addition, the involvement of distinct proteases of different APCs in the thymic cortex or medulla for MHC class II presentation suggests that different peptide repertoires generate for either positive or negative selection in order to minimize extensive thymocyte deletion.

Thymus-specific serine protease (TSSP), discovered during a screen for cTEC-specific genes, is another lysosomal protease with a potentially crucial role in MHC class II antigen processing[157-159]. Although the CD4 polyclonal repertoire shows no significant alteration in TSSP-deficient mice[160], there is a severe impairment of positive selection in OVA- or H-Y-specific CD4 T-cells when TECs lack TSSP[161]. Consistent with its endosomal localization, these data demonstrate that TSSP participates in the generation of peptides for positive selection. A link between mutations in *PRSS16*, the gene coding for TSSP, and human autoimmune diabetes susceptibility[161] prompted an investigation of the development of CD4 T-cells specific to some islet antigens, such as phogrin, in non-obese diabetes (NOD) TSSP-deficient mice. The differentiation of phogrin-specific CD4 T-cells is highly defective in TSSP-deficient NOD mice. What is more, bone marrow chimeras highlight the importance of TSSP in thymic DCs for generating a unique peptide repertoire to be negatively selected. Data gained from chimeras show that differentiation of islet antigen-specific CD4 T-cells is affected when bone marrow-derived APCs lack TSSP expression[162]. Similarly, TSSP was found to regulate the selection of CD4 T-cells specific for some β-cell antigens in NOD mice[162]. Deletion of diabetogenic CD4 T-cells is enhanced in TSSP-deficient mice, further supporting a role for TSSP in MHC class II antigen processing.

After binding of high-affinity peptides to MHC class II molecules, the MHC II/peptide (MHCII/p) complexes are transported from the MIIC to the plasma membrane. However,

the molecular basis for this process is largely undefined. It is known that transportation of the MHCII/p complexes is driven by microtubule-based motors or actin-based myosin motors, and that in DCs, the late endosomal/lysosomal compartments are triggered by lipopolysaccharide to form tubule-like structures and then generate vesicles containing MHCII/p complexes that can fuse with the plasma membrane[163, 164] (Graphic 2).

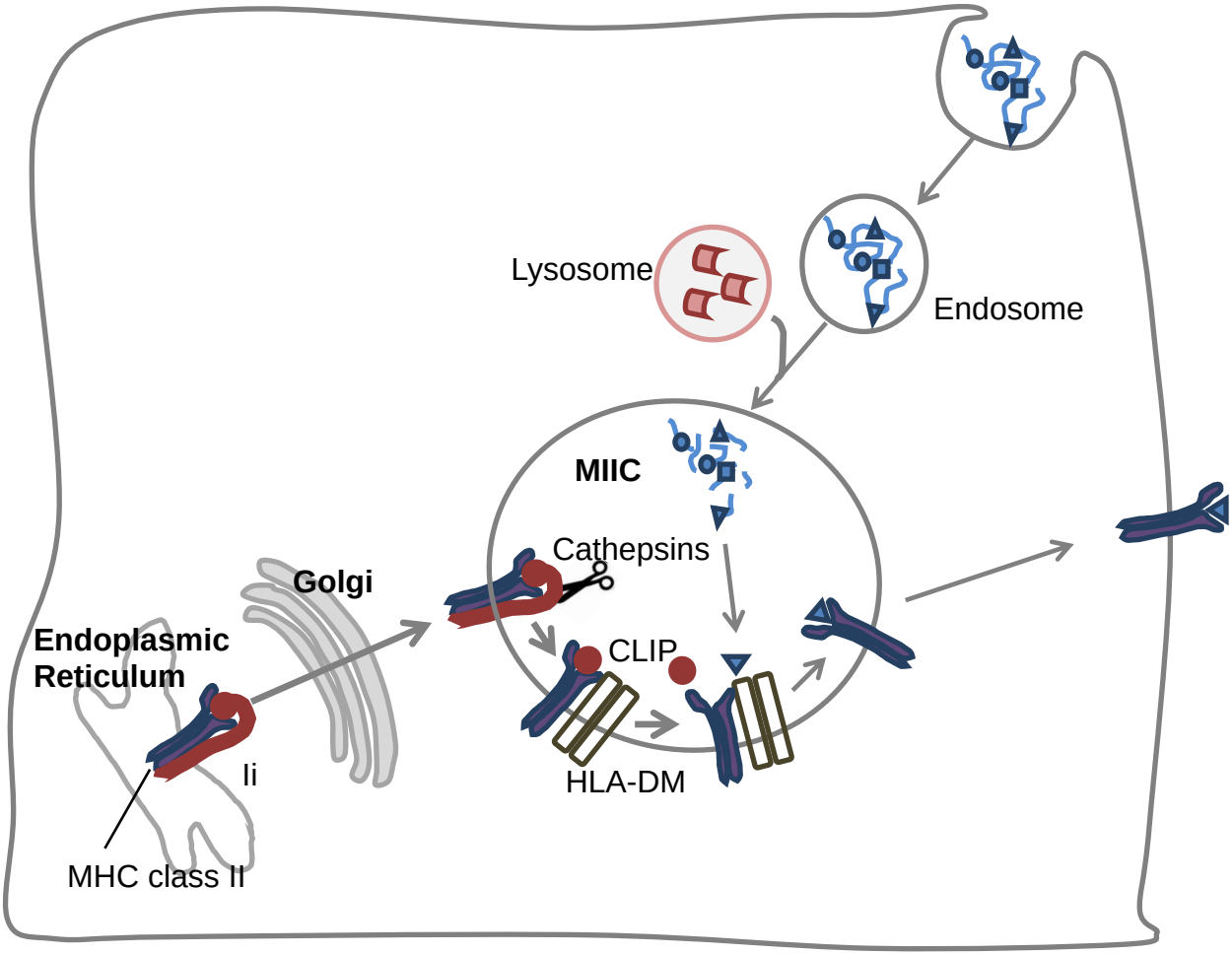

Graphic 2. The basic MHC class II antigen presentation pathway. MHC class II α- and β-chains are assembled in the endoplasmic reticulum (ER) and associated with the invariant chain (Ii). The Ii-MHC class II complexes are then transported through the Golgi to MHC class II containing compartments (MIICs) and fuse with late endosomal/lysosomal compartments that contain processed proteins during endocytosis. The MHC class II peptide loading groove remains be occupied by CLIP fragments which would be exchanged to peptides derived from the late endosomal/lysosomal compartments with the help of the HLA-DM chaperon. MHC class

II molecules with peptides are then transported to the plasma membrane for antigen presentation.

1.3.2 Alternative MHC class II antigen loading pathways

Several lines of evidence support the notion that intracellular antigen can also access MHC class II presentation pathway. In early studies, an analysis of peptides eluted from MHC class II molecules revealed that a substantial amount of natural MHC class II ligands (up to 20%) were derived from cytosolic and nuclear proteins[165, 166]. This observation was further verified by analysis of a repertoire of 400 constitutive MHC II/peptide complexes in human B cells. While the largest fraction (40%) of peptides loaded onto MHC class II was of membrane origin, a relatively large proportion (roughly 35%) was derived from a diverse pool of intracellular-derived antigens, including metabolic enzymes, nuclear and cytoskeletal proteins, viral and tumor antigens, and mitochondrion-derived peptides[167].

The first evidence of presentation of these endogenous complexes came from studies by Long and colleagues on viral antigen presentation to CD4 T-cells. They found that cytosol-synthesized antigens from measles virus and type A influenza virus are endogenously presented to MHC class II, and further are recognized by CD4 T-cells for activation[168]. Increasing amounts of data now demonstrate that various intracellular antigens, including self-, model-, viral- and tumor-antigens can gain access to the endogenous MHC class II antigen presentation pathway[167, 169-171], thereby broadening the MHC class II ligand repertoire. The classical, endocytic antigen presentation pathway clearly does not explain satisfactorily why there is such a large proportion of intracellular- and organelle-derived epitopes presented on MHC class II molecules.

Earlier work suggested the existence of an endogenous processing pathway for MHC class II-restricted presentation[172], which revealed that both exogenous and endogenous antigens could be shuttled into MHC class II loading. Recently, studies have implicated multiple pathways to mediate MHC class II presentation of endogenous antigens in both professional and nonprofessional APCs. These pathways include the TAP-dependent pathway, intercellular antigen transfer, and the autophagy pathway.

Experimental evidence for the contribution of the TAP-dependent pathway to cytosolic MHC class II-restricted presentation comes from the study of Tewari and colleagues[173]. They revealed that proteasome-dependent cytosolic processing is required for the generation of two MHC class II-restricted epitopes from the HA and the neuraminidase (NA) glycoproteins of influenza virus. TAP and recycled MHC class II molecules were shown to be essential for epitopes to be presented onto the surface of APCs.

The supporting evidence for intercellular antigen transfer came from Taylor's group[174]; they showed that two nuclear antigens from EBV could gain access to the MHC class II pathway and be presented in EBV-transformed B cells. Endogenous MHC class II presentation of these two antigens could not be inhibited by treatment with 3-methyladenine (3-MA), which blocks autophagy. However, this presentation process could be observed in antigen-negative cells by co-cultivation with antigen-positive cells or exposure to their culture medium.

Autophagy, an intracellular bulk degradation process, is also thought to be responsible for endogenous MHC class II antigen presentation[169, 170, 175-177]. This will be discussed in detail in the following section.

1.3.3 Autophagy, a candidate pathway for endogenous antigen loading

Autophagy is a term derived from the Greek words for 'self-eating'. It is a highly conserved cellular homeostatic process in all eukaryotic organisms, and refers to a cellular degradation pathway in which portions of cytoplasmic constituents are segregated and transported to the lysosome for degradation. These degraded products will then be released and recycled in cellular bio-synthesis. Three major forms of autophagic cargo delivery pathways to lysosomes have been identified (shown in Graphic 3): microautophagy, chaperone-mediated autophagy, and macroautophagy[178, 179].

Microautophagy is a constitutively active, nonselective catabolic process in mammals. Components of cytosol portions first form tubules or vesicles, and then they are imported to the lysosomes via lysosomal membrane invaginations. Proteins are continuously degraded in the lysosomal lumen[180]. Studies on microautophagy have been limited to yeast and cell-free systems, and there is still little understanding of the molecular mechanism of microautophagy in mammals[181, 182].

Chaperone-mediated autophagy (CMA) is a selective autophagic pathway that delivers cytoplasmic contents to the late endosome/lysosome for degradation[183]. Unlike microautophagy, delivery of cargo via CMA does not involve the formation of vesicle compartments at the surface of the lysosomes. Instead, CMA substrates are directly translocated from the cytosol into the lysosomal lumen, and this process requires unfolding of the substrate proteins[184, 185]. A prerequisite of a CMA substrate is the presence of an amino acid sequence motif biochemically related to KFERQ[186]. KFERQ or KFERQ-like motifs are present in approximately 30% of cytosol soluble proteins, but rarely detected in organelles or membrane proteins, which suggests that only soluble proteins can be degraded through CMA. A chaperone, heat shock cognate 70 kDa protein (Hsc70), can recognize substrates bearing CMA motifs in the cytosol, and this recognition facilitates the delivery of substrates to the lysosomal membrane for binding to the cytosolic tail of lysosome-associated membrane protein 2 (LAMP-2A)[183]. Each substrate must bind to LAMP-2A for lysosomal translocation to take place, and so it was thought likely that the level of LAMP-2A at the lysosomal membrane would be CMA rate-limiting. This was confirmed by altering the transcriptional expression or by mediating the degradation and lysosomal distribution[187]. The binding of substrates to the surface of the lysosome drives the multimerization of LAMP-2A into a translocation complex, and with the assistance of Hsc70, the substrates are imported into the lysosome and then rapidly degraded. Furthermore, functional assays indicate that the CMA pathway promotes antigen presentation of cytoplasmic peptides onto MHC class II molecules in professional APCs[177].

Macroautophagy is the best genetically characterized catabolic mechanism by which eukaryotic cells adjust their biomass, remove long-lived proteins, or eliminate aged or

damaged organelles[188]. A potential role for macroautophagy in endogenous antigen loading has been intensively investigated in different *in vitro* systems[167, 169, 176, 189]. The focus of this study is the role macroautophagy plays in mTECs during negative selection. The molecular mechanisms of macroautophagy, its physiological functions, and role in antigen presentation will be discussed in the following paragraphs.

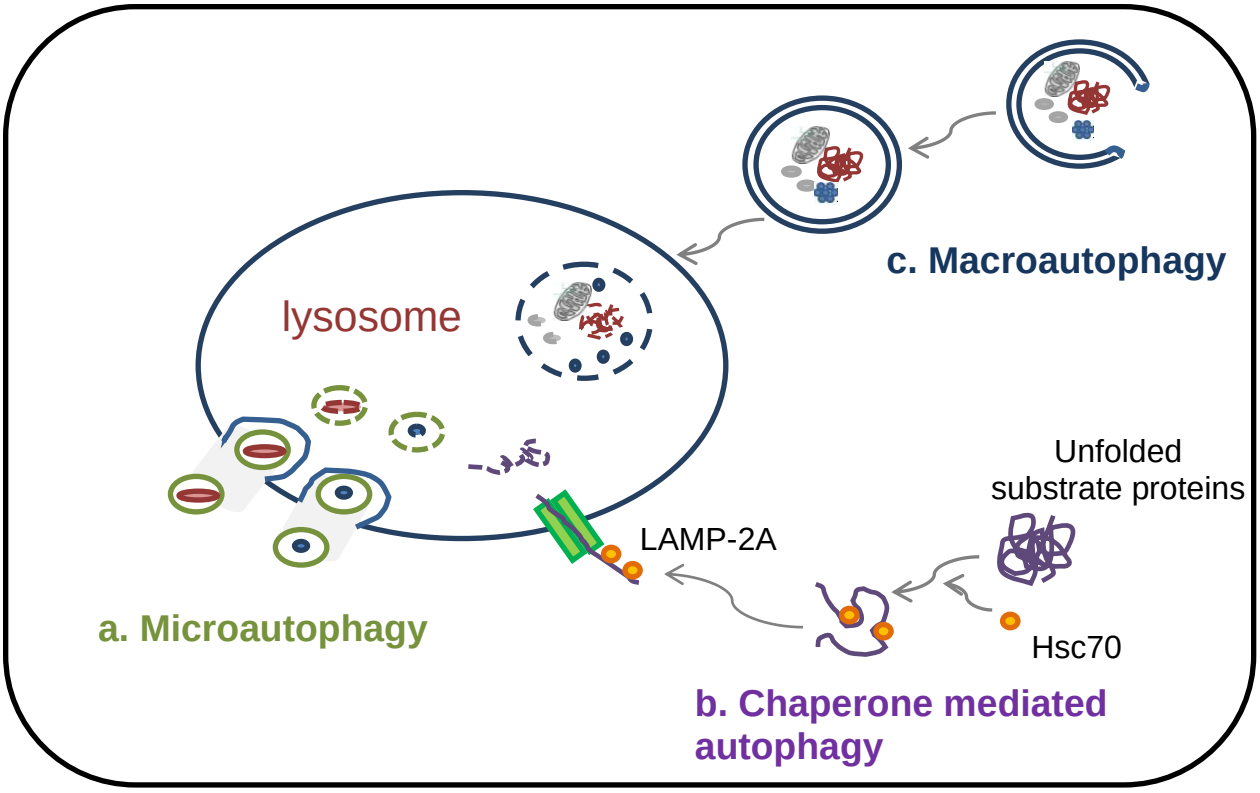

Graphic 3. Three different types of autophagic pathways in mammalian cells. (a) In microautophagy, intracellular materials are directly delivered into lysosomes for degradation via lysosomal membrane invaginations. (b) In chaperone mediated autophagy (CMA), substrate proteins are recognized by Hsc70, subsequently imported to lysosome by binding of LAMP-2A and rapidly degraded in there. (c) Macroautophagy is involved in the delivery of their engulfed cytoplasmic components to lysosomes for degradation.

1.4 Macroautophagy – process, physiological functions, and role in endogenous antigen loading routes

Macroautophagy (hereafter referred to as autophagy) is an evolutionarily conserved bulk degradation process for cytosolic proteins that involves the delivery of double

membrane sequestered cytoplasmic vesicles to the lysosome[190]. This process was first identified in resting rat hepatocytes in response to metabolic stress, such as starvation, and glucagon withdrawal[191, 192].

1.4.1 The biology of autophagy

In general, compared to normal conditions, cellular antophagic activity is markedly upregulated by numerous stimuli, such as nutrient starvation, physiological stress, pharmacological agents (rapamycin, chloroquine), or innate immune signals[193, 194].

Autophagy initiates when mammalian target of rapamycin (mTOR) is inhibited by nutrient starvation, which results in translocation of the ULK/Atg1 kinase complex (as mTOR substrate) from the cytosol to certain domains of the ER. The class III phosphatidylinositol-3-OH kinase (PI(3)K) complex is then recruited, as well as other related effectors[195], to trigger the initiation of an isolated membrane or 'phagophore', which contains a portion of cytoplasm from the cytosol. Consequently, the isolated membrane in association with other autophagy-related complexes elongates and engulfs cytoplasmic constituents, such as organelles or aggregated proteins, to become an enclosed double membrane structure known as the autophagosome. Finally, the outer membrane of the autophagosome fuses with a late endosome and/or lysosome to form a structure called the amphisome or autolysosome. Lysosomal hydrolytic enzymes then degrade the sequestered contents of the autophagosome together with its inner membrane[189] and the degraded products are recycled[196] (Graphic 4).

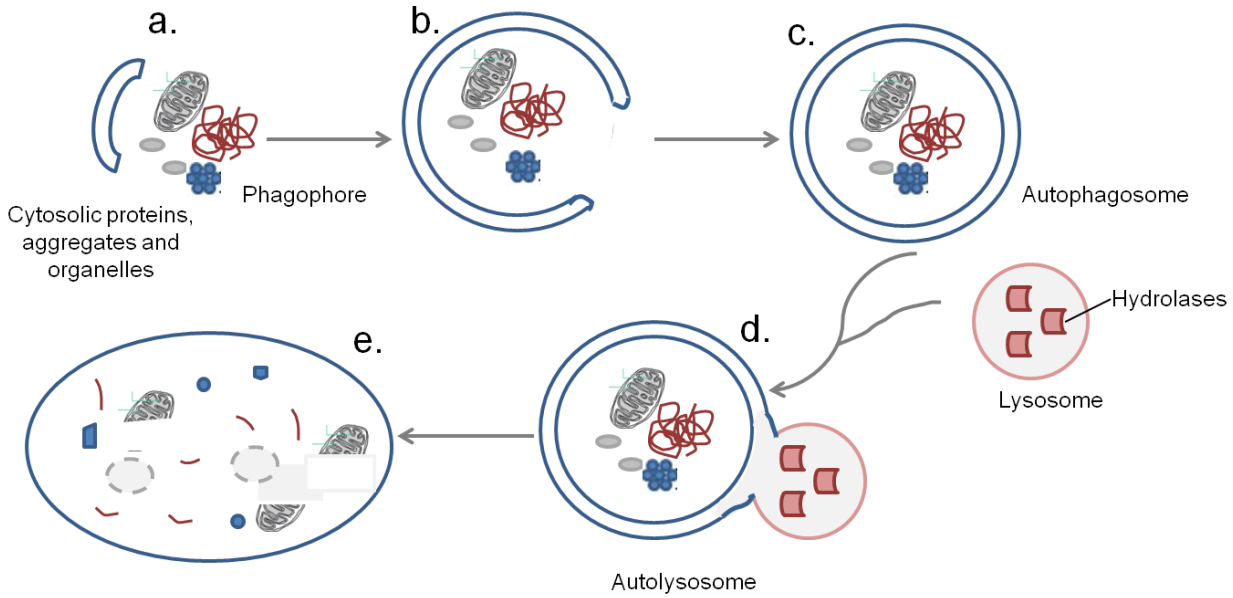

Graphic 4. The process of macroautophagy. (a) An isolated membrane engulfs a portion of cytoplasmic component, including ubiquitinylated protein aggregates or damaged organelles, (b) and the 'phagophore' further elongates with association of the antophagy-related complex (c) to form an enclosed double-membrane vesicle as autophagosome. (d) Subsequently, the outer membrane of the autophagosome fuses with a lysosome/late endosome to form autolysosome or amphisome; (e) the sequestered contents of autophagosome as well as the inner autophagosomal membrane are degraded.

The membrane dynamics of autophagosome formation are not fully understood. As a highly conserved process, autophagy-associated proteins coded by autophagy-related genes (Atg) are highly homologous from yeast to mammals[197]. Products of these genes have been isolated and well-characterized. Most of them are involved in two specialized ubiquitin-like modification systems that are required for elongation and formation of the autophagosome in mammals (Graphic 5). One is the autophagy-related gene 12 (Atg12)-Atg5 conjugation system, which is activated by Atg7 (E1-like) and Atg10 (E2-like). It makes the carboxyl terminus of Atg12 conjugating to Atg5 as a dimeric complex which functions together with Atg16 to generate the precursor of autophagosome[198]. The other system is the Atg8 (LC3, GATE16, and GABARAP as mammalian homologs) conjugation system[199]. This process initiates when the carboxyl terminal region of proLC3 is cleaved by Atg4B after translation. It makes the carboxyl terminal Gly of proLC3 to form LC3-I (the cytosolic form)[200]. With the assistance of Atg7 and Atg3 (E2-

like), LC3-I is covalently coupled to the phospholipid phosphatidylethanolamine (PE) via its carboxyl terminus to form the ubiquitin-like LC3-II (the membrane form), which can further incorporate into the newly synthesized outer and inner membrane of the autophagosome[201]. Consequently, generation of LC3-II has been viewed as the hallmark of autophagy, and can be evaluated biochemically (by measuring the level of LC3-II) or microscopically (by observing the localization pattern of fluorescently tagged LC3, as in GFP-LC3 mice)[193]. Formation of the autolysosome (the vesicle formed from the fusion of autophagosome and lysosome) results in rapid degradation of the contents, the inner membrane, and associated LC3-II, mediated by lysosomal proteases. LC3-II located on the outer membrane of the autophagosome is then cleaved by Atg4B and restored to LC3-I for further autophagosome formation[202].

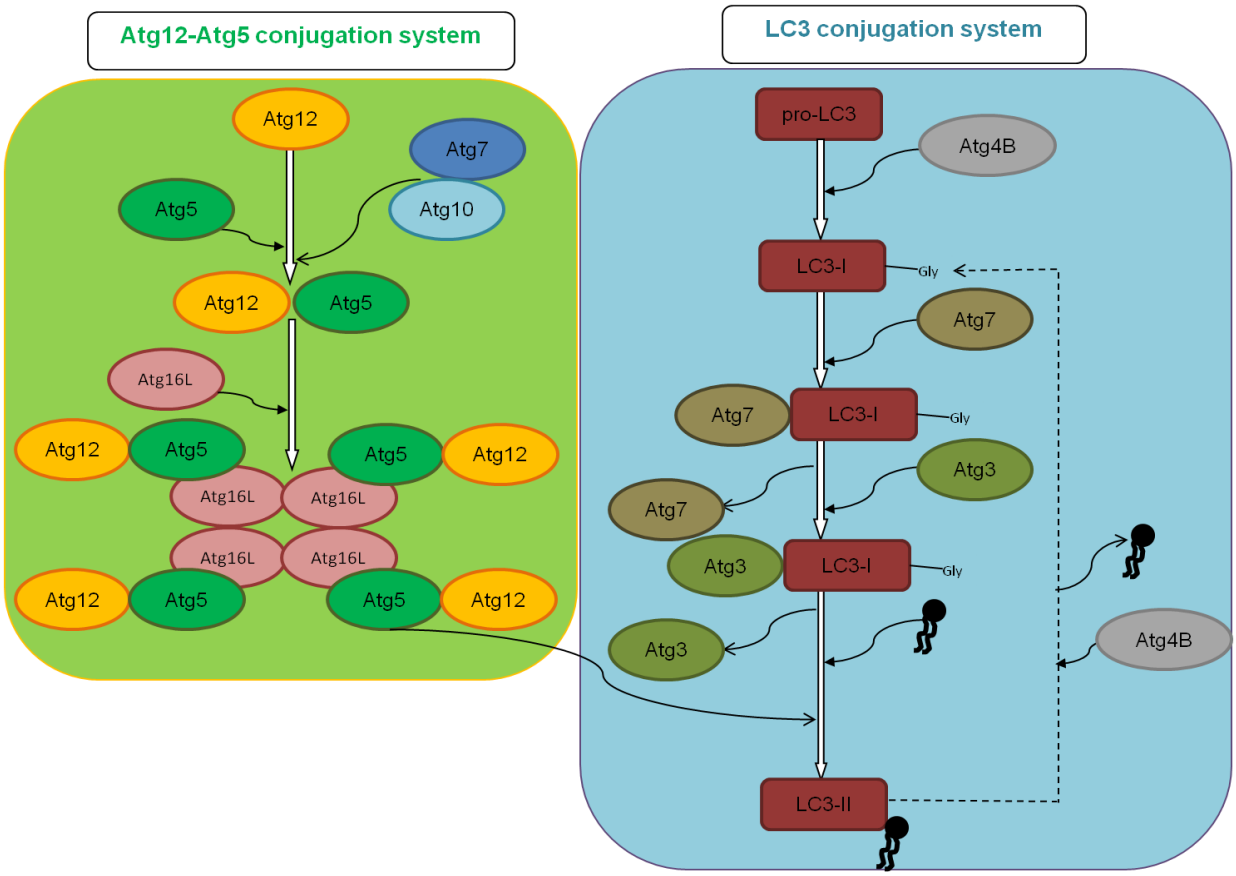

Graphic 5. Two ubiquitin-like conjugation systems involved in elongation and shape of autophagosome in mammals.

1.4.2 Physiological roles of autophagy in mammals

Autophagy plays a variety of roles in physiological processes in eukaryotic cells[203-205]. Autophagy occurs at low basal levels; however, it can be rapidly upregulated as an adaptive catabolic process in response to metabolic stress[179, 193]. It maintains cell homeostasis by turning over long-lived proteins and organelles, getting rid of toxic aggregated proteins, and eliminating damaged cytoplasmic components during stress or growth factor deprivation. Autophagy is activated in most cells to supply nutrients for essential anabolic needs under conditions of nutrient deprivation. During neonatal starvation in mice, carbohydrate and lipid reserves undergo autophagic degradation and are used as an energy source to survive; Atg5-deficient neonatal mice die within one day of starvation[206].

The broad spectrum of autophagy function is intricately linked to a wide range of healthy or pathological states[207, 208]. It has been speculated that autophagy may play a role in the prevention of autoimmunity and inflammatory disorders. Normal recycling of cytoplasmic contents, particularly in neural cells, via the autophagy pathway protects against the development of neurodegenerative disorders. By contrast, neural cell-specific Atg5 or Atg7 knockout mice accumulate abnormal intracellular proteins that form aggregates[207, 209].

Autophagy is essential for cellular homeostasis and functional maintenance as a pro-survival mechanism during nutrient deprivation[206]. The crucial role autophagy plays in T-lymphocyte development and function has been demonstrated by generating autophagy-deficient lymphocytes in irradiated recipients reconstituted with $Atg5^{-/-}$ fetal hematopoietic progenitor cells. CD4 and CD8 T-cells in $Atg5^{-/-}$ chimeras failed to undergo efficient TCR-induced proliferation; furthermore, $Atg5^{-/-}$ CD8 T-cells displayed increased cell death compared to wild-type (WT) littermates[210]. Autophagy also plays a role in B-cell development, mainly by regulating the development and survival of pre-B and B-1a cell subsets[211].

Autophagy contributes to the function of multiple aspects of both the innate and the adaptive immune response. In addition to degrading endogenous substrates, a selective

form of autophagy, known as xenophagy, contributes to the degradation of intracellular pathogens, including viruses, parasites, and bacteria[212-215]. Gutierrez *et al.* showed that inducing autophagy by treating macrophages with IFN-γ could overcome the block in phagolysosomal maturation that occurs during mycobacterial infection[216], which indicates that the autophagy pathway represents an efficient strategy for controlling intracellular pathogens. It has also been shown that the autophagic machinery of plasmacytoid DCs (pDCs) mediates delivery of viral RNA to endosomal toll-like receptors (TLRs), inducing the production of type I IFNs via TLR7 signaling[215].

The role of autophagy in immunity is not limited to the elimination of intracellular pathogens. It may also be a mechanism for antigen presentation. Indeed, data from recent studies imply a role for autophagy in regulating MHC class I-mediated cross-presentation of exogenous antigens[217]. Treatment with an inducer of autophagy enhances antigen cross-presentation[218]. Conversely, cross-presentation of antigen is significantly reduced by an autophagy inhibitor[219].

1.4.3 Autophagy and MHC class II antigen presentation

Recent studies reveal that autophagy is a potential mechanism for MHC class II endogenous antigen presentation. For example, presentation of cytosolic and nuclear antigens increases, on average by 50%, when cultured B-cell lines are starved to induce autophagy. For some individual ligands, the increase can exceed 130%, whereas membrane-bound antigen presentation is barely affected[167]. In contrast with proteasome-mediated antigen processing for coupling to MHC class I molecules, which favors proteins with a shorter half-life (e.g., defective ribosomal products (DRiPs)), autophagy substrates tend to be longer-lived, aggregated forms of ubiquitin-like proteins[209]. Currently, the ubiquitin-binding protein p62/SQSTM1 and autophagy-linked FYVE-domain-containing protein (Alfy) are the leading candidates for selective recognition of and targeting to the autophagy machinery. The p62 protein possesses both an LC3 recognition sequence and a ubiquitin-binding association (UBA) domain, which suggests that it serves as an adaptor linking polyubiquitinated substrates to Atg8/LC3 via UBA and LC3 interacting domains (LIRs) for autophagy-mediated

degradation[220, 221]. Alfy also colocalizes with autophagic marker LC3-II and ubiquitin-containing protein aggregates[222], suggesting Alfy may be a regulator for selective autophagy by targeting certain aggregated cytosolic proteins to autophagosomes. In addition, a nuclear factor E2-related factor 2 (Nrf2)-dependent stress response pathway has been implicated in the selection of aggregated proteins as substrates for autophagy[223]. Similarly, the pro-apoptotic factor NIX is used by mitochondria to mediate mitophagy as another form of selective autophagosomal degradation[224, 225].

Münz and colleagues initially showed that blocking autophagy inhibits endogenous MHC class II processing specifically for an EBV nuclear antigen, which results in decreased recognition by CD4 T-cells with specificity for this antigen[226]. Many other studies demonstrate that autophagy indeed contributes to the shuttling of intracellular antigens into the MHC class II loading pathway[167, 169, 170, 227]. However, it has not yet been clarified whether autophagy is a general and efficient pathway for MHC class II presentation of endogenous antigens. A later study by Münz's team[189] indicates that there is a substantial level of steady-state autophagy was continuously turned over in a variety of constitutive MHC class II-positive APCs, such as B-cell lines, monocytes, and DCs, and also in epithelial cell lines with IFN-γ-induced MHC class II expression. By observing GFP-LC3, they found that the autophagosome is frequently fused with MIIC, indicating that autophagosome cargo does indeed gain access to MHC class II for antigen presentation. It also raises the question of whether the multivesicular compartment formed by fusing of autophagosome and MIIC contains both MHC class II molecules and LC3 on its internal membranes. More importantly, targeting influenza matrix protein 1 (MP1) to the autophagosome as an LC3 fusion protein results in enhanced MHC class II presentation of MP1 and specific CD4 T-cell recognition, which suggests that autophagy constitutively and efficiently delivers cytosolic antigens for MHC class II presentation.

In accordance with these findings, it is plausible that autophagy-mediated MHC class II presentation of self-antigen plays a crucial role during thymic CD4 T-cell education. As the only non-hematopoietic cell type that constitutively expresses MHC class II molecules, TEC displays remarkably poor phagocytic activity[75], which suggests there is

an alternative MHC class II loading pathway. Analysis of GFP-LC3 mice indicates that starvation can significantly enhance autophagic activity in most tissues, including pancreas and muscle, which confirms the role of autophagy in the maintenance of energy homeostasis by recycling cytoplasmic components as a nutrient source[193]. However, in some other tissues, including thymic and lens epithelial cells, a higher basal level of autophagic activity, even in nutrient-rich conditions, is observed, and suggests that the number of autophagosomes in the TE may be among the highest in non-starved tissues. Indeed, roughly 70% of cTECs and 5–10% of mTECs contain high numbers of autophagosomes[228]. Furthermore, in line with the potential contribution of autophagy to the generation of MHC class II-bound peptides for T-cell selection, autophagosomes have been found fused with MIIC in thymic cryosections, with co-localization of LC3 with H2-DM-positive compartments[229]. This fusion strongly suggests that self-peptides expressed in the thymus can be shuttled into MHC class II molecules via the autophagy pathway in both cTECs for positive selection and mTECs for negative selection.

The most direct evidence[228] for the involvement of autophagy in positive selection of MHC class II-restricted TCRs in the TE was obtained in chimeras transplanted with autophagy-deficient thymi. This study showed that positive selection was impaired for some specific CD4 T-cells but enhanced for others, implying the alternation of the composition of MHC class II-bound peptides on cTECs occurs in the absence of autophagy in thymic epithelium, whereas selection of MHC class I-restricted TCRs was apparently unaffected. A similar setting was used to address whether the polyclonal T-cell repertoire selected by $Atg5^{-/-}$ TECs is self-tolerant; athymic nude mice were transplanted with either $Atg5^{-/-}$ or WT embryonic thymi. Only the recipients of $Atg5^{-/-}$ grafts started to lose weight 6 weeks post-transplantation, and compared to the controls had an increased number of activated peripheral CD4 T-cells. Inspection of internal organs revealed massive inflammatory infiltrates in the colon, liver, uterus, and lymph nodes. In line with autophagy-deficient TE perturbing the generation of selecting MHC II ligands, secondary transfer of the CD4 T-cells from diseased mice to WT recipient recapitulated all the autoimmune symptoms. However, it remains unclear whether the

escape of these autoreactive CD4 T-cells results from a lack of negative selection or the failure of deviation into Tregs, or is in fact lymphopenia caused by impaired positive selection.

2. Aim of the thesis

A growing number of studies have demonstrated that mTECs mediate central CD4 T-cell tolerance through direct presentation of endogenously expressed self-antigens[230-232]. As the only non-hematopoietic cell type that expresses MHC II molecules, TEC shows remarkably poor phagocytic activity[75]. Therefore, the pathway of MHC class II antigen loading in mTECs for negative selection of thymic $CD4^+$ T-cell remains poorly defined. Observations of colocalization of LC3 with MIIC compartments in the thymus[229] along with high numbers of autophagosomes presented in roughly 70% of cTECs and 5–10% of mTECs indicate that autophagy may shuttle intracellular materials into the MHC II loading pathway. A previous study from our lab further demonstrated that interference with autophagy specifically in TECs led to altered selection of certain MHC II restricted T-cells and resulted in multi-organ inflammatory infiltration[228]. Taken together, these results strongly suggest a contribution of autophagy for T-cell selection by focusing the MHC II/peptide repertoire of TECs on their intracellular milieu. However, it is not yet clear whether autophagy in mTECs contributes to induce central CD4 T-cell tolerance.

Here, we aimed to address this issue by generating transgenic mice that express a model antigen (human C-reactive protein, hCRP) specifically targeted to autophagosomes in $Aire^+$ mTECs and by examining the fate of *DEP*-specific $CD4^+$ T-cells.

3. Results

3.1 Cloning and functional evaluation of constructs targeting a model-antigen to autophagosomes

To obtain an autophagy substrate, an antigen was designed to deliberately introduce to autophagy degradation system. A tripartite hybrid protein was cloned (Figure1a). Briefly, a N-terminal fused Enhanced Green Fluorescent Protein (eGFP) was used as a reporter followed by a part of human C-reactive protein (hCRP) containing an epitope recognized by *DEP* specific TCR. LC3 was then fused in the C terminal of this fusion protein for autophagosome targeting (hereafter referred as GCL). During the process of autophagosome formation, the C-terminal region of proLC3 is cleaved, which exposes Gly_{120} to form LC3-I. Then the Gly_{120} site is conjugated to phosphatidylethanolamine (PE) for incorporation on both outer and inner membrane of autophagosome as LC3-II[199](Figure 1b). We also generated another construct with non-targeting to autophagosome by introducing a point mutant at position 120 of LC3. This mutation makes the residue change from Gly to Ala[201] (hereafter referred as GCL_{G120A}) (Figure 1a).

In order to visualize the targeting of these two constructs, HEK 293T cells were transfected with either GCL or GCL_{G120A} plasmid. Localization of hybrid proteins was monitored by fluorescence microscopy to examine whether antigen was fused with autophagosome or not. In Figure 1c, GFP distribution was even in the cytoplasm of both transfected cells that were cultured in full medium. However, GFP^+ punctae was only found in cells expressing GCL-vector in starvation medium supplemented with rapamycin (mTOR inhibitor which results in autophagy initiation), and no segregation of GFP dots could be observed in GCL_{G120A}-expressing cells under the same condition.

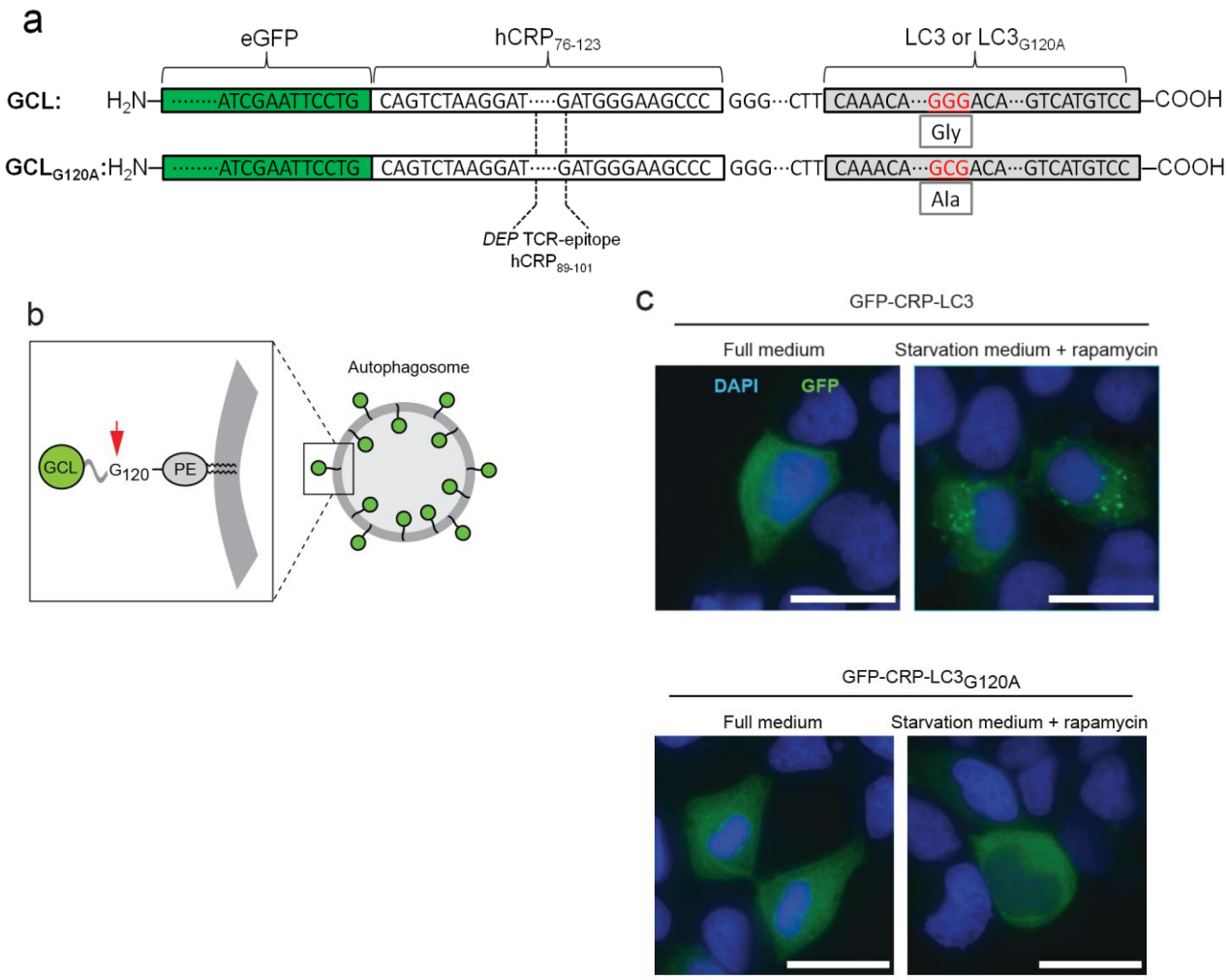

Figure 1. Targeting pattern of GCL and GCL_{G120A}. (a) Construct scheme of the GCL and GCL_{G120A}. (b) Schematic illustration of GCL targeting to autophagosome. GCL fusion proteins incorporate on both outer and inner membrane of autophagosomes via conjugation of LC3 to phosphatidylethanolamine (PE). (c) Assessment of localization of expressed proteins. HEK 293T cells were transfected with expression vectors encoding for GCL and GCL_{G120A} and then cultured in either full medium or starvation medium with rapamycin for 20h, the localization of expressed proteins was monitored by fluorescence microscopy. Scale bars indicate ×20μm. Panels show representative cells from one out of 2 independent experiments.

3.2 Generation and characterization of mTEC-specific GCL and GCL_{G120A} transgenic mice

To explore the role autophagy plays in mTECs to induce central CD4 T-cell tolerance, we generated transgenic mice expressing this fusion antigen specifically in mTECs. Two bacterial artificial chromosome (BAC) constructs containing 152kb upstream and

58kb downstream flanking regions of AIRE locus were cloned, along with the AIRE start codon replaced by an open reading frame encoding GCL or GCL_{G120A} as downstream of the β glubin intron (Figure 2a). By microinjection of these two constructs into fertilized eggs, seven or nine individual transgenic founders for the GCL or GCL_{G120A} constructs were generated, respectively. Due to introducing a restriction enzyme cutting site of Nru I into GCL_{G120A}, between GCL and GCL_{G120A} could be easily distinguished (shown in Supplementary Figure 1).

First, the expression pattern of GCL or GCL_{G120A} was examined. mRNA of various thymic stromal cell subsets from each founder was purified. The relative expression level of the transgene was quantified by real-time PCR (qPCR). The results indicated that mRNA expression of GCL or GCL_{G120A} in each founder was exclusively restricted into mTEC subpopulation, mainly in $mTEC^{hi}$ (phenotype as $CD45^{-}Epcam^{+}Ly51^{-}MHCII^{hi}CD80^{hi}$), partial expressed in $mTEC^{lo}$ (phenotype as $CD45^{-}Epcam^{+}Ly51^{-}MHCII^{lo}CD80^{lo}$), rarely in cTEC (phenotype as $CD45^{-}Epcam^{-}Ly51^{+}$) as well as DC (phenotype as $CD45^{+}CD11C^{+}$) (Supplementary Figure 2 and Figure 2b). Moreover, mRNA level of transgene expressing in mTECs varied among these founders (Supplementary Figure 2). To ascertain the transgene expression is truly in mTEC subset, the expression of AIRE gene was also analyzed. AIRE gene could be found highly expressing in $mTEC^{hi}$ and less in $mTEC^{lo}$ subpopulation, and hardly be detected in cTEC and DC subsets (Supplementary Figure 3 and Figure 2c).

Next, we aimed to figure out whether the expression of GCL or GCL_{G120A} proteins could be measured by quantifying GFP signal via FACS analysis. As we expected, GFP fluorescence signal became a mTEC-specific marker and varied from one transgenic line to another, while no signal was detected in either cTECs or DCs (Supplementary Figure 4a, 4b and Figure 2d). Furthermore, we found the higher transgenic mRNA level in mTECs corresponded to the stronger GFP signal, and the signal could be detected only in mTECs with a relatively higher expression level.

Based on qPCR data and FACS-analyses of GFP signal, a matched pair of transgenic lines was chosen for further investigation. Compared to the other transgenic founders,

these two mouse strains (referred to as Aire-GCL and Aire-GCL$_{G120A}$) expressed a relatively comparable, intermediate level of GCL or GCL$_{G120A}$ in mTEC^{hi} and mTEC^{lo} subpopulations (Figure 2b and 2d).

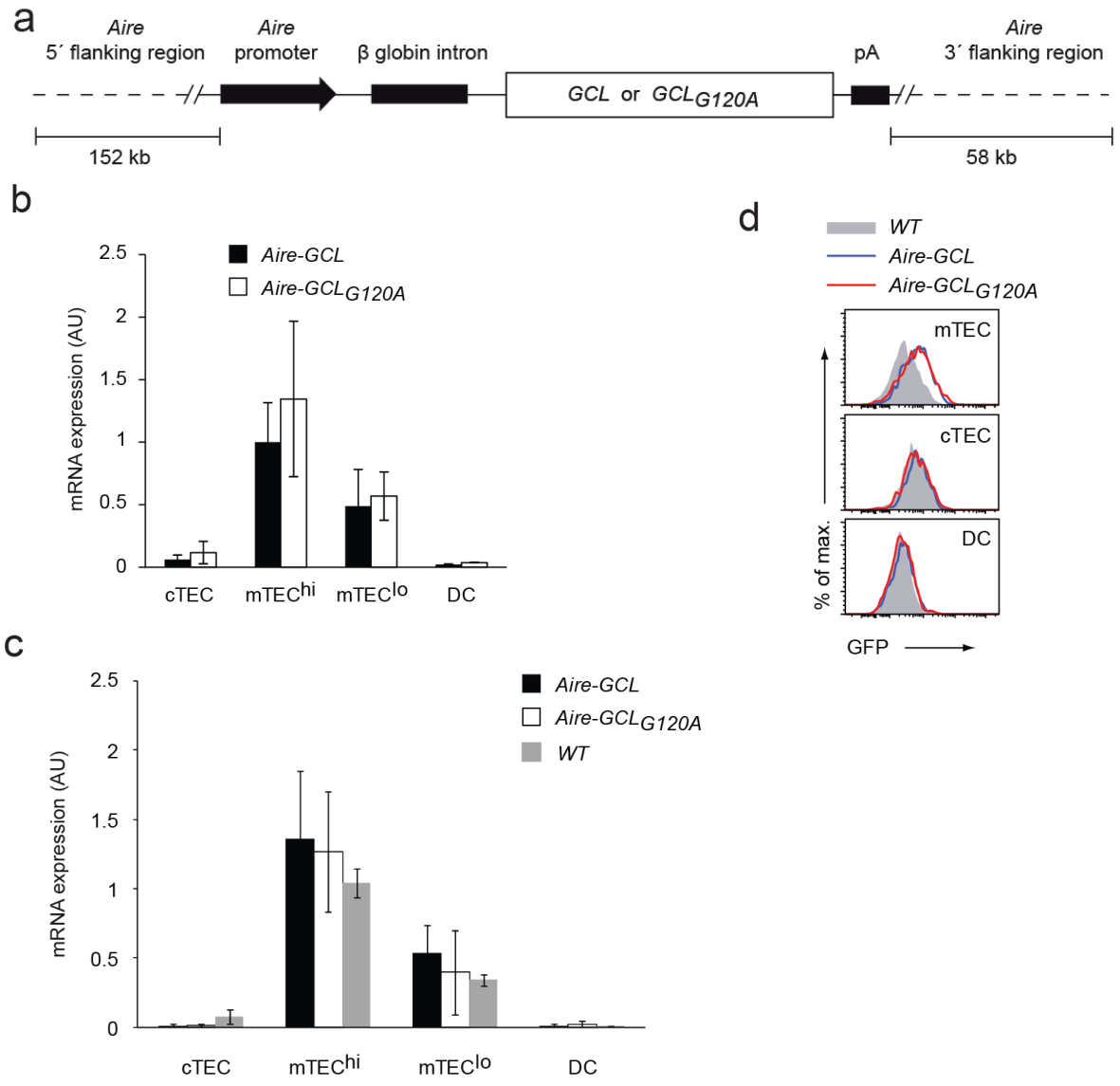

Figure 2. Generation of mTEC-specific GCL and GCL$_{G120A}$ transgenic mice and analysis of transgene expression. (a) Scheme of the Aire-GCL and Aire-GCL$_{G120A}$ BAC transgenic constructs to drive a specific expression of the fusion protein in mTECs (pA=poly-adenylation signal). (b) Quantitative analysis of transgenic mRNA expression. Different stromal cell types (cTEC, mTEC^{hi}, mTEC^{lo} and DC) were isolated from 2-week-old Aire-GCL or Aire-GCL$_{G120A}$ mice and transgenic mRNA level was assessed by qPCR. (c) The graph showed the relative expression of AIRE mRNA in respective stromal cells from 2-week-old Aire-GCL, Aire-GCL$_{G120A}$ mice or WT littermates. Values from (b) and (c) are normalized to expression in mTEC^{hi} from

Aire-GCL mice and indicated the mean±standard deviation from 3 independent experiments with pooled material from at least 4 thymi. None of the differences between individual subsets from Aire-GCL and Aire-GCL_{G120A} mice were statistically significant. (d) Transgenic proteins expression by different thymic stromal cell populations (mTEC, cTEC and DC) of WT (gray), Aire-GCL (blue) or Aire-GCL_{G120A} (red) thymi was determined by FACS analysis. Data are representative of 2 independent experiments, each with 5 mice.

3.3 Different direct presentation in GCL and GCL_{G120A} mTECs

3.3.1 GCL but not GCL_{G120A} is directly presented by mTECs

So far, our experiments had established the mice in which the expressing transgene was restricted into the mTEC subset. To address whether this expression pattern induces direct presentation by mTECs, or the mTEC-derived antigen is eventually processed and indirectly presented by neighboring DCs, we isolated mTECs and DCs from both lines separately and measured the capacity of APCs to activate $hCRP_{89-101}$-specific T hybridoma cells with an NFAT-driven GFP reporter.

Upon 20h-incubation with Aire-GCL mTECs, 16% of $hCRP_{89-101}$-specific T hybridoma cells turned into GFP^+ (see in Figure 3a). However, the same observation could not be found in T cell hybridomas stimulated by mTECs from Aire-GCL_{G120A} mice, only a weak response was elicited (P=0.008, vs. WT controls; Figure 3b)). In contrast, the percentage of GFP^+ cells stimulated by DCs from either Aire-GCL or Aire-GCL_{G120A} was not as high as stimulated by Aire-GCL mTECs, the response only maintained a marginal level as compared with WT DCs (P=0.048 and P=0.013, respectively; Figure 3b). Taken together, for GCL (the autophagy substrate), its antigen presentation mediated by mTECs is much more efficient than the variant GCL_{G120A} that express in a comparable level yet has one AA exchange to block the autophagosome targeting.

3.3.2 Mutation does not impact MHC class II expression and function in Aire-GCL_{G120A} mTECs

Since the weaker T cell stimulation capacity of Aire-GCL_{G120A} mTECs was measured as comparing with Aire-GCL mTECs, it raises the concern that the point mutation which abolishes autophagosome targeting might result in the alteration of mTEC function,

such as impaired MHC class II expression, and further leads to weak capacity on peptide presentation.

In order to address this issue, the surface MHC class II expression of mTECs from Aire-GCL, Aire-GCL_{G120A} mice and WT littermates was examined. A similar expression level of MHC class II on mTECs was observed (Figure 3c). Furthermore, mTECs from indicated groups were purified and cultured with T cell hybridomas to analyze their peptide presentation capacity in the presence of CRP peptides (6μg/ml). In Figure 3d, up to 80% of *DEP* T hybridoma cells recognition was activated by Aire-GCL or Aire-GCL_{G120A} mTECs with peptide pulsed and the percentage of increased GFP^+ cells had no significant difference compared to WT mTECs with peptides (P=0.1283 and P=0.0709, respectively).

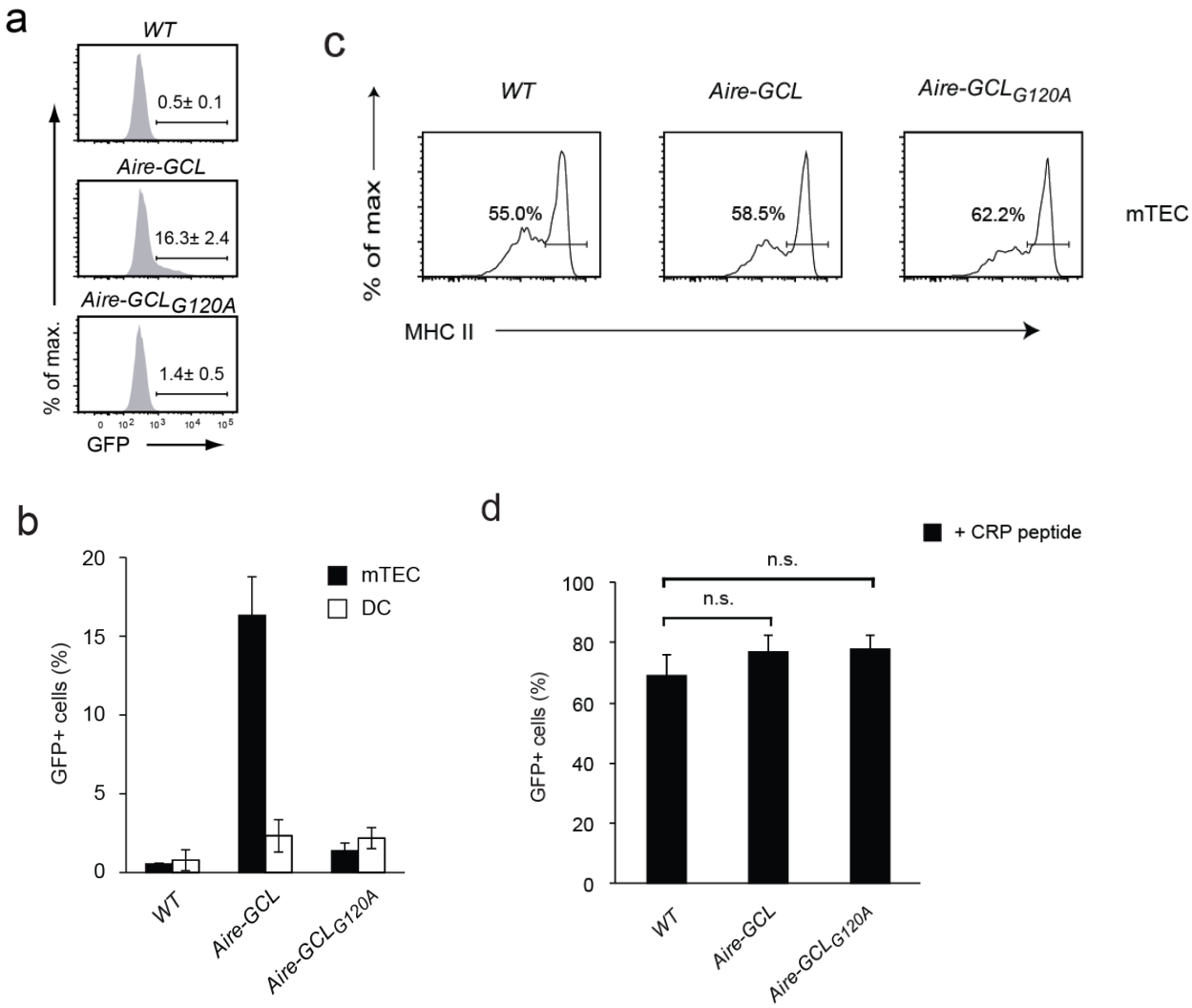

Figure 3. Characterization of antigen presentation capacity of Aire-GCL mTECs. (a) Assessment of antigen presentation capacity *in vitro*. *Ex-vivo* isolated mTECs from 5-week-old WT, Aire-GCL and Aire-GCL_{G120A} mice were cultured with NFAT-GFP reporter hybridoma cells expressing $hCRP_{89-101}$-specific *DEP*-TCR. After 20h, GFP expression of T hybridoma cells was measured by FACS analysis. The bar diagram depicts the frequency of GFP^+ hybridoma cells stimulated by mTEC from each group. (b) Summary of the percentage of T hybridoma cells with GFP-fluorescence stimulated by mTEC (black bars) or DC (white bars) from indicated groups. (c) Freshly mTECs of Aire-GCL and Aire-GCL_{G120A} thymi were isolated and MHC II expression level was measured by FACS. Values are representative from one out of two independent experiments with pooled material from at least 6 thymi. (d) Assessment of peptide presentation *in vitro*. The bar diagram shows the percentage of GFP^+ hybridoma cells stimulated by *Ex-vivo* isolated mTEC from indicated mice in the presence of 6µg/ml CRP peptide. Values from (a),(b),(d) are representative of 3 independent experiments with pooled material from at least 6 thymi. (n.s.= not significant.)

3.4 mTECs directly present GCL, but not GCL_{G120A}, for negative selection

3.4.1 A similar 'late' negative selection displays in both double transgenic strains

To assess the consequence of distinct antigen presentation patterns of mTECs in both lines on central tolerance of $CD4^+$ T-cells, Aire-GCL and Aire-GCL_{G120A} mice were bred with *DEP* TCR-*tg* mice bearing a TCR recognizing epitope CRP_{89-101}[232]. In Figure 4a and 4b, compared to *DEP* TCR transgenic mice as controls, both double transgenic mice showed a similar extent of 'late' negative selection which self-reactive T-cell deletion occurred at the CD4 SP stage. It correlated with a relative and absolute number reduction of CD4 SP thymocytes to roughly 20%. Among these remaining CD4 SP thymocytes, expression of α chain and ß chain of *DEP* specific TCR had a considerable downregulation. In contrast, a statistically reduction in the absolute numbers of Tregs was found (Figure 4c). These data indicate that immune tolerance of *DEP* TCR-specific thymocytes predominantly operates via T-cell deletion in both lines.

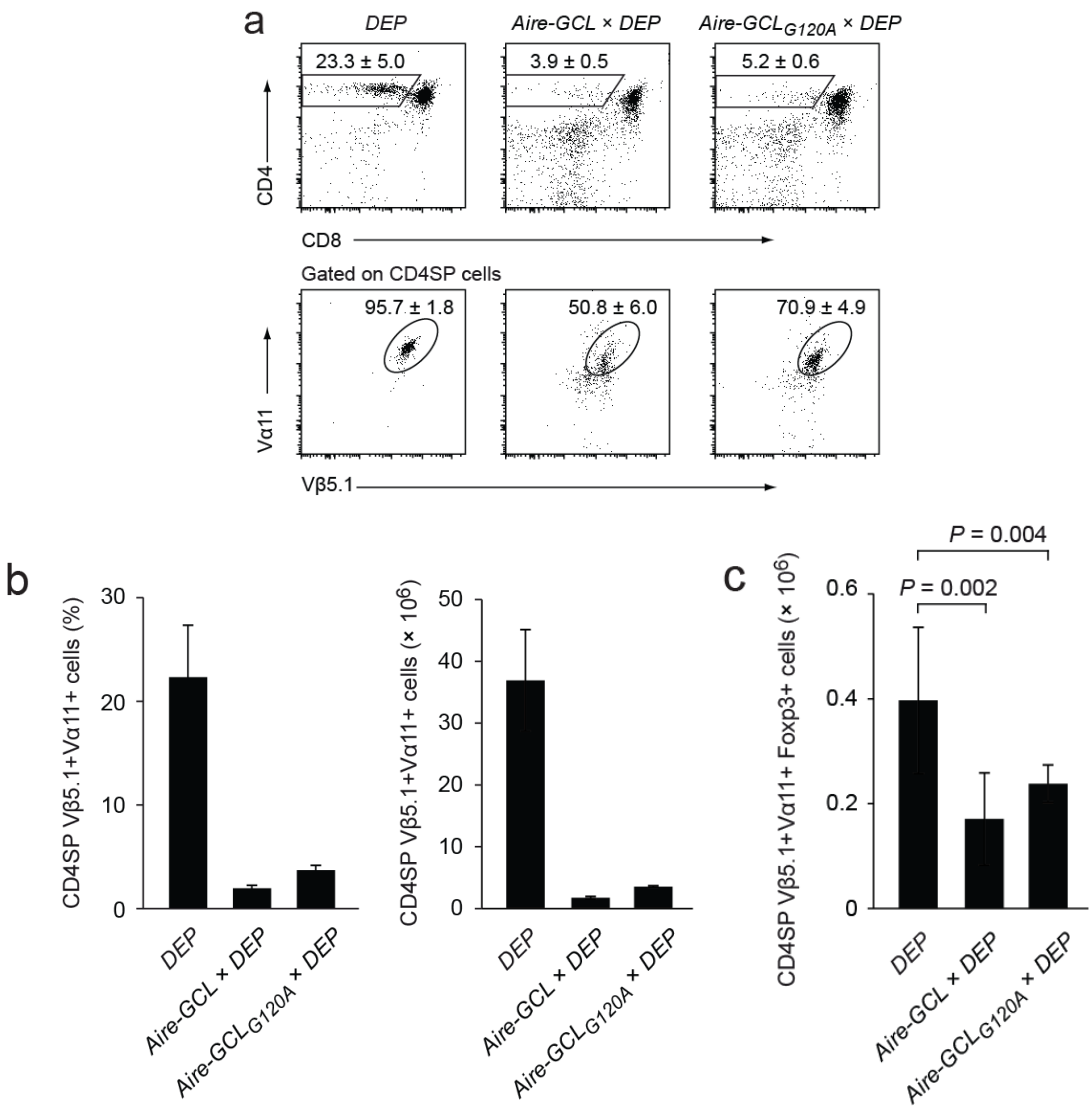

Figure 4. Negative selection of hCRP$_{89\text{-}101}$ specific CD4$^+$ T-cells in double transgenic mice. (a) CD4$^+$ T-cell development in 4- to 5-week-old *DEP* single transgenic mice, Aire-GCL×*DEP* and Aire-GCL$_{G120A}$×*DEP* double transgenic mice. The plots depict that the average percentage ± stdev of CD4 SP profiles (upper row) and of *DEP*-TCR$^+$ cells (Vα11$^+$Vβ5.1$^+$) among gated CD4 SP thymocytes (lower row). (b) The bar diagram shows the percentage and absolute numbers of CD4 SP Vα11$^+$Vβ5.1$^+$ cells among total thymocytes in (a). Data in (a) and (b) are from ≥10 mice per genotype. (c) Summary of the absolute numbers of CD4 SP Vα11$^+$Vβ5.1$^+$ Foxp3$^+$ cells among total thymocytes. Data in (c) are from at least 5 mice per genotype. (*P* values are indicated)

3.4.2 Antigen exclusively expressed in thymic epithelium is sufficient to mediate negative selection

Based on observations in Figure 4b shown distinct antigen presentation patterns of Aire-GCL or Aire-GCL_{G120A} mTECs resulted in the similar extent of *DEP* T-cell deletion in corresponding double transgenic mice, we therefore hypothesize whether different antigen presentation routes contribute to T-cell deletion in each line.

Briefly, to determine whether antigen exclusively expressed in thymic epithelium is available and sufficient to mediate a comparable extent of negative selection in Aire-GCL and Aire-GCL_{G120A} mice. Irradiated Aire-GCL, Aire-GCL_{G120A} or WT recipients were reconstituted with *DEP* TCR-*tg* bone marrow (BM) for four to five weeks and T-cell development was analyzed. As we expected, WT recipients which received *DEP* BM had a normal percentage of *DEP* TCR-specific CD4 T-cells (in Figure 5a and 5c), indicating positive selection was not impaired. However, when *DEP* BM was transferred into either Aire-GCL or Aire-GCL_{G120A} mice, most of *DEP* TCR-specific CD4 T-cells were deleted due to recognized as self-reactive thymocytes, which represented the similar extent of negative selection as the respective double transgenic mice in Figure 4.

3.4.3 Direct presentation via GCL mTECs versus indirect presentation by GCL_{G120A} DCs is essential for clonal deletion

To understand the contribution of DC versus mTEC in CD4 T-cell tolerance induction, different BM chimeras were generated by removing DC from the system. To this end, mice that carried diphtheria toxin α chain (DTA) under the control of a loxP-flanked stop cassette in the ubiquitously expressed ROSA26 locus were utilized and crossed to CD11c-Cre mice, which led to the physical ablation of DC (ΔDC)[233]. And then the BM from *DEP* TCR-tg ΔDC were transferred into irradiated Aire-GCL, Aire-GCL_{G120A} or WT mice, which abolished the ability of DC to present antigen in the thymus. Results showed the percentage of *DEP* $CD4^+$ T-cells in Aire-GCL mice receiving BM from ΔDC had no change compared to mice injected with *DC*-sufficient BM. In contrast to efficient $CD4^+$ T-cell deletion in Aire-GCL_{G120A} mice with transferring of *DEP* TCR-tg BM, there was a significant enlargement of $CD4^+$ T-cells in mice receiving *DEP* TCR-tg ΔDC BM ($P<0.001$; Figure 5b and 5c). However, this *DEP* specific CD4 T-cell rescue caused by a lack of DCs is not complete. Comparing with WT controls, there was still a significant decreased percentage of $CD4^+$ T-cells in Aire-GCL_{G120A} mice receiving *DEP* TCR-tg

ΔDC BM (P=0.0013; Figure 5b and 5c), which suggests there is the existence of autonomous presenting mTEC-induced negative selection in Aire-GCL$_{G120A}$ mice. Collectively, these findings suggest distinct antigen presentation routes operate in Aire-GCL and Aire-GCL$_{G120A}$ mice for induction of CD4^{+} T cell tolerance, which means autophagosome-targeted GCL is capable to be directly presented by mTECs and this direct presentation is sufficient to induce a robust negative selection. While in Aire-GCL$_{G120A}$ mice, cross presentation mediated by DCs seems to be the main mode to induce an efficient clonal deletion.

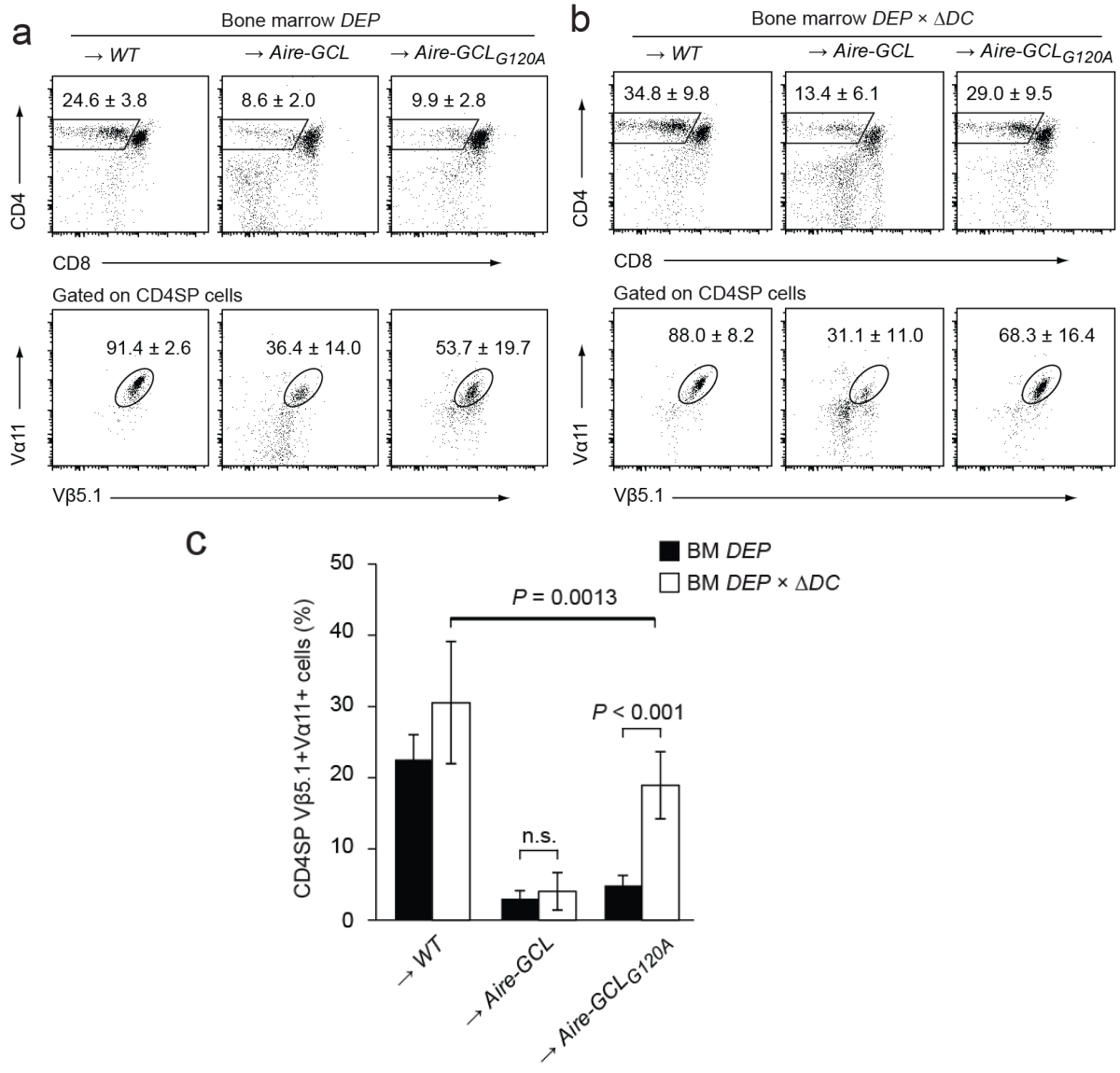

Figure 5. mTECs directly presenting GCL, but not GCL_{G120A}, are essential for negative selection. (a) $CD4^+$ T-cell development in WT, Aire-GCL or Aire-GCL_{G120A} recipients 4-5 weeks after irradiation and reconstitution with *DEP* bone marrow. The average frequencies of CD4 SP T-cells are shown (± stdev) in upper row and of *DEP*-TCR^+ cells ($V\alpha11^+V\beta5.1^+$) among gated CD4 SP thymocytes are depicted (± stdev) in lower row. Values are representative of at least 10 chimeras per group. (b) $CD4^+$ T-cell development in WT, Aire-GCL or Aire-GCL_{G120A} recipients of *DEP*×Δ*DC* bone marrow cells were analyzed after 4-5 weeks reconstitution. Dot plots show the average frequency± stdev of CD4 SP T-cells (upper row) and of DEP-TCR^+ cells ($V\alpha11^+V\beta5.1^+$) among gated CD4 SP thymocytes (lower row). Data are representative of at least 9 chimeras from each group. (c) Summary of the percentage of CD4 SP $V\alpha11^+V\beta5.1^+$ cells among total thymocytes in (a) and (b). (*P* values are indicated; n.s.= not significant.)

3.5 Direct antigen presentation by Aire-GCL mTECs is autophagy-dependent

3.5.1 Autophagy deficiency impairs negative selection mediated by direct pathway

To address the role of autophagy played on mTECs in direct presentation of intracellular antigens, different thymus chimeras with interference of autophagy in TECs were generated. Irradiated WT mice that were reconstituted with DEP-*tg* MHC $II^{-/-}$ [234] bone marrow were used as the recipients of thymus grafts. In this system, it abolished indirect antigen presentation of DCs due to the disrupted MHC class II expression on DCs. In Figure 6a and 6c, an unimpaired, efficient positive selection of *DEP* TCR-specific thymocytes was shown in non-antigen expressing chimeras transplanted with Atg5 $^{+/-}$ or Atg5 $^{-/-}$ thymi, which consists with our previous reports[228]. When the grafted epithelium expressed endogenous GCL and was autophagy-sufficient, negative selection occurred and the percentage of remained thymocytes was less than 20% (Figure 6b and 6c). A similar extent of T-cell deletion as the setting described in Figure 5b and 5c was observed, and it is convinced that direct presentation mediated by AIRE-GCL mTECs is sufficient to induce negative selection. In contrast, when the transplanted Aire-GCL epithelium was autophagy-deficient, a significant reduction of *DEP* T-cell deletion could be observed ($P<0.001$; Figure 6b and 6c). However, an incomplete *DEP* specific CD4 T-cell deletion still existed in chimeras grafted Aire-GCL thymi compared with WT controls under the autophagy-deficient condition ($P<0.001$; Figure 6b and 6c). Collectively, negative selection mediated by direct presentation in AIRE-GCL mTECs at least in part depends on the autophagy pathway. Additionally, the pathway that mediates direct

presentation by mTECs observed in Aire-GCL$_{G120A}$ mice (Figure 5c) is autophagy-independent, since there was no difference in the extent of deleted *DEP* T-cells between Atg5-sufficient and Atg5-deficient Aire-GCL$_{G120A}$ grafted thymi (P=0.1749; Supplementary Figure 5).

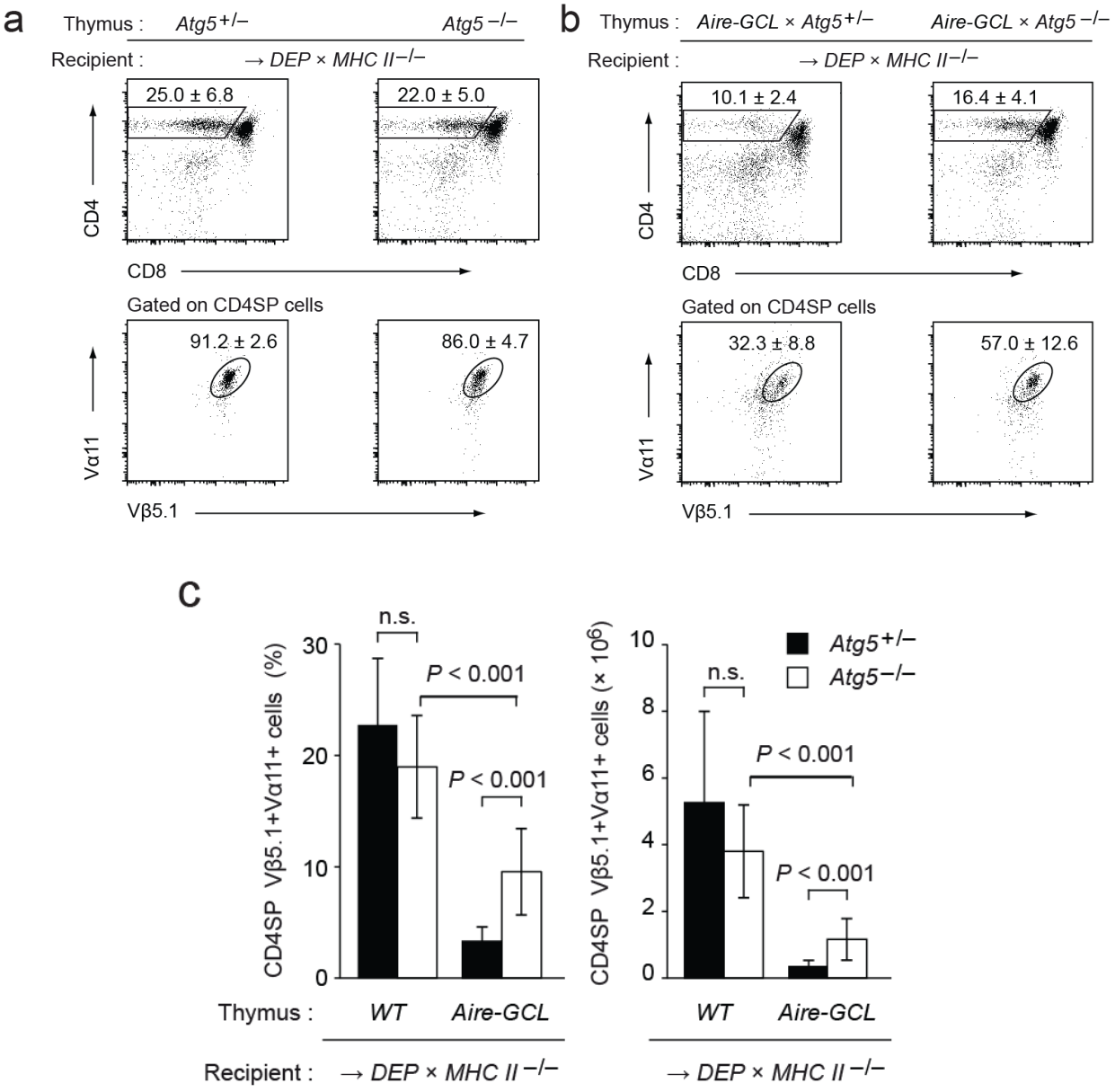

Figure 6. Negative selection mediated by direct presentation in Aire-GCL mTECs is partly autophagy-dependent. (a) Autophagy deficiency does not impact positive selection of *DEP* cells. CD4$^+$ T-cell development in Atg5$^{+/-}$ or Atg5$^{-/-}$ thymi lobes transplanted into *DEP*×*MHC II*$^{-/-}$ recipients measured after 4-6 weeks reconstitution. The dot plots depict the average frequency of CD4 SP T-cells are shown (± stdev) in upper row and of *DEP*-TCR$^+$ cells

(Vα11$^+$Vβ5.1$^+$) among gated CD4 SP thymocytes are depicted (± stdev) in lower row. Values are representative of at least 11 chimeras per group. (b) Defective negative selection of *DEP* cells is shown in Aire-GCL thymi with autophagy deficiency. Histograms show staining of CD4$^+$ SP T-cells for *DEP-TCR* from Aire-GCL×Atg5$^{+/-}$ or Aire-GCL×Atg5$^{-/-}$ thymi lobes 4-6 weeks after transplantation into *DEP*×*MHC II*$^{-/-}$ recipients. Numbers in the dot plots indicate the average frequency ((± stdev) of CD4 SP T-cells (upper row) and of *DEP*-TCR$^+$ cells (Vα11$^+$Vβ5.1$^+$) among gated CD4 SP thymocytes (lower row). Data are representative of at least 13 chimeras in each group. (c) Summary of the frequencies and absolute numbers of CD4 SP Vα11$^+$Vβ5.1$^+$ cells among total thymocytes in (a) and (b). (*P* values are indicated; n.s.= not significant.)

3.5.2 Autophagy deficiency impairs the endogenous antigen presentation

In Figure 6b and 6c, a significant reduction on the percentage of deleted thymocytes could be found in *DEP* MHC II$^{-/-}$ recipients transplanted with Aire-GCL autophagy-deficient lobes, which suggests negative selection mediated by Aire-GCL mTECs depends on autophagy pathway. As a result, the issue of whether direct presentation capacity of Aire-GCL mTECs would be impaired when the autophagy pathway was interfered is investigated. mTECs from thymus chimeras described in Figure 6 were isolated and used to stimulate T cell hybridomas. In Figure 7a, although the percentage of GFP$^+$ hybridomas stimulated by Aire-GCL Atg5 $^{+/-}$ mTECs from grafted lobes was not as high as those stimulated by Aire-GCL mTECs described in Figure 3a, it still generated 6% GFP$^+$ cells from the co-culture system, a statistically significant response was induced by Aire-GCL mTECs with autophagy-sufficient compared to mTECs with GCL-expressing, but autophagy-deficient (P=0.0084; as shown in Figure 7b). Thus, these data suggest that the defective efficiency on direct presentation of Aire-GCL mTECs caused by interfering with autophagy is responsible for the severe impaired negative selection shown in Figure 6b and 6c.

To investigate the possibility of impaired peptide presentation capacity in Aire-GCL mTECs resulted from Atg5 deficiency, hCRP$_{89\text{-}101}$-specific T hybridoma cells were cultured with mTECs from GCL-expressing Atg5$^{+/-}$ or Atg5$^{-/-}$ grafted lobes in the presence of CRP peptide (6μg/ml). Data indicated that no matter autophagy pathway was interfered or not, Aire-GCL mTECs induced a similar level of GFP$^+$ hybridomas upon culturing with peptides (see Figure 7c). At the same time, we observed the MHC II expression was not affected when Atg5 was deficient in mTECs. A slightly higher, but

comparable level of MHC II was expressed on mTECs from Aire-GCL Atg5 $^{+/-}$ or Aire-GCL Atg5 $^{-/-}$ lobes compared with mTECs from WT littermates (Figure 7d).

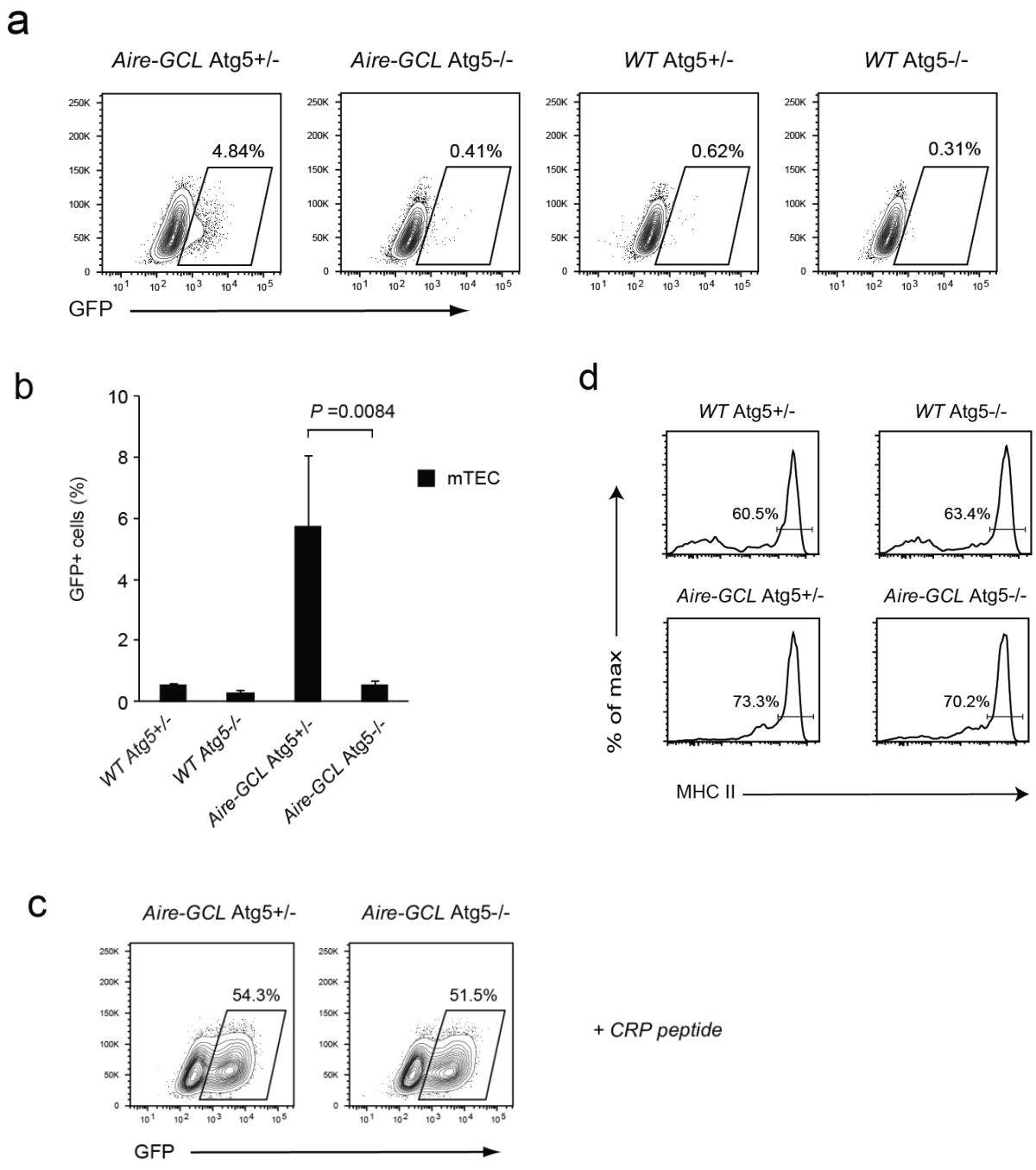

Figure 7. Characterization of antigen presentation by Aire-GCL mTECs with interference of autophagy. (a) Assessment of antigen presentation capacity *in vitro*. *Ex-vivo* isolated mTECs from GCL-expressing Atg5$^{+/-}$ or Atg5$^{-/-}$ grafted lobes as well as WT littermates were cultured with NFAT-GFP reporter hybridoma cells expressing hCRP$_{89-101}$-specific *DEP*-TCR.

After 20h, GFP expression of T hybridoma cells was measured by FACS analysis. Values show the frequency of stimulated GFP^+ hybridoma cells from one out of three independent experiments with pooled material from ≥6 grafted lobes. (b) Summary of the percentage of hybridomas with GFP-fluorescence stimulated by mTECs from indicated groups. Values are representative of 3 independent experiments with pooled material from at least 6 grafted lobes (*P* values are indicated). (c) Assessment of peptide presentation *in vitro*. Values show the percentage of GFP^+ hybridoma cells by *Ex-vivo* isolated mTEC from indicated groups in the presence of 6µg/ml hCRP peptide. (d) Freshly mTECs from indicated groups were isolated and MHC II expression level was measured by FACS. Values from (c) and (d) are representative from one out of two independent experiments with pooled material from at least 6 grafted lobes.

3.6 A redundant role of mTECs and DCs from Aire-GCL thymi on negative selection

Although direct presentation by Aire-GCL mTECs is essential for negative selection, the contribution of DCs in Aire-GCL system to present autophagosome-targeted GCL is still not clear. The investigation system used in Figure 5b highlights the crucial role of indirect presentation by Aire-GCL_{G120A} DCs played on induction of negative selection. Additionally, the data from Figure 3b indicates the antigen presentation capacity between Aire-GCL_{G120A} and Aire-GCL DCs is comparable. Thus, we are wondering if central tolerance in Aire-GCL mice would be affected in the presence of 'presentation-competent' DCs when direct presentation by mTECs is diminished.

To verify it, *DEP* MHC II sufficient mice as recipients were transplanted with Aire-GCL $Atg5^{+/-}$ or Aire-GCL $Atg5^{-/-}$ embryonic lobes as well as wide type littermates. In Figure 8a, five weeks after reconstitution, most of *DEP* $CD4^+$ T-cells were positively selected and showed a normal percentage in either $Atg5^{+/-}$ or $Atg5^{-/-}$ transplanted lobes in which no antigen was expressed. However, in Aire-GCL $Atg5^{+/-}$ transplanted lobes roughly two third of *DEP* thymocytes were deleted, which was consistent with a strong CD4 T-cell deletion occurred in Aire-GCL $Atg5^{+/-}$ lobes transplanted into MHC II deficient *DEP-Tg* mice. In contrast, a similar extent of $CD4^+$ T-cell deletion was achieved in *DEP* MHC II sufficient recipients even though the transplanted Aire-GCL epithelium was autophagy-deficient (Figure 8b,c, compared Figure 6b,c). Thus, indirect presentation by DCs is capable to compensate autophagy-dependent direct presentation by mTECs in Aire-GCL system.

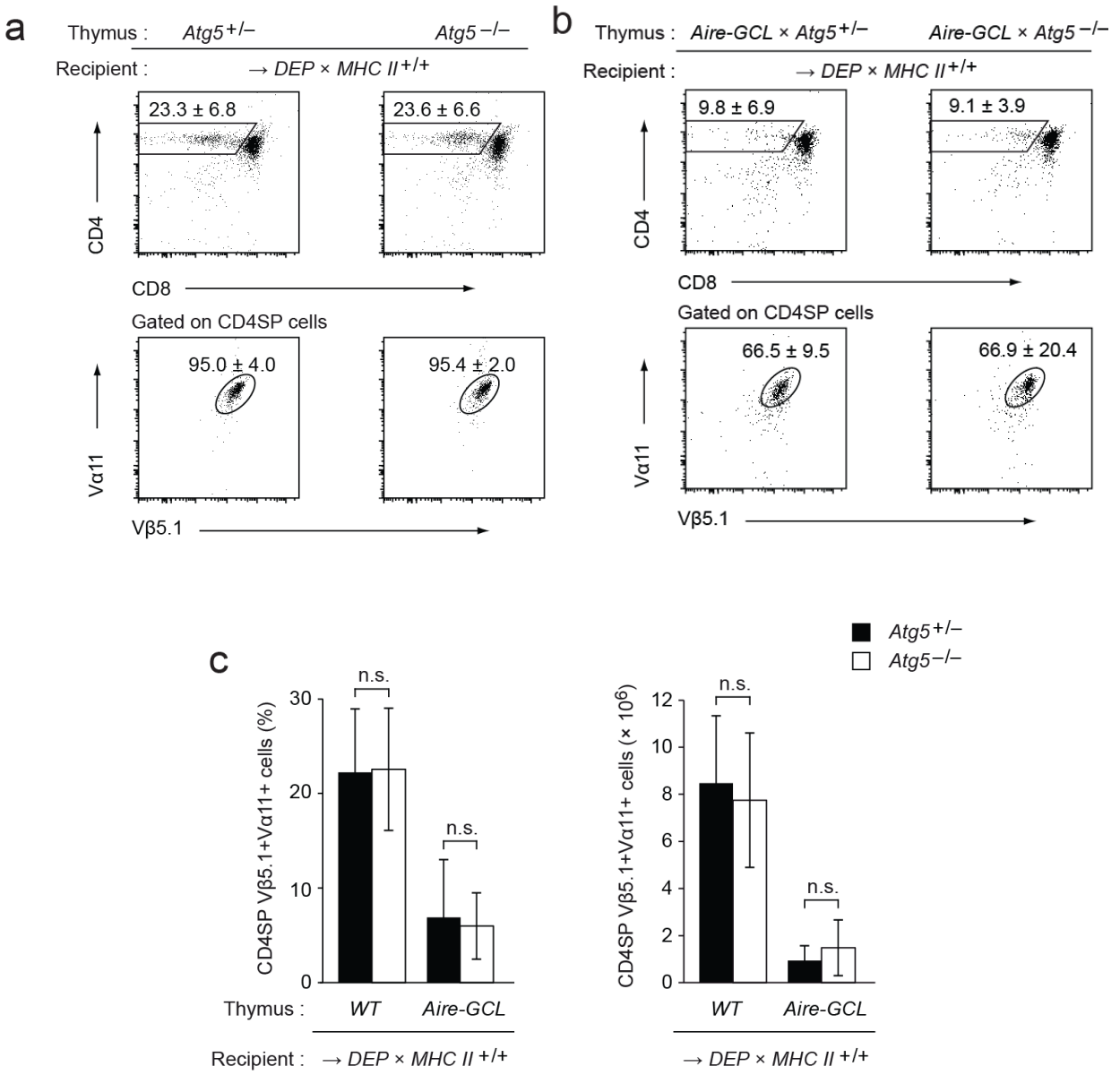

Figure 8. Direct presentation by mTECs and indirect presentation by DCs in Aire-GCL thymus operate in parallel. (a) Analysis of thymus chimeras of interfering with autophagy in TECs. *DEP*×*MHC II*$^{+/+}$ mice as recipients were transplanted with Atg5$^{+/-}$ or Atg5$^{-/-}$ thymi lobes, 4-6 weeks later, *DEP* CD4^{+} T-cell development was measured. The dot plots depict the average frequency of CD4 SP T-cells are shown (± stdev) in upper row and of DEP-TCR^{+} cells (Vα11^{+}Vβ5.1^{+}) among gated CD4 SP thymocytes are depicted (± stdev) in lower row. Values are representative of at least 19 chimeras per group. (b) In the presence of 'presentation-competent' DCs, a non-impaired *DEP* T-cell deletion occurs in Aire-GCL TECs with autophagy

deficiency. $CD4^+$ SP T-cells for *DEP-TCR* from Aire-GCL×$Atg5^{+/-}$ or Aire-GCL×$Atg5^{-/-}$ thymi lobes 4-6 weeks after transplantation into *DEP*×*MHC II*$^{+/+}$ recipients were stained and analyzed. The average frequency of CD4 SP T-cells are shown (± stdev) in upper row and of DEP-TCR^+ cells ($V\alpha11^+V\beta5.1^+$) among gated CD4 SP thymocytes are depicted (± stdev) in lower row. Values are representative of at least 10 chimeras per group. (c) Summary of the frequencies and absolute numbers of CD4 SP $V\alpha11^+V\beta5.1^+$ cells among total thymocytes in (a) and (b). (n.s.= not significant.)

3.7 A crucial role of autophagy-dependent direct presentation by mTECs at lower antigen expression level

3.7.1 Antigen expression level in a second Aire-GCL strain

Considering the data that much more GFP^+ hybridomas were generated when stimulated by Aire-GCL mTECs compared to Aire-GCL DCs (Figure 3b), while these DCs are also capable to mediate efficient negative selection in Aire-GCL system (Figure 8b). It arises the hypothesis that negative selection can be co-mediated via direct presentation by mTECs as well as indirect presentation by DCs when the amount of endogenous antigen expressed by mTECs exceeds the minimal requirement for induction of negative selection. Thus, the issue of whether DC-mediated negative selection depends on the amount of mTEC-expressed antigen is investigated.

To test this hypothesis, a second Aire-GCL strain was used to perform analysis. Comparison of mRNA expression level indicated that a less mRNA expression of roughly 3-4 fold decrease was measured in $mTEC^{hi}$ and $mTEC^{lo}$ subpopulations from the second Aire-GCL strain (referred to as Aire-GCL^{lo}) than the Aire-GCL line (Figure 9a). The GFP fluorescent in Aire-GCL^{lo} mTECs could not be detected, which indicates lower transgenic proteins were expressed (Figure 9b).

3.7.2 Fewer antigen expression on Aire-GCL^{Lo} mTECs displays weaker antigen presentation capacity

Next, we assessed antigen presentation capacity of Aire-GCL^{lo} mTECs with lower antigen expression level. There are less GFP^+ cells stimulated by Aire-GCL^{lo} mTECs compared to Aire-GCL mTECs (1.64±0.21% vs. 12.58±3.14%)(Figure 9c).

In order to have a more precise comparison on direct presentation capacity of mTECs between Aire-GCL and Aire-GCL^{lo} strains, a peptide titration curve was drawn to depict activation of T hybridoma cells when stimulated by co-cultured WT mTECs in the presence of different concentration (with titrated doses) of hCRP peptide. By comparison of Figure 9c and 9d, the percentage of stimulated T hybridoma cells by Aire-GCL mTECs was similar to that of WT mTECs added with 1.2μg/ml peptide (12.58±3.14% vs. 15.55%), while the percentage of stimulated hybridomas by Aire-GCL^{lo} mTECs was similar to that of WT mTECs added with 455ng/ml peptide (1.64±0.21% vs. 1.99%). By calculation, it was roughly a 3-fold weaker direct presentation capacity in Aire-GCL^{lo} mTECs than Aire-GCL mTECs.

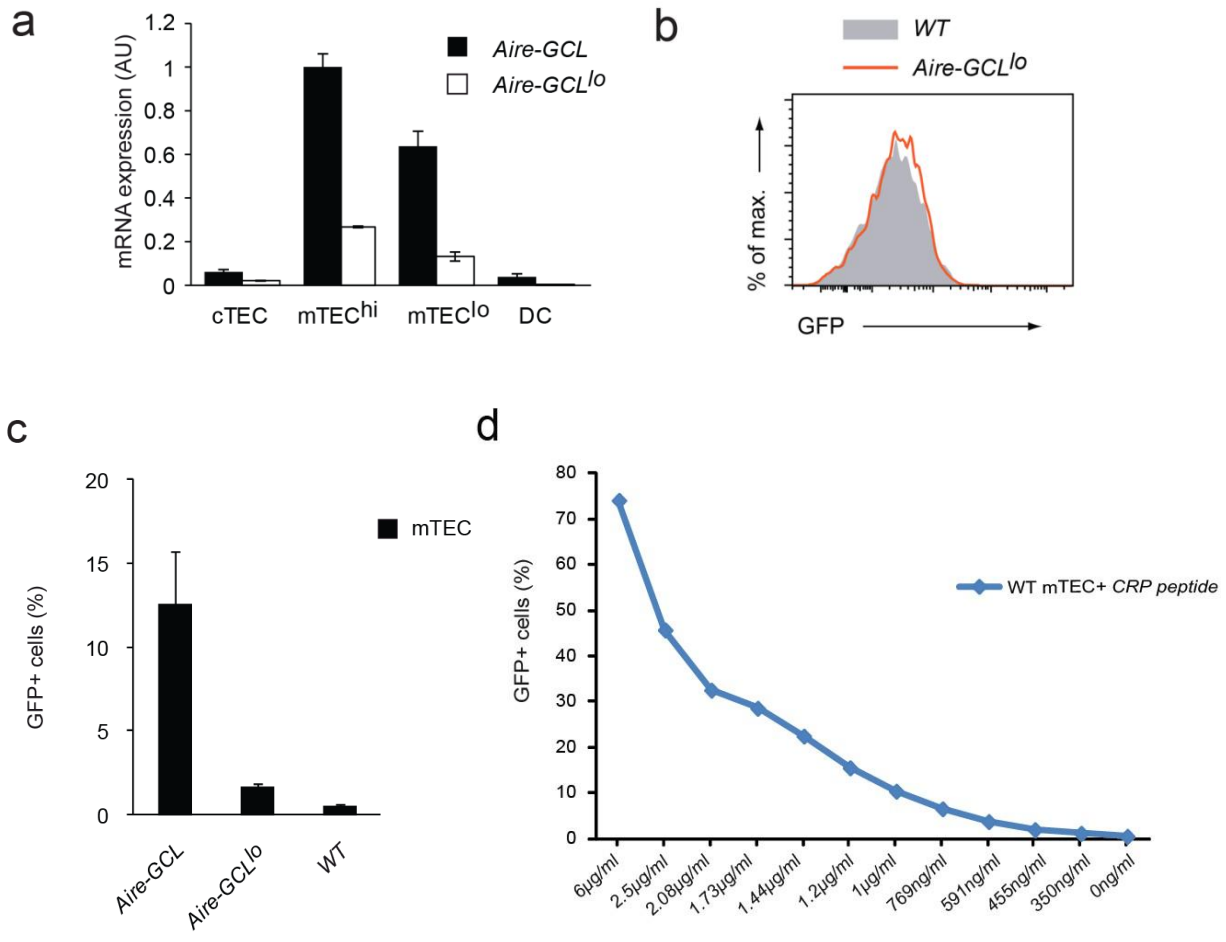

Figure 9. A lower antigen expression level in Aire-GCL^{lo} mTECs performs a weaker antigen presentation capacity. (a) Expression analysis of GCL transgenic mRNA. GCL mRNA was isolated from purified different thymic stromal subsets defined as in Figure 2b from

Aire-GCL or Aire-GCL^{lo} mice and the relative transgenic mRNA expression level was determined by qPCR. Values are normalized to expression in mTEC^{hi} from Aire-GCL mice and indicate the mean±standard deviation from 3 independent biological replicates. (b) Quantification of transgenic protein expression was assessed by measurement of GFP fluorescence in mTECs from Aire-GCL^{lo} mice (red), WT mTECs (gray) as a negative control. Values are representative of 3 independent experiments with pooled cells from at least 4 thymi. (c) Assessment of antigen presentation capacity. Freshly isolated mTECs from Aire-GCL, Aire-GCL^{lo} or WT mice cultured with hCRP$_{89\text{-}101}$ specific T hybridoma cells, 20h later, frequencies of stimulated GFP^{+} hybridoma cells were measured. The bar diagram shows the percentage of hybridomas with GFP-fluorescence stimulated by mTEC from indicated mice. Values are representative of 3 independent experiments with pooled cells from at least 6 thymi. (d) CRP peptide 1.2-fold titration standard curve was drawn by analysis of the percentage of GFP^{+} T hybridoma cells stimulated by *ex vivo* isolated WT mTECs (c) in the presence of different concentration of CRP peptide. n=1 per peptide concentrate, one of two experiments is represented.

3.7.3 In Aire-GCL^{lo} mice, mTEC performs an essential role in mediating central CD4^{+} T-cell tolerance

Next, thymocyte development in Aire-GCL^{lo} × *DEP* TCR-*tg* double transgenic mice was analyzed. Irrespective of the considerable differences on antigen expression level between Aire-GCL^{lo} and Aire-GCL lines, a similar extent of negative selection was observed in Figure 10a and 10b. Then the role of Aire-GCL^{lo} mTECs to mediate negative selection in BM chimeras (*DEP*→ Aire-GCL^{lo} and *DEP*×ΔDC→ Aire-GCL^{lo}) was examined. Negative selection occurred no matter DCs were present or not, indicating direct presentation by Aire-GCL^{lo} mTECs is efficient to mediate CD4 T-cell deletion (Figure 10c-e). To further assess the role autophagy plays on Aire-GCL^{lo} mTECs to mediate central CD4^{+} T-cell tolerance, thymus chimeras that impeded on autophagy were generated. T-cell deletion was not affected in transplanted grafts with GCL expressing and Atg5 sufficient. In contrast, T-cell deletion was completely abolished in transplanted Aire-GCL^{lo}-expressing lobes with Atg5 deficiency, showing the total *DEP* thymocytes were rescued from negative selection (Figure 11a and 11b). Taken together, these results demonstrate autophagy-dependent endogenous loading on mTECs plays a crucial role for central CD4 T-cell tolerance under an antigen limiting condition.

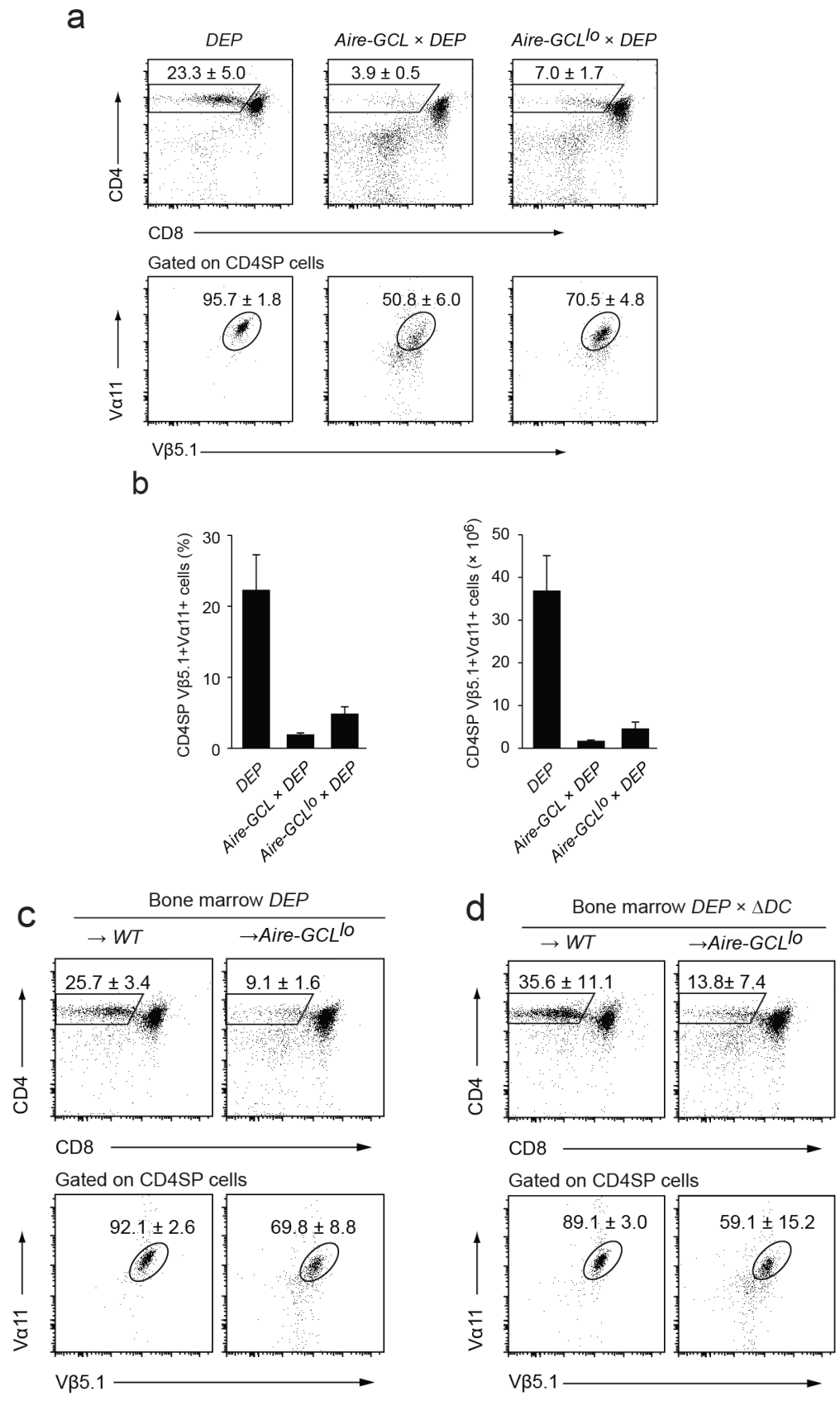
a
DEP
Aire-GCL × DEP
Aire-GCLlo × DEP
23.3 ± 5.0
3.9 ± 0.5
7.0 ± 1.7
CD4
CD8
Gated on CD4SP cells
95.7 ± 1.8
50.8 ± 6.0
70.5 ± 4.8
Vα11
Vβ5.1
b
CD4SP Vβ5.1+Vα11+ cells (%)
CD4SP Vβ5.1+Vα11+ cells (× 10^6)
DEP
Aire-GCL × DEP
Aire-GCLlo × DEP
c
Bone marrow DEP
→ WT
→Aire-GCLlo
25.7 ± 3.4
9.1 ± 1.6
92.1 ± 2.6
69.8 ± 8.8
d
Bone marrow DEP × ΔDC
35.6 ± 11.1
13.8± 7.4
89.1 ± 3.0
59.1 ± 15.2

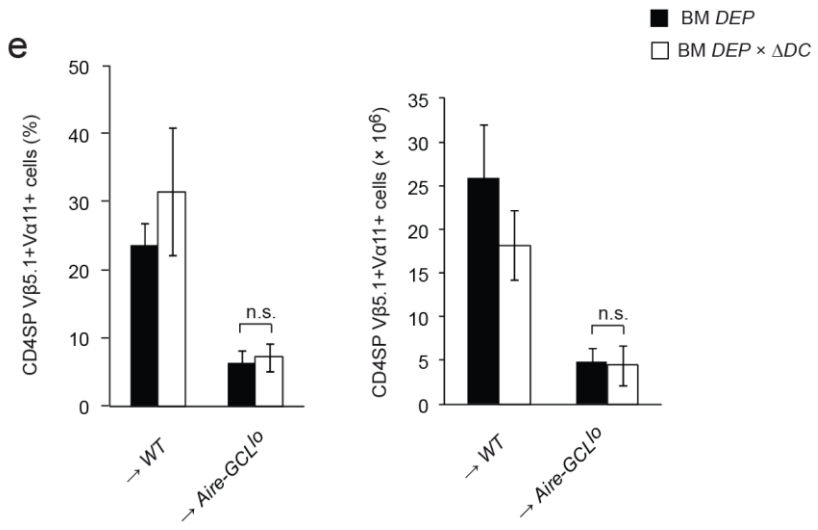

Figure 10. Thymocyte development in Aire-GCL^{lo} × *DEP* TCR-tg double transgenic mice and reconstituted BM chimeras. (a) Negative selection in Aire-GCL^{lo} × *DEP* TCR-tg double transgenic mice. Thymi of 4 to 5-week-old *DEP* single transgenic mice, Aire-GCL×*DEP* and Aire-GCL^{lo}×*DEP* double transgenic mice were analyzed by FACS. Numbers in the dot plots indicate the average frequency ((± stdev) of CD4 SP T-cells (upper row) and of DEP-TCR^{+} cells (Vα11^{+}Vβ5.1^{+}) among gated CD4 SP thymocytes (lower row). (b) Summary of the frequencies and absolute numbers of CD4 SP Vα11^{+}Vβ5.1^{+} cells among total thymocytes in (a). Data in (a) and (b) are from at least 8 mice per group. (c) Analysis of CD4^{+} T-cell development in 4-5 weeks reconstituted bone marrow chimeras in which *DEP* bone marrow were transferred into irradiated Aire-GCL^{lo} or WT recipients. The average frequency of CD4 SP T-cells are shown (± stdev) in upper row and of *DEP*-TCR^{+} cells (Vα11^{+}Vβ5.1^{+}) among gated CD4 SP thymocytes are depicted (± stdev) in lower row. Values are representative of at least 7 chimeras per group. (d) Analysis of CD4^{+} T-cell development in *DEP*×ΔDC bone marrow chimeras. WT or Aire-GCL^{lo} recipients were reconstituted with *DEP*×ΔDC bone marrow and chimeric animals were assessed 4-5 weeks later. Numbers indicate the average frequency of CD4 SP T-cells are shown (± stdev) in upper row and of *DEP*-TCR^{+} cells (Vα11^{+}Vβ5.1^{+}) among gated CD4 SP thymocytes are depicted (± stdev) in lower row. Values are representative of at least 11 chimeras per group. (e) Summary of the frequencies and absolute numbers of CD4 SP Vα11^{+}Vβ5.1^{+} cells among total thymocytes in (c) and (d). (n.s.= not significant.)

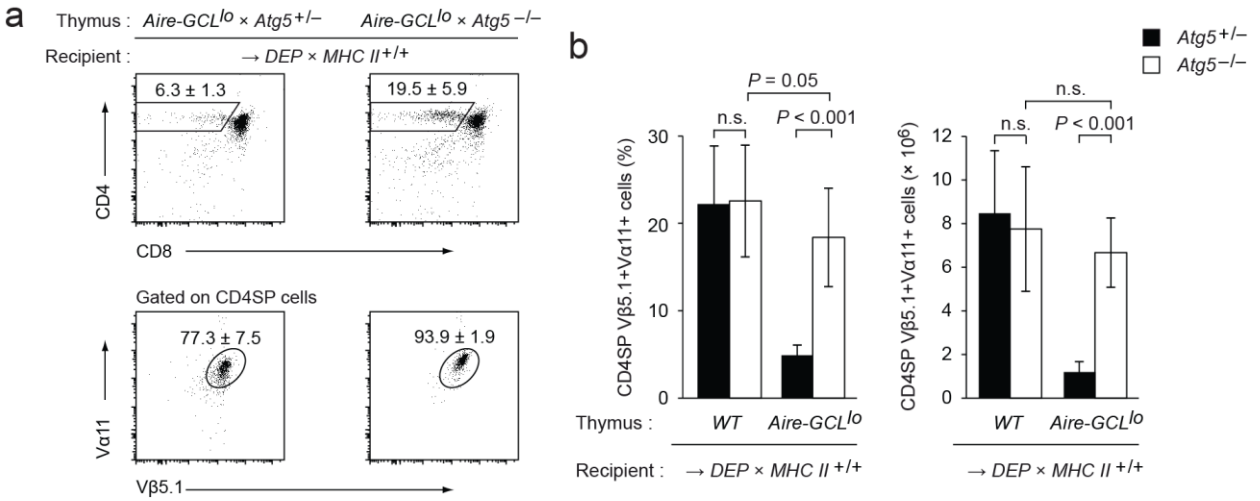

Figure 11. At limiting antigen expression in Aire-GCL^{lo} mice, autophagy-dependent direct presentation by mTECs plays an essential role in central CD4^{+} T-cell tolerance induction. (a) Escape of negative selection on *DEP* T-cells in transplanted Aire-GCL^{lo} lobes upon interference with autophagy in TECs despite in the presence of 'cross presentation-competent' DCs. Plots depict CD4^{+} and *DEP*-TCR^{+} staining of thymocytes from Atg5$^{+/-}$ or Atg5$^{-/-}$ thymi lobes transplanted into *DEP*×*MHC II*$^{+/+}$ recipients measured after 4-6 weeks reconstitution. The average frequency of CD4 SP T-cells are shown (± stdev) in upper row and of DEP-TCR^{+} cells (Vα11^{+}Vβ5.1^{+}) among gated CD4 SP thymocytes are depicted (± stdev) in lower row. Values are representative of at least 17 chimeras in each group. (b) Frequencies and absolute numbers of CD4 SP Vα11^{+}Vβ5.1^{+} cells among total thymocytes in (a) as compared to WT Atg5$^{+/-}$ (n=19)or Atg5$^{-/-}$ (n=20)thymic lobes. (*P* values are indicated; n.s.= not significant.)

4. Discussion

Immunologists have focused on the topic of mTECs since the discovery of the autoimmune regulator Aire and its link to the promiscuous gene expression of tissue-restricted antigens (TRAs) in mTECs[157]. The mTEC subset is relatively short lived and rapidly replaced[76]. TRAs expressed by mTECs can be efficiently transferred to DCs for antigen presentation, which highlights the role of mTEC as antigen reservoir in eliminating autoreactive thymocytes and preventing organ-specific autoimmunity[84, 235]. As TEC is the only non-hematopoietic cell that constitutively expresses high levels of MHC II, the recognition of MHC class II/peptides on mTECs contributes to the removal (*negative selection*) or deviation (*Treg induction*) of autoreactive CD4 T-cells[228].

There is a growing number of studies demonstrating that mTECs mediate central CD4 T-cell tolerance through direct presentation of endogenously expressed self-antigens[105, 231, 232]. The most direct evidence supporting the autonomous capacity of mTECs in CD4 T-cell tolerance came from the study by Hinterberger *et al*, in which a C2TA-specific short hairpin RNA (shRNA) was designed to knock down 90% of MHC class II expression on mTECs and the diminished MHC class II expression led to the impaired negative selection of CD4 polyclonal and TCR-specific thymocytes along with the defective Treg generation[230]. As TECs display a poor efficiency in capturing and processing extracellular antigens, other intracellular processing pathways for MHC class II-associated antigens presentation in mTECs are proposed to contribute to mediate central CD4 T-cell tolerance.

Macroautophagy, a bulk protein degradation process that delivers cytoplasmic components into lysosomal compartments, has been implicated to shuttle intracellular materials into the MHC class II[167, 189]. Previous results from our lab showed that interference with autophagy in TECs led to an altered selection of certain MHC II-restricted T cell specificities and resulted in multi-organ inflammatory infiltration[228]. However, it remains unclear whether a breakdown of CD4 T-cell central tolerance is caused by a defective clonal deletion and/or an impaired Treg deviation mediated by autophagy-deficient mTECs or homeostatic expansion of autoreactive T-cells due to

impaired positive selection induced by interfering with autophagy on cTECs. We addressed this issue by generating a transgenic mouse which expressed a model antigen specifically targeted to autophagosome in Aire^{+} mTECs and evaluating the efficiency of autophagy pathway on intracellular antigen shuttling to MIIC in mTECs. Based on this, its contribution on mTECs for central CD4 T-cell tolerance was investigated.

4.1 Autophagy pathway required for antigen processing to mediate endogenous antigen presentation by mTECs

Since being discovered, autophagy has been regarded as a non-selective bulk degradation process. During the initial formation of autophagosome, the isolated membrane indiscriminately engulfs cytoplasmic materials, then elongates and further fuses with lysosomes to degrade the sequestered content[236, 237]. However, autophagosomes can also degrade substrates in a selective manner[238]. Unlike non-selective autophagy, selective autophagy contains little bulk cytosol between the cargo and the vesicle inner membrane[239, 240]. In mammals, there are two well characterized examples of selective autophagy: aggregate-prone proteins[241] and bacteria-containing autophagosomes[242]. A polyubiquitin-binding protein p62 (SQSTM1) selectively recognizes and links polyubiquitinated proteins with LC3 for further recruiting them to autophagosomes[220].

LC3, a mammalian homologue of Atg8, is an essential lipid-anchored protein on the surface of preautophagosomal and autophagosomal membranes[201, 243]. Its incorporation into autophagosomes can be monitored in autophagy reporter (GFP-LC3) mice[193]. In MHC class II positive APCs, autophagosomes were found to be continuously fusing with multivesicular MIIC. More importantly, by fusion of an antigen to autophagosome-associated LC3 protein, MHC class II presentation of this antigen increased by 20-fold[189] which implicates this specific antigen-targeting to autophagosomes can deliver antigens into MHC class II loading route. That is because as the degradation of LC3 in the inner autophagosomal membrane occurs, the fused antigen will be also degraded, which provides an opportunity to make the degraded peptides bound with MHC class II molecules for antigen presentation. On the basis of this, the tripartite hybrid protein,

GCL was generated. Meanwhile, another construct, GCL_{G120A} was generated and expressed as a cytosolic antigen. Due to the mutation from Gly to Ala in LC3 protein of GCL_{G120A}, it makes the cleavage at the C-terminal region of proLC3 unavailable, thus abolishes the conjugation of LC3 to autophagosomal membrane[201]. This abolishment results in the expressed hCRP protein cannot be targeted into autophagosome. Our results are consistent with these descriptions presented above. In our study, under nutrient deprivation, GFP^+ punctae could be observed in HEK 293T cells that expressed GCL-vector, in contrast, no segregation of GFP dots were detected in GCL_{G120A}-expressing HEK 293T cells.

To investigate whether autophagosome-targeting facilitates antigens to be shuttled into mTEC-mediated endogenous MHC class II loading, we generated Aire-GCL and Aire-GCL_{G120A} mice, in which two closely related variants were expressed in a comparable level in mTECs. Analysis of T hybridoma cells activation revealed that contrary to GCL_{G120A}, the GCL variant (as an autophagy substrate), was directly presented by mTECs and was quantifiable. This observation is in agreement with report described that autophagosome-targeting antigen preferentially gained access to MIIC for endogenous antigen presentation[189]. As follows, negative selection on Aire-GCL×*DEP* and Aire-GCL_{G120A}×*DEP* double transgenic mice was compared. A similar extent of negative selection occurred, exhibiting a severe decrease in the total numbers of *DEP* $CD4^+$ thymocytes as well as Treg. Although more Treg differentiation was not found in our experiment, there is convincing evidence given that induction of Treg can be mediated by both mTECs[105, 230] and DCs[71] in some TCR transgenic models.

Since the experiment described above did not observe more favorable T-cell deletion in Aire-GCL×*DEP* mice, in order to better understand the role of mTEC played on negative selection, different BM chimeras were designed to remove DCs from the system. Analysis of the BM chimeras (*DEP*×ΔDC→Aire-GCL) showed the presence of mTEC-mediated direct presentation alone is sufficient to induce robust *DEP* TCR-specific $CD4^+$ T-cell deletion. Furthermore, to investigate whether direct presentation depends on autophagy in Aire-GCL line, a system with interference of autophagy pathway on mTECs was introduced. Analysis of the grafted Aire-GCL×$Atg5^{+/-}$ or Aire-GCL×$Atg5^{-/-}$

lobes in *DEP*×MHC II$^{-/-}$ recipients showed that autoreactive *DEP* CD4^{+} T-cells rescued from clonal deletion as a disrupted Atg5 gene was introduced into mTECs, along with the results from *in vitro* assay showed that direct presentation by Aire-GCL mTECs was completely eliminated by interfering with autophagy. These findings strongly support our hypothesis that autophagy pathway participates in central CD4 T-cell tolerance by facilitating direct presentation of endogenous self-antigens in mTECs.

However, this CD4 T-cell clonal deletion induced by mTEC-mediated direct presentation seems not always to depend on autophagy pathway. The study by Aichinger, M. in the *ePCC/mPCC* system[244] suggested different subcellular distributions of self-antigens might require distinct pathways to gain access to MHC class II in mTECs for negative selection. In this system, pigeon cytochrome C (PCC) antigen is expressed in its native form as a mitochondrial neo-self-antigen in *ePCC*; while PCC antigen is expressed as a membrance protein on the cell surface in *mPCC* via addition of a membrane anchor[245]. At first, efficient negative selection of *AND* CD4 T-cells was not interfered in grafted ePCC- or mPCC-expressing lobes with elimination of antigen presentation capacity of DCs. It suggested both forms of PCC could be presented directly and efficiently by mTECs and further induced *AND* CD4 T-cell deletion. Furthermore, the role of autophagy on TECs for negative selection was analyzed in the *AND*-Tg×CIITA$^{-/-}$ recipients grafted with ePCC×Atg5$^{-/-}$ or mPCC×Atg5$^{-/-}$ lobes. The direct presentation of ePCC, but not of mPCC, was abolished due to the interference of autophagy in TECs. It has been reported that cell organelles, such as mitochondria, can be selectively recruited to autophagosomes by anchoring to the inner autophagosomal membrane. With fusion of lysosome/late endosome, autophagosome with its contents are degraded. Thus, this process provides a feasible pathway for mitochondrial ePCC to be shuttled into MHC class II loading pathway (pathway (a) in Graphic 6). In contrast, as a membrane antigen, direct presentation of mPCC by mTECs is independent on autophagy. It is probably because a portion of the plasma membrane along with molecules coming from the cell surface is pinched off during the typical process of endocytosis, and these engulfed molecules may include certain newly synthesized, cell surface-residing membrane proteins (such as mPCC mentioned here). And then these

contents enter the cytosol as the form of endocytic vesicles. After internalized as early endosomes and further matured into late endosomes, the vesicles are delivered to the lysosome lumen as well as their sequestered molecules. It makes these membrane proteins finally gain access to the MHC class II antigen presentation pathway via endocytosis (pathway (b) in Graphic 6), and importantly, this process does not require autophagy. The study by Dengjel et, al. provided direct evidence to support the existence of distinct pathways in mediating MHC class II presentation for organelle-derived versus membrane-bound antigens[167]. The presentation of intracellular-derived antigens, including organelles, was significantly increased in a cultured B cell line upon induction of autophagy, whereas the presentation of membrance-bound proteins was barely affected.

4.2 The contribution of mTECs versus DCs for central $CD4^+$ T-cell tolerance upon a certain threshold of antigen abundance

Previous studies have reported the expression of Aire in DCs[246] and we reproduced this observation of a low expression level of Aire gene in DCs. Therefore, it is crucial to understand the contribution of DC as antigen reservoir to induce negative selection. In BM chimeric mice (Aire-GCL×*DEP*→WT), in which only the hematopoietic cells could potentially express hCRP antigen, no deletion of *DEP* TCR-specific $CD4^+$ T-cells was observed (personal communication with Tomoyoshi, Y.), which excluded the possibility of DC as the only source of antigen providing to mediate negative selection. In contrast, BM chimeras (*DEP*→Aire-GCL or *DEP*→Aire-GCL_{G120A}) recapitulated the phenotype of double transgenic mice described above; most of *DEP* TCR-specific thymocytes were deleted, which indicates the expression of antigen exclusively in thymic epithelium is sufficient to induce negative selection.

Two mechanisms account for mediating this remarkable deletion of antigen-specific $CD4^+$ T-cells described above. One is the direct presentation mediated by mTECs, and the other one is the indirect pathway via DC. However, the contribution of thymic epithelial versus hematopoietic cell on negative selection is still controversial. Based on existing experimental evidence, we propose at least two parameters governing the requirement for direct pathway via mTECs and/or DC-mediated cross-presentation to

induce central tolerance. One is the subcellular localization of antigen, and the other is the antigen dose.

Antigens displayed by mTECs seem to preferentially reflect the intracellular milieu of this cell type. We suggest that this pool comprises a variety of membrane-associated self-antigens (for instance, membrane proteins from *mPCC* and RIP-mOVA system) as well as autophagy substrates (cellular organelles, such as mitochondria or the nucleus). In contrast, antigen presentation by hematopoietic APCs in the thymus, especially DCs, appears to be optimized to include secretory self-antigens, such as mTEC-derived soluble self-antigens in RIP-OVA^{hi} system (pathway (c) in Graphic 6). These newly synthesized self-antigens may release into the extracellular space and then are endocytosed, processing and presented by neighboring tDCs. The most direct evidence came from the observation that OT-II thymocytes were significantly deleted when mTEC were the only APC in BM chimeras (OT-II MHC II$^{-/-}$→RIP-mOVA) compared with WT control (OT-II MHC II$^{-/-}$→WT); whereas in BM chimeras (OT-II MHC II$^{-/-}$→RIP-OVA^{hi}), those OT-II CD4^{+} T-cells rescued from negative selection in the absence of hematopoietic APCs compared to WT control (OT-II MHC II$^{-/-}$→WT)[231]. However, to some origins of self-antigen, the issue requiring for tolerance induction mediated by antigen transferring and presentation via DCs is still not fully understood. It remains unclear why negative selection in Aire-GCL$_{G120A}$ at least in part depends on cross presentation via DCs (pathway (c) and/or (d) in Graphic 6). The possible explanation is that antigen in GCL$_{G120A}$ seems not to be preferentially targeted for mTEC-mediated direct presentation, which consists with the finding that MP1 specific CD4^{+} T-cell recognition of MP1-LC3($_{G120A}$) was even weaker than that of MP1-LC3[189]. Moreover, In *in vitro and in vivo* assay, it had demonstrated that intercellular materials could be constitutively, unidirectional transferred from epithelial cells towards DCs[121, 122]. A mature phenotype of thymic DCs harboring the capacity to acquire TEC-derived cytoplasmic proteins and to mediate the most efficient cross presentation was indentified[122]. Thus, in Aire-GCL$_{G120A}$, DC-mediated cross presentation might be the major mode to induce efficient CD4^{+} T-cells deletion. Additionally, mTEC-mediated autonomous presentation is also involved to mediate negative selection, even though

the direct presentation via mTECs is not autophagy-dependent, which was confirmed by our observation in Figure 5c and Supplementary Figure 5, separately.

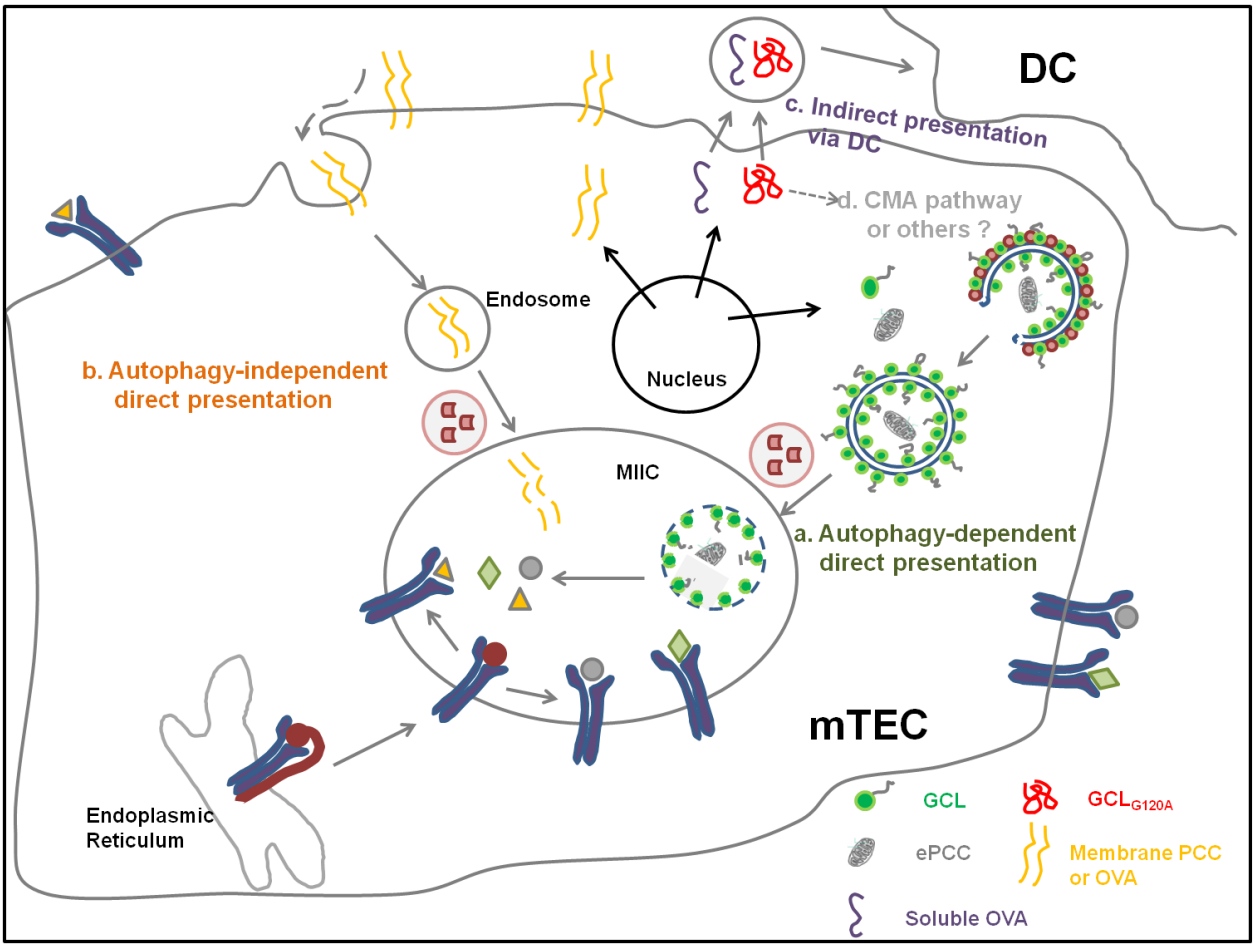

Graphic 6. The different subcellular localizations of mTEC-derived antigen require distinct MHC class II antigen presentation pathways. (a) Autophagy-dependent mTEC-mediated direct presentation: autophagy substrates (such as mitochondrial ePCC and autophagosomal targeting GCL) are specifically targeted into autophagosomes. After fusing with late endosomal/lysosomal compartment, autophagy substrates are degraded in MIIC; the resulting peptides bind to MHC class II ligands and then transport to the cell surface for presentation. (b) Autophagy-independent direct presentation via mTECs: mTEC-expressed membrane proteins (like mPCC and mOVA) on the cell surface can be endocytosed to early endosomes. After fusing with lysosomes, antigens are degraded and gain access to MHC class II loading pathway of mTECs. (c) DC-mediated cross-presentation: mTEC-derived soluble antigens (like OVA) and cytoplasmic antigens (like GCL$_{G120A}$) can be uptaken, and subsequently

processed by tDCs for presentation on their MHC class II molecules. (d) Cytoplasmic hCRP antigen in GCL_{G120A} may take other pathways (such as CMA) to mediate direct presentation by mTECs.

Moreover, the amount of antigen expressed in mTECs is likely to be a driving force to influence the contribution of direct pathway mediated by mTECs and indirect pathway mediated by DCs, which further to determine the fate of $CD4^+$ T-cells. In our findings, we observed efficient *DEP* $CD4^+$ T-cell deletion in Aire-GCL×*DEP* double transgenic lines even though the expressing transgene varied among lines. Furthermore, negative selection of *DEP* TCR-specific T-cells was barely impaired in a series of bone marrow or thymus chimeras which antigen presentation by mTECs or DCs was eliminated in the Aire-GCL line. Conceivably, a certain degree of redundancy function of DCs participates in inducing a robust $CD4^+$ T-cell negative selection in this system. However, by analyzing negative selection induction in the Aire-GCL^{lo} system, it reveals that autophagy-dependent mode is essential to induce mTEC-mediated direct presentation. The role of DCs played on antigen presentation for central tolerance is excluded in the lower transgene expressing system. Comparing to Aire-GCL line, mTECs in this Aire-GCL^{lo} system perform a 4-fold fewer mRNA expression for transgene, consequentially elicit 3-fold weaker *DEP* T hybridoma stimulation capacity. Collectively, we hypothesize a certain threshold of antigen abundance might exist in influencing the contribution of mTECs versus DCs for central CD4 T-cell tolerance. That is, when the amount of an endogenously expressed antigen by mTECs is above this threshold, the extra antigen can be transferred to neighboring DC, which leads cross-presentation mediated by DCs for negative selection; otherwise the establishment of negative selection will solely depend on mTECs via an endogenous MHC class II loading pathway.

4.3 Concluding remarks and future perspectives

Direct antigen presentation mediated by mTECs and indirect pathway via DC-mediated presentation of mTEC-derived antigen are proposed to mediate central $CD4^+$ T-cell tolerance. It has become apparently that mTECs and DCs differ in their capacity to process antigens, which results in a largely non-overlapping self-antigen pool being

sampled and presented for T-cell development. However, the pathways involved in mediating mTECs to present the intracellular milieu onto their MHC class II ligands are still not fully defined. Growing evidence indicate that autophagy can operate as a potential pathway for MHC class II endogenous antigen presentation by TECs. In that way, it contributes to the composition of MHC class II-bound peptides on cTECs, and further regulates thymocytes developing during positive selection. Here we present evidence that autophagy on mTECs contributes to induce negative selection of thymic $CD4^+$ T-cell and is essential for the generation of a self-tolerant T-cell repertoire.

Taken together, a model has been proposed here to illustrate the contribution of autophagy-dependent endogenous presentation by mTECs and cross-presentation by DCs for $CD4^+$ T-cell tolerance in the case of available amount of antigen provided by mTECs as a determinant (see Graphic 7). It implicates the patterns of how TRAs expressed by $Aire^+$ mTECs might be presented to mediate central $CD4^+$ T-cell tolerance. However, whether one of the two Aire-GCL systems could represent to expression of physiological self-antigens in mTECs still needs further investigations. Besides the study on its function in thymic T-cell education, further studies will be conducted on the issue whether autophagy may also participate in the establishment of peripheral tolerance to $CD4^+$ T-cells.

In our study, we focused on the role of autophagy on mTECs for central $CD4^+$ T-cell tolerance. However, other alternative pathways might operate in the thymic epithelial and/or DCs and are further involved in mediating MHC class II antigen loading. CMA is an interesting candidate. It promotes endogenous antigens to be presented onto MHC class II ligands of professional APCs during function assays[177]. However, because of the involvement of LAMP-2A and Hsc70 in many basic cellular processes, the genetic manipulation to investigate the contribution of CMA on MHC class II loading is hard to achieve. In LAMP-2-knockout mice, the issue of CMA contributing to MHC class II loading became complex due to the absence of all three isoforms of the LAMP-2 protein (LAMP-2A, B and C)[247]. Therefore, generation of miRNA transgenic mice specific for LAMP-2A might be a possible approach. Furthermore, it is found that CMA and autophagy are functionally compensable for each other. Blockage of CMA via RNA

interference against LAMP-2A could result in a constitutive autophagy activity and vice versa[248, 249]. Thus, the question on what mediates the crosstalk between CMA and autophagy pathway also needs to be solved. Additionally, the mechanism of other endogenous loading pathways, including microautophagy and the TAP-dependent pathway, remains to be elucidated.

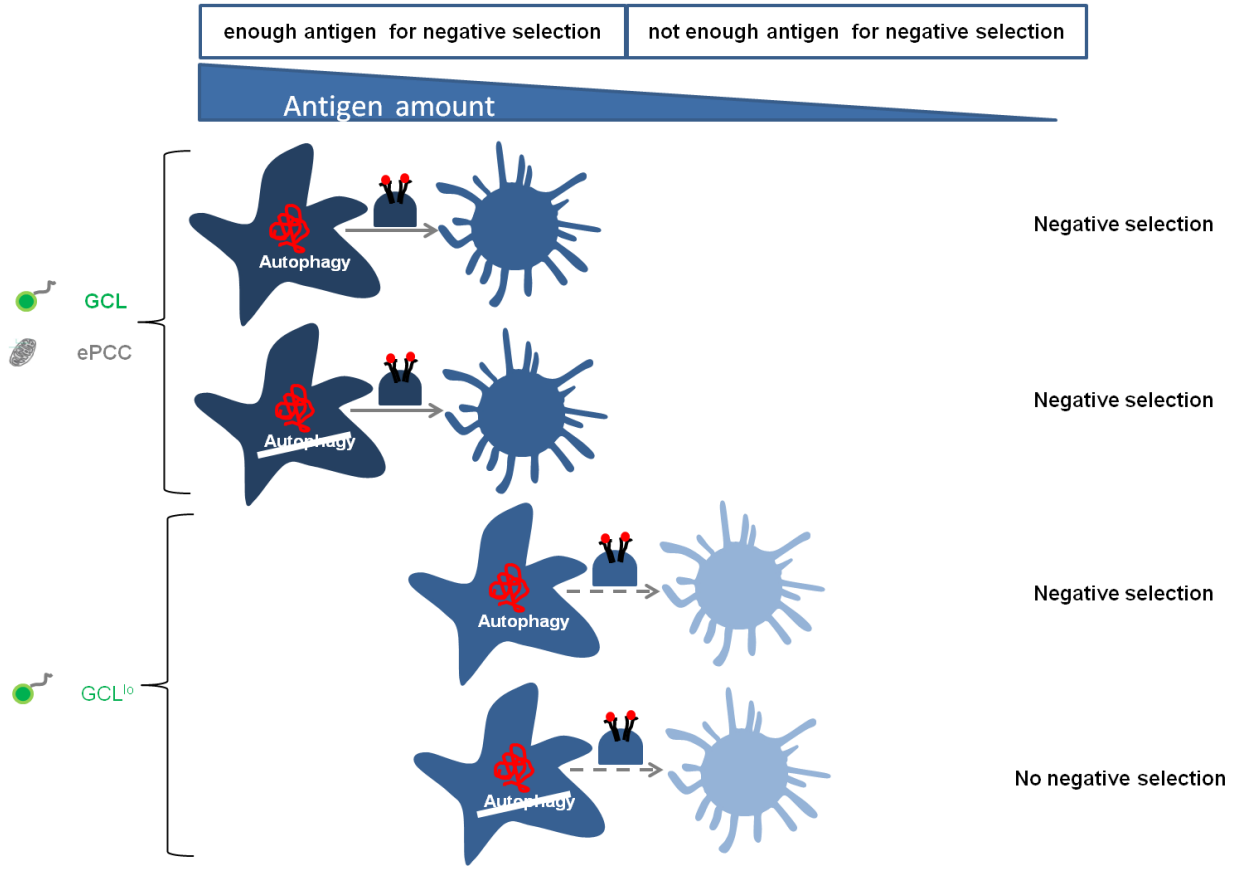

Graphic 7. The proposed model for intracellular mTEC-derived antigen transferring and its consequences on negative selection to CD4$^+$ T-cells. Endogenous presentation by mTECs and cross-presentation by DCs co-operate to mediate CD4$^+$ T-cell tolerance with sufficient antigen provided by mTECs (Aire-GCL and ePCC system) in one side, however, both pathways perform in a redundant manner. When mTEC-mediated direct presentation is abolished via interference of autophagy-related genes, DCs uptake those spreading antigens to drive the negative selection process due to the existence of antigen transferring. In the other side, when antigen expressed by mTECs is in a limiting dose (Aire-GCL^{lo} system), not enough antigen can be transferred to DCs, the role of DCs in negative selection will be completely replaced by direct presentation of endogenous self antigens by mTECs, and autophagy on mTECs will facilitate this endogenous MHC class II loading route.

Supplementary Figure 1

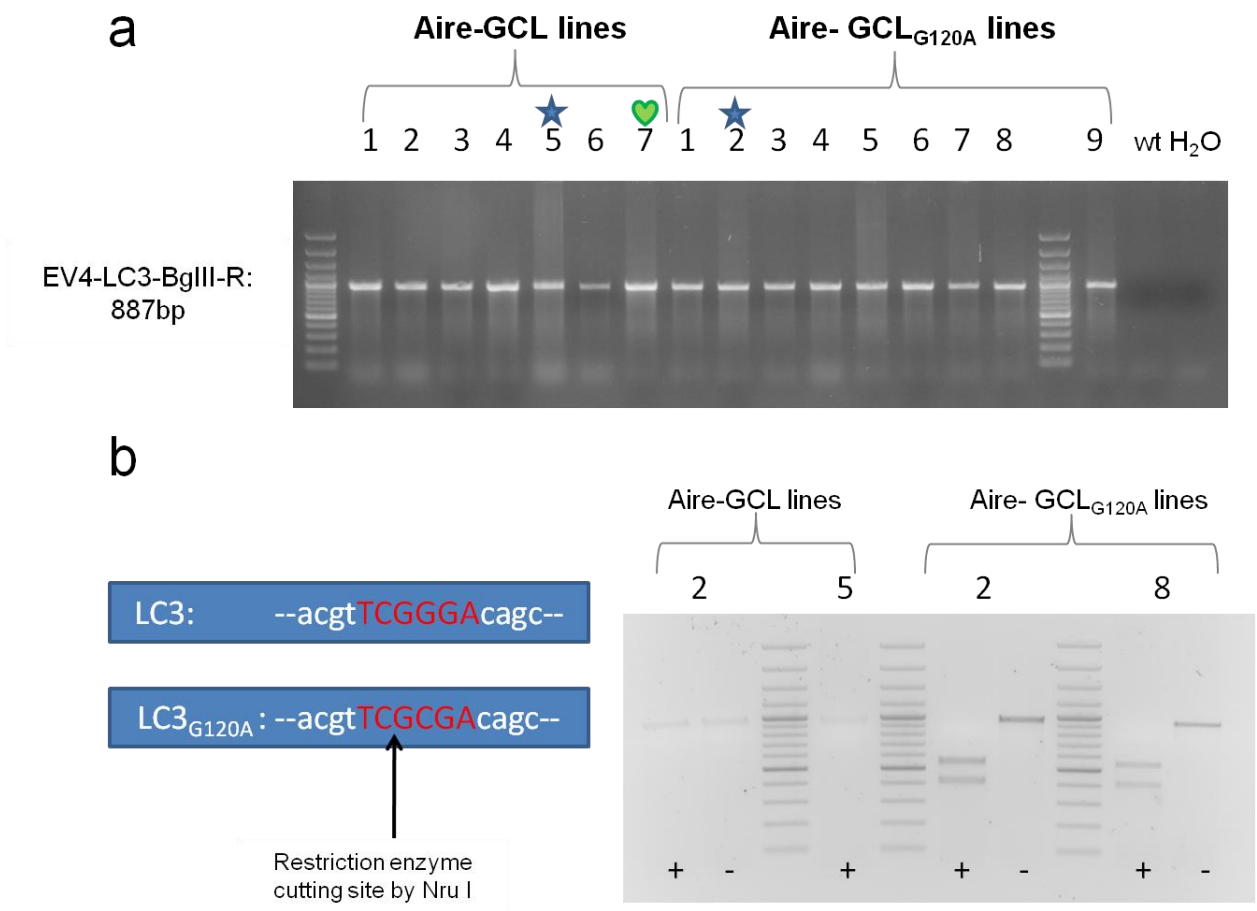

Figure S1. A point mutation of GCL$_{G120A}$ can be distinguished by recognition of the restriction enzyme cutting site. (a) PCR genotyping to founder lines using EV4 and LC3-BglII-R primers. Note: No.5 (star) and No.7 (heart) from Aire-GCL founders are referred to as Aire-GCL and Aire-GCL^{lo} lines used in the whole experiment; and No.2 (star) from Aire-GCL$_{G120A}$ founders is referred to as Aire-GCL$_{G120A}$ line used in the research project. (b) Amplified PCR products from genomic DNA of Aire-GCL and Aire- GCL$_{G120A}$ were digested with or without Nru I.

Supplementary Figure 2

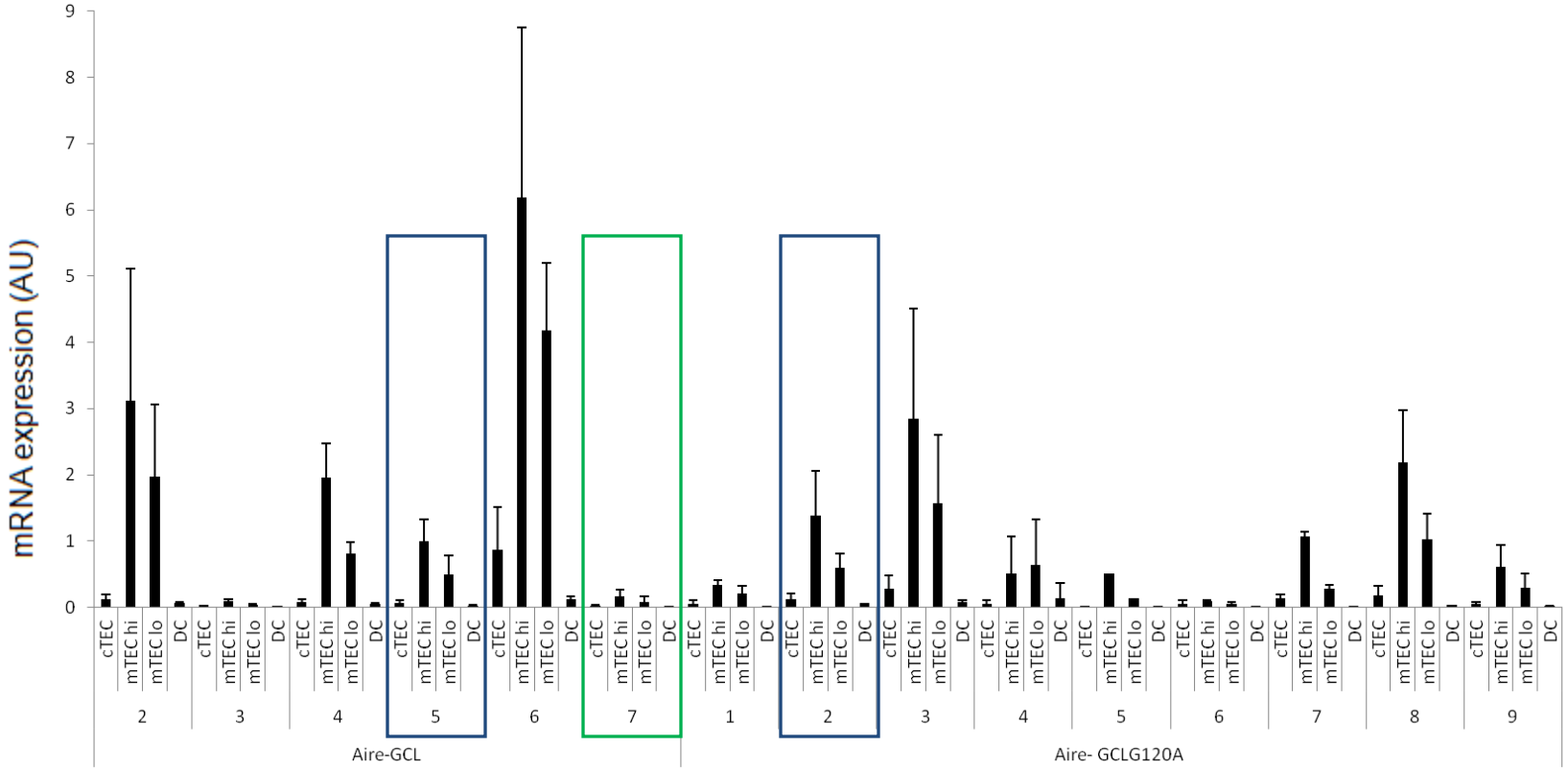

Figure S2. Quantitative analysis of transgenic mRNA expression in all transgenic founders. The graph showed the relative expression of transgenic mRNA in respective stromal cells from Aire-GCL and Aire- GCL_{G120A} transgenic mice. Values are normalized to expression in $mTEC^{hi}$ from Aire-GCL No.5 and indicated the mean±standard deviation from 3 independent biological replicates. Note: No.5 (with blue frame) and No.7 (with green frame) from Aire-GCL founders are referred to as Aire-GCL and Aire-GCL^{lo} lines used in the whole experiment; and No.2 (with blue frame) from Aire-GCL_{G120A} founders is referred to as Aire-GCL_{G120A} line used in the research project. (Data not include Aire-GCL No.1, and only 1 biological replicates from Aire- GCL_{G120A} No.5).

Supplementary Figure 3

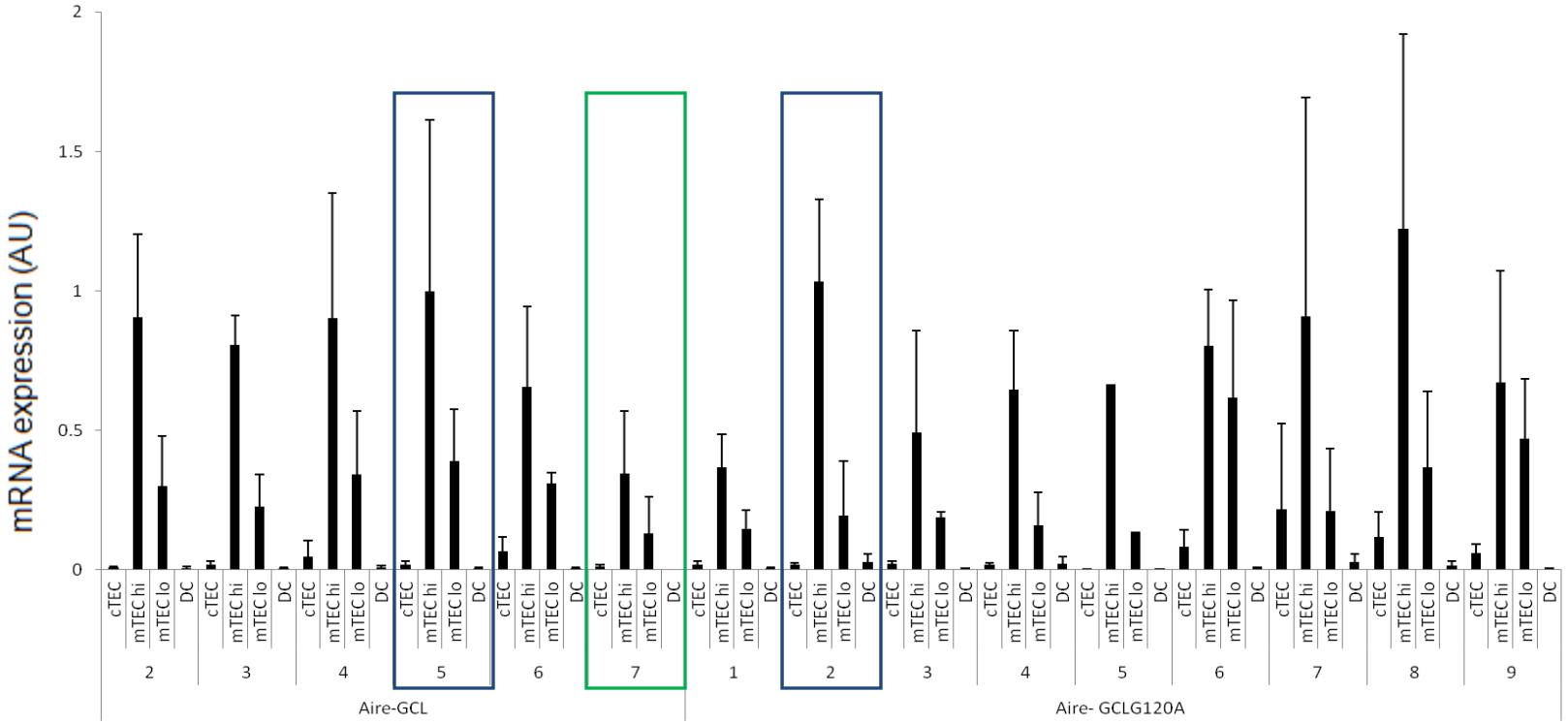

Figure S3. Quantitative analysis of Aire mRNA expression in all transgenic founders. The graph showed the relative expression of Aire mRNA in respective stromal cells from Aire-GCL and Aire- GCL_{G120A} transgenic mice. Values are normalized to expression in $mTEC^{hi}$ from Aire-GCL No.5 and indicated the mean±standard deviation from 3 independent biological replicates. No.5 (with blue frame) and No.7 (with green frame) from Aire-GCL founders are referred to as Aire-GCL and Aire-GCL^{lo} lines used in the whole experiment; and No.2 (with blue frame) from Aire-GCL_{G120A} founders is referred to as Aire-GCL_{G120A} line used in the research project. (Data not include Aire-GCL No.1, and only 1 biological replicates from Aire- GCL_{G120A} No.5).

Supplementary Figure 4a

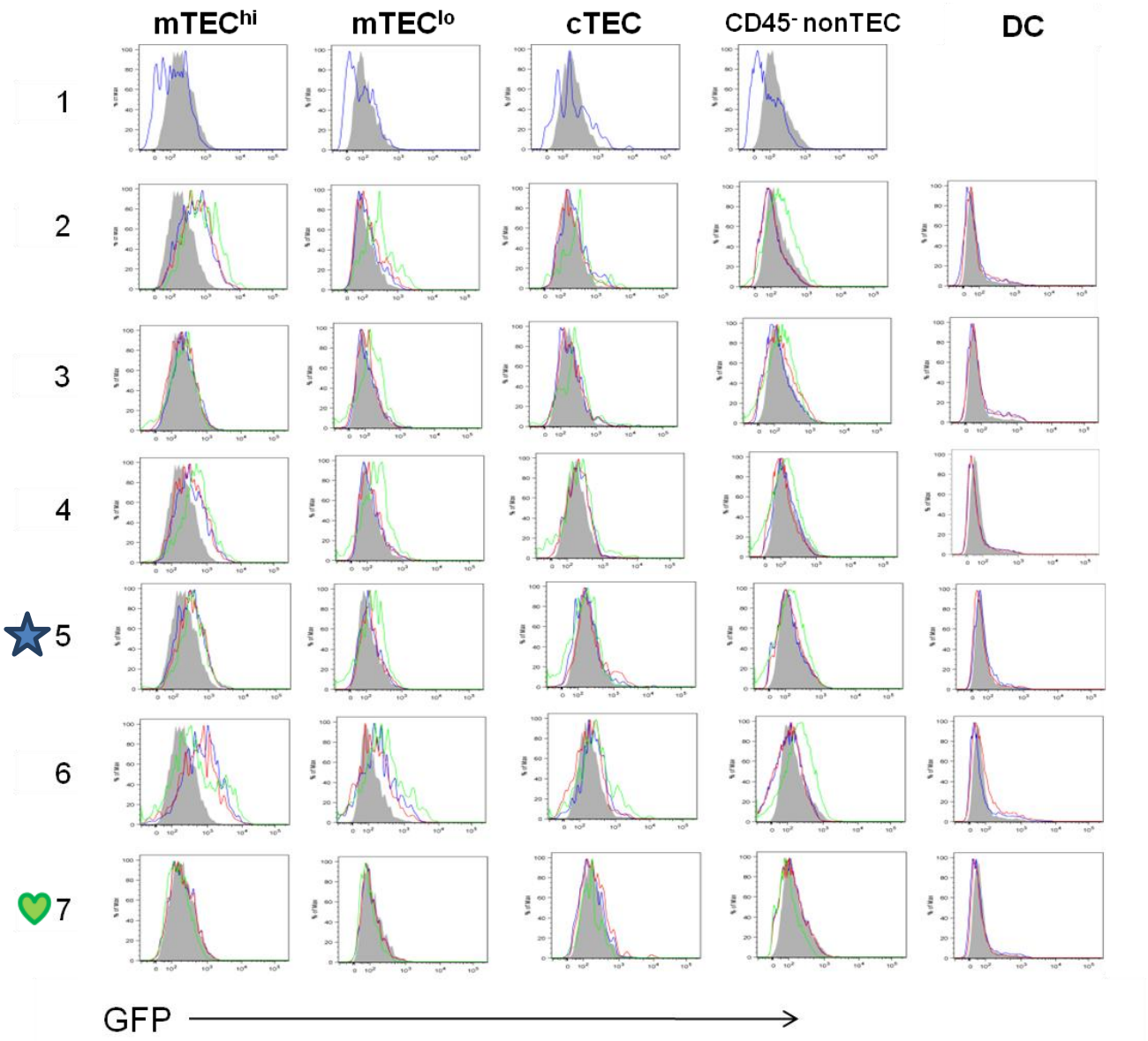

Figure S4a. Analysis of transgenic protein expression in all Aire-GCL mice. The graph showed the transgenic protein expression determined by FACS of respective stromal cells from Aire-GCL mice (blue, red, green) compared with WT mice (gray). Note: No.5 (star) and No.7 (heart) from Aire-GCL founders are referred to as Aire-GCL and Aire-GCL^{lo} lines used in the whole experiment. Data are representative of 2-3 independent experiments, each with 4 mice.

Supplementary Figure 4b

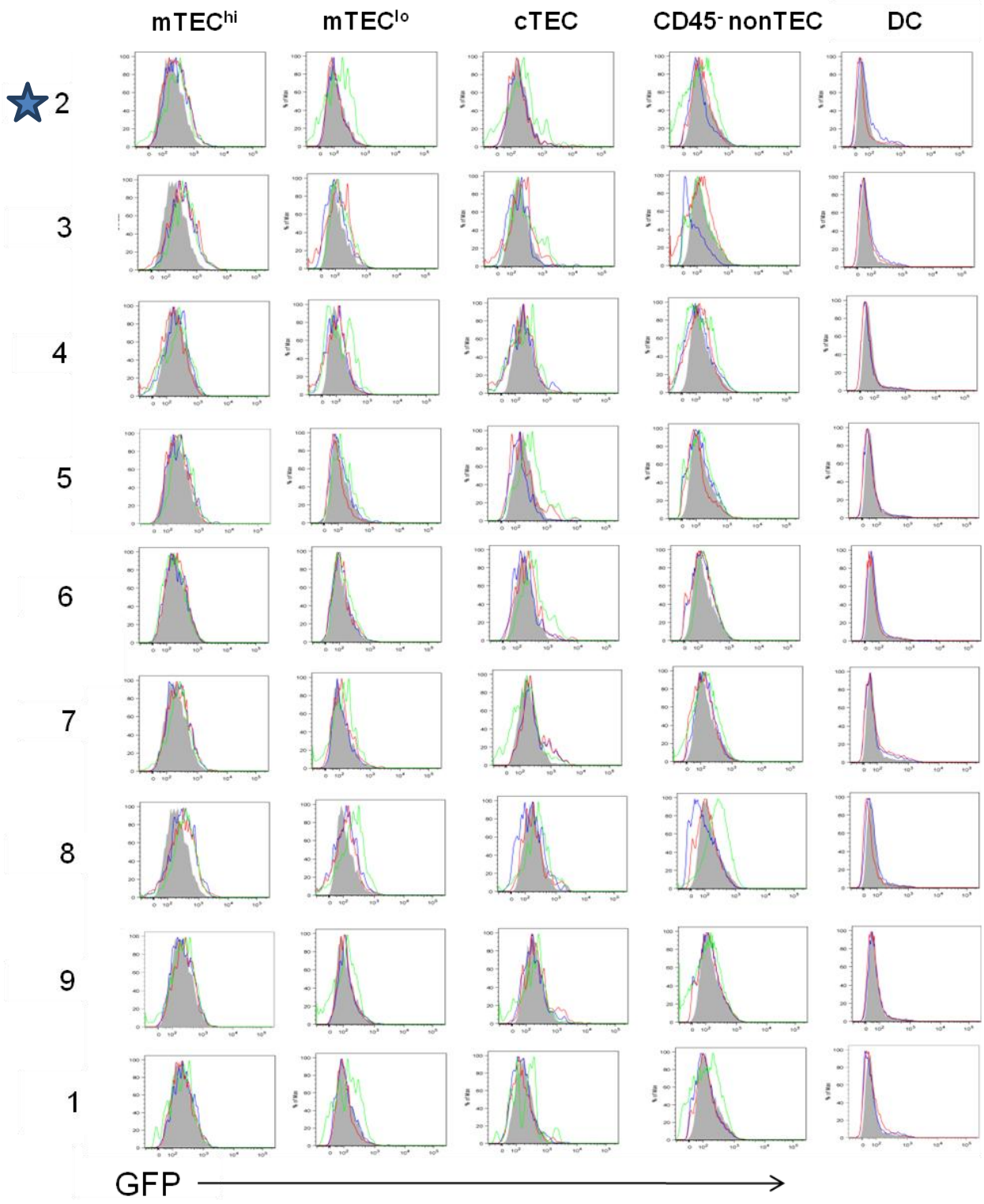

Figure S4b. Analysis of transgenic protein expression in all Aire-GCL$_{G120A}$ mice. The graph showed the transgenic protein expression determined by FACS of respective stromal cells from Aire-GCL$_{G120A}$ mice (blue, red, green) compared with WT mice (gray). No.2 (star) from Aire-GCL$_{G120A}$ founders is referred to as Aire-GCL$_{G120A}$ line used in the research project. Data are representative of 2-3 independent experiments, each with 4 mice.

Supplementary Figure 5

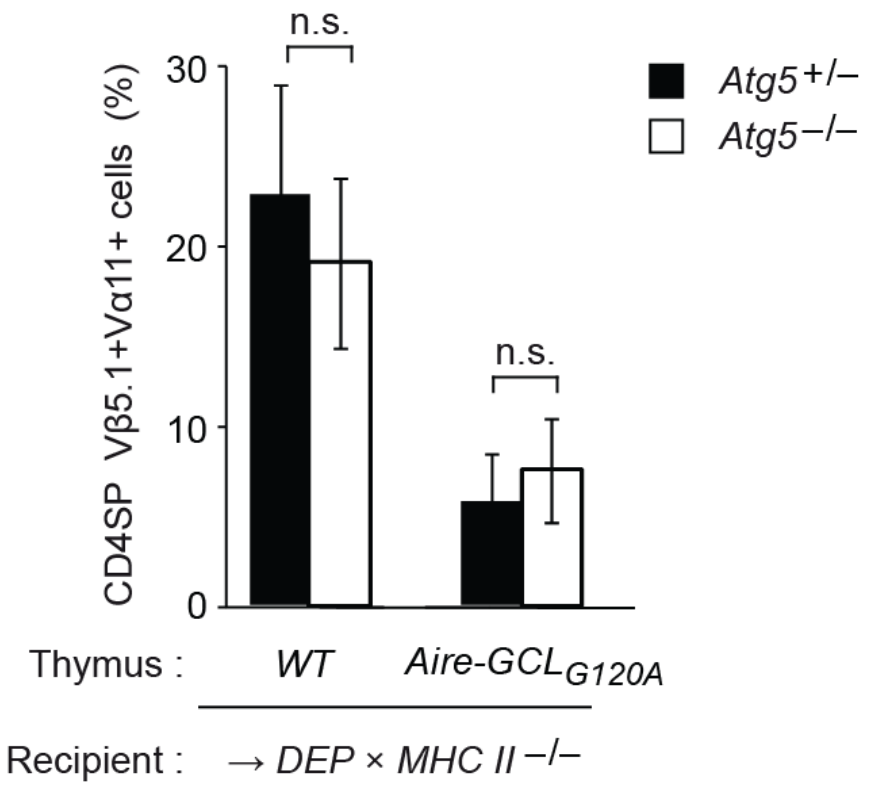

Figure S5. Negative selection mediated by direct antigen presentation by Aire-GCL$_{G120A}$ mTECs is autophagy-independent. Atg5$^{+/-}$ or Atg5$^{-/-}$ thymi lobes from indicated groups were transplanted into *DEP*×*MHC II*$^{-/-}$ recipients and CD4^{+} T-cell development was measured after 4-6 weeks reconstitution. Summary of the frequencies of CD4 SP Vα11+Vβ5.1+ cells among total thymocytes (P values are indicated; n.s.= not significant.). Data are representative of at least 10 chimeras in each group.

5. Materials and Methods

Mice

TCR-*DEP* [232], MHC class II$^{-/-}$ (H2-Ab1$^{-/-}$) [234], Atg5 $^{+/-}$ [206], ΔDC mice[233] has been described elsewhere. C57BL/6 mice were purchased from Charles River. All mice were breed in individually ventilated cages in the animal facility of the Institute for Immunology of the University of Munich, Germany. All animal studies were done according to the local regulations.

Antibodies and flow cytometry

Phycoerythrin (PE)-conjugated monoclonal antibodies (mAbs) to Vα11.1/11.2 (RR8-1), Ly51 (BP-1), Phycoerythrin-Cy7 (PE-Cy7)-conjugated streptavidin, Fluorescein isothiocyanate (FITC)-conjugated mAbs to Vβ5.1/5.2 (MR9-4) and Biotin-conjugated CD80 (16-10A1), CD4 (RM4-5), CD8a (53-6.7) were purchased from Becton Dickinson. PE-Cy7-conjugated mAbs to CD4 (GK1.5), CD11c (N418), Phycoerythrin-Cy5 (PE-Cy5)-conjugated mAbs to CD8a (53-6.7), CD45 (30-F11), Allophycocyanin (APC)-conjugated mAbs to I-A/I-E (M5/114.15.2), EpCAM (G8.8), Allophycocyanin-cy7 (APC-cy7)-conjugated mAbs to CD25 (PC61), EpCAM (G8.8) and Biotin-conjugated B220 (RA3-6B2) were purchased from BioLegend. Monoclonal Ab to MHC class II (P7.7) was purified from hybridoma supernatant and conjugated to Alexa Fluor 647 by using the Alexa Fluor 647 conjugation kit from Molecular Probes. 4', 6-Diamidin-2'-phenylindol-dihydrochlorid (DAPI) was purchased from Invitrogen. Surface staining of antibodies were performed according to standard procedures at a density of 1-2 x 10^6 per 50 µl and volumes were scaled up accordingly.

Intracellular staining of Foxp3 was performed according to the manufacturers' protocol by using APC-conjugated mAbs to Foxp3 (FJK-16s, eBioscience).

Flow-cytometric analyses were performed on a FACSCanto II (Becton Dickinson) using FACS DIVA (Becton Dickinson) for acquisition and FlowJo (Tree Star) for analysis.

Cloning of GCL or GCL_{G120A} BAC targeting construct

LC3 and $LC3_{G120A}$ cDNA were a kind gift from Prof. Noboru Mizushima.

In briefly, using designed primers to introduce the appropriate restriction sites, the following elements were amplified, subcloned and inserted into pBluescript vector backbone in the listed order (5' to 3'): β-glubin intron was subsequently clones as a HindIII/EcoRV fragment, that was PCR amplified from pSG5 construct using primers EV8 (CATGAAGCTTGATCGATCCTGAG) and EV9 (GTCAGATATCAATAACCAGCACGTTGC), following with eGFP was 3' terminally fused to β-glubin intron sequence as an EcoRV fragment, eGFP coding sequence was PCR amplified from pTAGGFP construct, using EcoRV F (CCGATATCCGCCACCATGAGCGG) and EcoRV R (AAGATATCCCTGTACAGCTCGTC) primers, after that with $hCRP_{76-123}$ sequence, which contains *DEP*-TCR recognized epitope, was amplified as SmaI/PstI fragment from Hogness 57 construct using primers EV4 (GATCCTGCAGTCTAAGGATATAGGATAC) and EV5 (CGATCCCGGGCTTCCCATCTACCCAGAAC) amplified and subcloned, and LC3 and $LC3_{G120A}$ cDNA BamHI/Xbal digestion fragment was fused at the 3' terminus to hCRP. To destroy triple Myc tag, that was N-ternimally fused to the LC3 protein and its mutated version, LC3 and $LC3_{G120A}$ cDNA was PCR amplified from original pCI-neo construct using primers Forward 5'- CCGGGATCCCCGTCCGAGAAGACCTT-3', Reverse 5'-TTCTCTAGAGCACCATAGTTATAAACCAG-3' which introduced BamHI and Xbal restriction sites, finally BamHI/Xbal fragment was inserted. The resulting construct was used for subsequent BAC modification.

Constructs containing a β –globin intron followed by cDNAs encoding for GCL or GCL $_{G120A}$, respectively, and a poly-A signal were inserted by homologous recombination into the mouse BAC RP23-77011 which contained 58kb downstream and 152kb upstream from the transcription start site of AIRE (BACPAC). The targeting vector contained homology boxes spanning nucleotides -379 to -2 (5': box1) and 17 to 399 (3': box2) of the *Aire* gene. A neomycin resistance gene flanked by FRT sites was used to select successfully recombined clones and was subsequently removed.

Autophagy induction *in vitro* and Microscopic Analysis

pMSCV GCL or GCL_{G120A} :

HEK 293T cells were transiently transfected with pMSCVneo vectors containing the plasmids encoding for GCL or GCL_{G120A} by calcium phosphate method. In briefly, HEK 293T cells were cultured in High Glucose DMEM medium with 5% FCS (vol/vol; Biochrom). To avoid cell density is too high, the growing cells should be split at least 2× one day before transfection. Meanwhile, 10mM HEPES was added, cell concentration was carefully adjusted into 1×10^5 in 1ml medium and cultured for further transfection. The other day, 2.5µg plasmid DNA dissolved in 112.5µl H_2O was fully mixed with 12.5µl pre-warmed $CaCl_2$ by vortexing, and then 125µl pre-warmed HeBS Buffer was added. In the following step, this mixture was added into growing cells, after 6-8h culture, freshly pre-warmed medium was added; and after another 48h culture, transfected cells seeded onto coverslips in 12-well plates were either starved with medium (Earles balanced salt solution with 0.5 µM Rapamycin; both from Sigma-Aldrich) or cultured in full medium (DMEM with 8% [vol/vol] FCS; Biochrom) for another 24 h. Subsequently, coverslips were mounted onto glass slides with Prolong Gold antifade reagent containing DAPI (Molecular Probes) and analyzed by fluorescence microscopy.

2×HeBS Buffer:

16.4g NaCl
11.9g HEPES
0.21g Na_2HPO_4 in 800ml H_2O

Generation of Aire-GCL and Aire-GCL_{G120A} Mice

BAC modification

Transformation of BAC with pBAD

DH10β bacteria containing the BAC RP23-77011 which used for modification was inoculated in 4ml LB-Cl medium (LB supplemented with Chloramphenicole (12.5µg/ml)) and incubated overnight at 37°C. 1ml from the enrichment bacteria was taken and the bacteria pellets were harvested by centrifuging at 10,000rpm/min for 2min and resuspended by 1ml ice-cold 10% glycerol. After washing for three times, the pellets were resuspended in 100ul 10% glycerol and 500ng pBAD vector was added for transformation via electroporation using following settings (100Ω, 25µFD, 2.5KV). Immediately 1ml LB medium without antibiotics was added and incubated at 37°C for 1h. After that, 100µl bacteria was streaked on LB-Cl+Amp plates (LB supplemented with Chloramphenicole and Ampicillin (100µg/ml)) and incubated overnight at 37°C.

Transformation with recombination cassette

3 colonies were inoculated in 5ml LB-Cl+Amp medium and incubated overnight at 37°C. The next day, 1ml cultured bacterial liquid was added into 70ml LB-Cl+Amp medium and incubated at 37°C, 300rpm/min for growing till the OD_{600} value reached to 0.13. After that, 14% L-Arabinose (final concentration is 0.2%) was added, bacteria was incubated continuously at 37°C with 300rpm/min shaking speed till the OD_{600} value reached to 0.34, this incubation time should be less than an hour. Next, bacteria was precipitated by spinning down at 7000rpm/min for 5min and resuspended with 1ml ice-cold 10% glycerol on ice, and then plastic centrifuge tubes were filled up with glycerol, washed for three times. After washing step, the supernatant was discarded and bacteria pellets were resuspended in remained glycerol (around 300ul in volumes). 500µg in 5ul GCL or GCL_{G120A} digested fragment by restriction enzymes of *NotI* and *PvuI* was added for transformation by electroporation with the following setting (200Ω, 25µFD, 2.5KV) and then 2ml LB medium was immediately added. After 1.5h-incubation at 37°C, 100ul bacterial liquid was added on LB-Kana+Cl plates (LB plates with Kanamycin (25ug/ml) and Chloramphenicole) for streaking and incubated overnight at 37°C.

PCR screen of clones positive for the insert

20 single colonies which grown on LB-Kana+Cl plates were picked up and lysed in 20µl sterile H_2O by pipetting. 1µl lysate was used to test the successful recombination by

PCR and three pairs of primers were chosen.KA9 (ACAGCCACTCCTGTCTTTGC) and KA10 (TCCTTCTCCTTCAGACGGAG) identified the empty vectors, KA9 and EcoRV R (AAGATATCCCTGTACAGCTCGTC) amplified the positive clones, BamF (GGATCCCCGTCCGAGAAGACCTT) and KA10 were used to check for the loss of neomycin. TD_{Long} 54×30 PCR program was used in all cases.

TD_{Long} 54 x 30 program:

94° C 3:00 → 1 cycle

94° C 0:45
60° C 0:45
72° C 2:00
} 2 cycles

94° C 0:45
58° C 0:45
72° C 2:00
} 2 cycles

94° C 0:45
56° C 0:45
72° C 2:00
} 2 cycles

94° C 0:45
54° C 0:45
72° C 2:00
} 30 cycles

72° C 10:00 1 cycle

Deletion of kanamycin resistance

The positive clones identified by PCR were picked for 1000-fold dilution; one drop from the diluted solution was streaked onto on LB-Kana+Cl plates and incubated overnight at 37°C. 50 clones were picked in the next day and transferred onto two different fresh plates (LB-Amp and LB-Kana+Cl plates) by inoculating loop. After overnight-incubation at 37°C, the clones which grown on LB-Kana+Cl plates but not LB-Amp were picked, indicating the recomninase plasmid has been lost in bacteria.

The picked clones were inoculated in 5ml LB medium overnight at 37°C. One day later, 1ml cultured bacteria was added into 100ml LB-Tet+Kana+Cl medium (LB medium supplement with Tetracycline and Kanamycin and Chloramphenicole) and incubated at 37°C till the OD_{600} value reached to 0.5. And then cultured bacteria was diluted from 100ml to 250ml and continued to incubate till the OD_{600} value reached to 0.5 again. Next the cultures were rapidly chilled by swirling in water/ice mixture, 100ml bacteria was transferred and centrifuged at 4000rpm/min for 7min at 4°C. After centrifugation, the bacteria pellets were resuspended gently in 10ml TFBI (transformation buffer I: 30mM KOAc, 50mM $MnCl_2$, 100mM KCl, 10mM $CaCl_2$, 15% glycerol (v/v), do not adjust pH, sterilize by filtration) and filled up with TFBI. The bacteria was harvested by spinning down at 4000rpm/min for 7min at 4°C, and pellets were resupended gently with 1ml TFBII (transformation buffer II: 10mM Na-Mops (pH 7.0), 75mM CaCl2, 10mM KCl, 15% glycerol). Mixed 50 µl bacteria and 2µl containing 300ng flp-plasmid gently in an Eppendorf tube and incubated on ice for 30min, transferred into 42°C water bath for 1min, and then 350µl LB medium was added for 1h-incubation at 30°C. After that, 20µl bacteria were streaked onto LB-Tet plate (LB plate supplement with Tetracycline) and incubated overnight at 30°C. In order to delete the kanamycin resistance from bacteria, 10 clones were picked up and transferred into 2ml LB medium without antibiotics with 30°C incubation for 1h and following with 37°C incubation for 5h, which gives them a chance to lose the flp-plasmid. And then 20µl was taken for streaking onto each of LB-Amp, LB-Kana+Cl or LB-Cl plate. The next day, 6 clones which only grown on LB-Cl plate but not on either LB-Amp or LB-Kana+Cl plate were picked and cultured in 5ml LB-Cl medium overnight at 37°C. The correct inserted fragment and direction was

checked from the picked clones via make DNA mini-preparation, PCR amplification and sequencing. 50µl from 1000-times diluted culture of 3 correct clones was used for streaking onto LB-Cl plates.

Large scale preparation of BAC DNA and purification

A single colony with the correctly targeted BAC was picked from a freshly streaked LB-CL plate and incubated in a starter culture of 4ml LB-CL medium for approximately 8h at 37°C with 300rpm/min shaking. 500µl of the starter culture were added into 4 flasks which contain 500ml LB-CL medium and cultured at 37°C 300rpm/min for 14h to make bacteria growing. When time is up, bacteria were harvested in 200ml plastic centrifuge tubes by centrifugation at 6,000g in a refrigerated superspeed centrifuge equipped with a GSA rotor (Sorvall) at 4°C. BAC isolation was carried out according to the manufacturer recommendation of the large construct kit (Qiagen) with some modification to the supplied protocol. Pellets from 500ml of the 14h cultured bacteria were resuspended in 30ml Buffer P1 with RNase A (Qiagen), supplemented with LyseBlue reagent (Qiagen). Hereafter, 30ml Buffer P2 (Qiagen) were added and the plastic centrifuge tubes were agitated gently, but thoroughly, to make sure the solution were completely mixed, as indicated by a homogenously blue solution, and then kept the mixture incubating at room temperature for 5min. Next added 30ml chilled Buffer P3 and agitated the plastic centrifuge tubes gently, but thoroughly, to make sure the solution were fully mixed with a symbol which blue color fade out and a fluffy white material formed. It is crucial to be as gentle as possible here, as too harsh agitation will result in shearing and subsequent exonuclease digestion of large amounts of BAC DNA. After keeping incubation on ice for 10min, the mixture was centrifuged at 14,000g in the same rotor as before for 30min at 4°C. Cleared supernatant containing BAC DNA was separated from non pelleted debris by filtering through a water-prewetted folded filter (supplied in the kit), and DNA was precipitated by adding 0.6 volumes room-temperature isopropanol (Fluka) and centrifuging at 14,000g for 30min at 4°C. After carefully decanting the supernatant, DNA pellets were washed with 5ml room-temperature 70% (v/v) ethanol (sigmal) and air-dried for 3min. Next the DNA pellets were dissolved in 9.5ml Buffer EX (Qiagen) carefully and completely by very gentle

shaking. After that, ATP (sigma) to a final concentration of 3.16mM and 300µl ATP-dependent exonuclease (supplied with the large construct kit) was added and incubated in a water bath at 37°C for 60min in order to remove the genomic DNA and nicked BAC DNA. Next 10ml Buffer QS (Qiagen) was added to the DNA sample, filtered through a 70µm cell strainer (BD Falcon), and loaded onto QIAGEN-tip 500 columns which were pre-equilibrated with Buffer QBT (Qiagen), The empty columns were washed twice with 30ml Buffer QC (Qiagen) and DNA was eluted with 15ml pre-warmed Buffer QF (Qiagen). Eluted DNA was precipitated by adding 0.7 volumes room-temperature isopropanol and then centrifuged at 3,000g for 60mins at 4°C, and washed with 5ml room-temperature 70% ethanol, again pelletted at 3,000g for 60min at 4°C and air dried for approximately 10min and dissolved at room temperature in 200-400µl aqua ad injectabile (Braun), depending on pellet size.

The purified BAC was immediately linearized with the appropriate restriction enzyme *NruI*. Briefly, the BAC was incubated at 37°C in the presence of 100U *NruI* (New England Biolabs) in the presence of the appropriated reaction buffer in 400µl reactions. Completeness of reactions was verified on a 1% (w/v) agarose (Sigma)/TAE gel. Following linearization BAC DNA was cleaned up using a standard phenol based extraction protocol. Briefly, 1 volume of phenol:Chloroform:isoamylalcohol (25:24:1) (Sigma) was added, thoroughly mixed and centrifuged at 10,000g for 10min. The aqueous phase was then transferred into a fresh tube and 0.1 volumes of 3M sodium acetate pH5.2 (Sigma) was added followed by the addition of 3 volumes of absolute ethanol (AppliChem), vigorous mixing and incubation for 10min at room temperature to precipitate the DNA. The DNA was pelletted by centrifugation at 20,000g for 10min followed by 5 washing steps with 70% (v/v) ethanol (Sigma). After briefly air drying the pellet, the DNA was dissolved in *aqua ad infectabile* (Braun) followed by the addition of 1 volume 2×BAC injection buffer. Finally the BAC DNA was quantified on a 1% (w/v) agarose/TAE gel by running it along with 100bp and 1kb length markers (Fermentas).

10× injection buffer

1830ml H_2O

160ml TRIS (1M, pH 7.5)

4ml EDTA (0.5M)

NaCl (100mM final)

BAC DNA preparation for pronuclear injections

Tg mice were generated by injection of linearized BAC DNA into pronuclei of C57BL/6 zygotes. For pronulear injuctions DNA was diluted in injection buffer to a concentration of 1 ng/ml. Microinjection was performed by Ronald Naumann at the Max Planck Institute of Molecular Cell Biology and Genetics, Dresden, Germany.

Generation of NFAT-GFP Reporter Hybridoma Cells

The T1CRP-54.4 hybridoma expressing the *DEP* TCR was infected with the retroviral vector which contains the construct SIN-(NFAT)x-GFP ([250]provided by H. Spits, Academisch Medisch Centrum, Amsterdam). Subclone 32–14 was used for in vitro stimulation experiments.

Preparation and Purification of Thymic Stromal Cells

Thymi were disenthralled from connective tissue and fat, cut into very small pieces using scissors and transferred to pre-warmed digestion medium (IMDM containing 0.2 mg/ml Collagenase (Roche), 0.2 mg/ml DispaseI (Roche), 2% FCS, 25mM HEPES (pH 7.2) and 25 µg/ml DNase I (Roche)). 1ml digestion medium was used per thymus. Digestion was performed in a FACS tube at 37 °C for 35min (the single cell suspension was resuspended in every 5min with a 1000µl pipette) , and then cells in the FACS tube were transferred on ice and digestion process was blocked by adding 1:100 0.5M EDTA and then incubated for 10min. cells were filtered and washed with FACS buffer once. The supernatant was discarded and pellet was resuspended in 1ml high density percoll (GE Healthcare; ρ=1.115), then carefully added 1ml low density percoll (ρ=1.055) on the top, following added 1ml FACS buffer and did gradient centrifuge (4°C, 30min, 1350g). After that, the upper interphase, containing the desired low density fraction, was removed and resuspened in 3ml FACS buffer, and were ready to staining.

The Percoll solutions were prepared as follows:

High density percoll (ρ=1.115)	Low density percoll (ρ=1.055)
9×Percoll stock (ρ=1.134) 1×PBS (10×) 25mM HEPES pH=7.2 (final)	1×Percoll (ρ=1.115) 1.09×PBS (1×)

Antigen Presentation Assay

2×10^4 T1CRP-54.4/ SIN-(NFAT)x-GFP (clone 32-14) hybridoma cells were co-cultured with 1×10^4 thymic APC s in 150µl High Glucose IMDM w/o Phenol Red (PAA) supplemented with 8% FCS (v/v) (Biochrom). After culturing for 20h, GFP expression was measured by FACS.

Bone Marrow Chimeras

The femurs of the donor mice were isolated and placed in a petrel dish (on ice) containing sterile PBS buffer (pH=7.2), and then the femurs were flushed to harvest bone marrow with PBS buffer by using a 25G 5/8 needle. To remove bits of bone, the cell suspension was filtered and collected in a 50ml tube, and then centrifuged at 600g for 5min. After that, cells were washed with FACS buffer once; in order to deplete of T-cells and B-cells in bone marrow, cell pellets were resuspended in master mixture of biotin-labeled antibodies (CD4, CD8 and B220) and incubated on ice for 20min. After washing with FACS buffer, pellets were resuspended with appropriated amounts of streptavidin MACS beads (Miltenyi Biotec) and incubated at 4°C for 20min. After incubation, cells were washed, resuspended with MACS buffer and went through column. The flow through fractions were harvest and washed with FACS buffer. The cell number was counted and adjusted into the suitable concentration, and 5×10^6 bone marrow cells in 300µl was injected i.v into recipient mice, which got two times of 550 rad irradiation.

Thymus Transplantation

E14-16 thymi were transplanted under the kidney capsule of female animals. $Atg5^{-/-}$ embryonic thymi and $Atg5^{+/-}$ WT controls in individual experiments were obtained from $Atg5^{+/-}$pregnant female after mating to the same $Atg5^{+/-}$ male.

Semiquantitative RT-PCR

Sorted different subsets of thymic stromal cells (purity ≥90%) were used for RNA purification. Total RNA from no less than 10,000 cells was purified by using miRNeasy Mini Kit (Qiagen); the procedure was executed according to manufacturer's instruction . DNA carryover in isolated RNA was removed with a process named on-column DNase digestion. Reverse-transcription for purified RNA was conducted by using iScript cDNA synthesis kit (Biorad) according to the manufacturer instructions.

qPCR in a 10µl reaction (4µl cDNA template+1µl mixed primers+5µl SsoFast EvaGreen Supermix (Biorad)) was performed with duplicates in a CFx96 Real-Time thermal cycler (BioRad) according to the manufacturer instruction. Primers were used in 500nm for each.

qPCR reaction program:

95° C 30s → 1 cycle

95° C 3s
56° C 5s
} 40 cycles

65-95° C, 3s/step 1 cycle

Primers used for qPCR:

gene	primer	sequence
Aire-GCL or Aire-GCL_{G120A}	YW103	5' TTCTGGGTAGATGGGAAGCC 3'
	YW104	5' CCCTTGTATCGCTCTATAATCACT 3'
Aire	Aire fwd	5' GAGTCACAGCACCTTCCTCTT 3'
	Aire rev	5' GGGACAGCCGTCACAACA 3'
β-actin	β-actin fwd	5' GGTGGGAATGGGTCAGA 3'
	β-actin rev	5' GAGCATAGCCCTCGTAGAT 3'

Statistical Analysis

Statistical significance was assessed using the unpaired two-tailed Student's *t* test.

Supplementary Methods-Genotyping Primers

Genotyping

DNA preparation

Tails were incubated in 50µl digestion buffer at 55°C for 5h, and then proteinase K was inactivated at 95°C for 5min.

Gitocher digestion buffer (10×)

670mM Tris pH 8.8

166mM ammonium sulfate

65mM $MgCl_2$

0.1% Gelatin

Digestion buffer

3µl Proteinase K (10mg/ml stock)

2.5µl Triton (10% stock)

5µl Gitocher Buffer (10×)

0.5µl β-Mercapto-ethanol

39µl H_2O

PCR Red-buffer (5×)

250mM KCl

50mM Tris pH 8.3

43% Glycerol

7.5mM $MgCl_2$

2mM Cresol Red

For genotyping, the following primers were used:

gene	primer	sequence
Aire-GCL or -GCL_{G120A}	GCL fwd	5' GATCCTGCAGTCTAAGGATATAGGATAC 3'
	GCl rev	5' TTCAGATCTGCACCATAGTTATAAACCAG 3'
TCR-*DEP*	LK28 fwd	5' CGAGAGGAAGCATGTCTAAC 3'
	LK29 rev	5' ACCGCGGTCATCCAACACAG 3'
CD11c-Cre	Cre fwd	5' CGATGCAACGAGTGATGAGG 3'
	Cre rev	5' GCATTGCTGTCACTTGGTCGT 3'
DTA	DTA fwd	5' TACATCGCATCTTGGCCACG 3'
	DTA rev	5' CCGACAATAAATACGACGCTG 3'
MHC II wt	MHC II wt fwd	5' TTCGTGTACCAGTTCATGGG 3'
	MHC II wt rev	5' TAGTTGTGTCTGCACACCGT 3'
MHC II ko	MHC II ko fwd	5' TTCGTGTACCAGTTCATGGG 3'
	MHC II ko rev	5' CCTGCCGAGAAAGTATCCA 3'
Atg5 wt	LK 39 fwd	5' GAATATGAAGGCACACCCCTGAAATG 3'
	LK 41 rev	5' GTACTGCATAATGGTTTAACTCTTGC 3'
Atg5 ko	LK 40 fwd	5' ACAACGTCGAGCACAGCTGCGCAAGG 3'
	LK 41 rev	5' GTACTGCATAATGGTTTAACTCTTGC 3'

PCR program:

TD 54 x 30: for TCR-DEP, DTA-floxed, MHC II ko, Aire-GCL and Aire- GCL_{G120A} genotyping.

94° C 3:00 → 1 cycle

94° C 0:45
60° C 0:45
72° C 1:00
} 2 cycles

94° C 0:45
58° C 0:45
72° C 1:00
} 2 cycles

94° C 0:45
56° C 0:45
72° C 1:00
} 2 cycles

94° C	0:45	
54° C	0:45	30 cycles
72° C	1:00	
72° C	10:00	1 cycle

CD11c-Cre genotyping program:

94° C	3:00	1 cycle
94° C	0:30	
56° C	0:30	38 cycles
72° C	1:00	
72° C	10:00	1 cycle

Atg5 genotyping program:

94° C	3:00	1 cycle
94° C	0:30	
58° C	0:30	36 cycles
72° C	0:30	
72° C	10:00	1 cycle

6. References

1. Takeuchi, O. & Akira, S. Pattern recognition receptors and inflammation. Cell 140, 805-820 (2010).
2. Flajnik, M.F. & Du Pasquier, L. Evolution of innate and adaptive immunity: can we draw a line? Trends in immunology 25, 640-644 (2004).
3. Wada, H. et al. Adult T-cell progenitors retain myeloid potential. Nature 452, 768-772 (2008).
4. Bell, J.J. & Bhandoola, A. The earliest thymic progenitors for T cells possess myeloid lineage potential. Nature 452, 764-767 (2008).
5. Owen, J.J. & Ritter, M.A. Tissue interaction in the development of thymus lymphocytes. The Journal of experimental medicine 129, 431-442 (1969).
6. Haynes, B.F. & Heinly, C.S. Early human T cell development: analysis of the human thymus at the time of initial entry of hematopoietic stem cells into the fetal thymic microenvironment. The Journal of experimental medicine 181, 1445-1458 (1995).
7. Lind, E.F., Prockop, S.E., Porritt, H.E. & Petrie, H.T. Mapping precursor movement through the postnatal thymus reveals specific microenvironments supporting defined stages of early lymphoid development. The Journal of experimental medicine 194, 127-134 (2001).
8. Ara, T. et al. A role of CXC chemokine ligand 12/stromal cell-derived factor-1/pre-B cell growth stimulating factor and its receptor CXCR4 in fetal and adult T cell development in vivo. Journal of immunology 170, 4649-4655 (2003).
9. Liu, C. et al. The role of CCL21 in recruitment of T-precursor cells to fetal thymi. Blood 105, 31-39 (2005).
10. Wurbel, M.A. et al. Mice lacking the CCR9 CC-chemokine receptor show a mild impairment of early T- and B-cell development and a reduction in T-cell receptor gammadelta(+) gut intraepithelial lymphocytes. Blood 98, 2626-2632 (2001).
11. Rossi, F.M. et al. Recruitment of adult thymic progenitors is regulated by P-selectin and its ligand PSGL-1. Nature immunology 6, 626-634 (2005).
12. Shortman, K. & Wu, L. Early T lymphocyte progenitors. Annual review of immunology 14, 29-47 (1996).
13. Zuniga-Pflucker, J.C. & Lenardo, M.J. Regulation of thymocyte development from immature progenitors. Current opinion in immunology 8, 215-224 (1996).
14. Radtke, F., Fasnacht, N. & Macdonald, H.R. Notch signaling in the immune system. Immunity 32, 14-27 (2010).
15. Maillard, I., Fang, T. & Pear, W.S. Regulation of lymphoid development, differentiation, and function by the Notch pathway. Annual review of immunology 23, 945-974 (2005).
16. Peschon, J.J. et al. Early lymphocyte expansion is severely impaired in interleukin 7 receptor-deficient mice. The Journal of experimental medicine 180, 1955-1960 (1994).
17. Fry, T.J. & Mackall, C.L. The many faces of IL-7: from lymphopoiesis to peripheral T cell maintenance. Journal of immunology 174, 6571-6576 (2005).
18. Porritt, H.E., Gordon, K. & Petrie, H.T. Kinetics of steady-state differentiation and mapping of intrathymic-signaling environments by stem cell transplantation in nonirradiated mice. The Journal of experimental medicine 198, 957-962 (2003).
19. Shortman, K., Egerton, M., Spangrude, G.J. & Scollay, R. The generation and fate of thymocytes. Seminars in immunology 2, 3-12 (1990).
20. Krangel, M.S. Mechanics of T cell receptor gene rearrangement. Current opinion in immunology 21, 133-139 (2009).
21. von Boehmer, H. Unique features of the pre-T-cell receptor alpha-chain: not just a surrogate. Nature reviews. Immunology 5, 571-577 (2005).

22. Yamasaki, S. et al. Mechanistic basis of pre-T cell receptor-mediated autonomous signaling critical for thymocyte development. Nature immunology 7, 67-75 (2006).
23. Trampont, P.C. et al. CXCR4 acts as a costimulator during thymic beta-selection. Nature immunology 11, 162-170 (2010).
24. Janas, M.L. et al. Thymic development beyond beta-selection requires phosphatidylinositol 3-kinase activation by CXCR4. The Journal of experimental medicine 207, 247-261 (2010).
25. Maillard, I. et al. The requirement for Notch signaling at the beta-selection checkpoint in vivo is absolute and independent of the pre-T cell receptor. The Journal of experimental medicine 203, 2239-2245 (2006).
26. Uematsu, Y. et al. In transgenic mice the introduced functional T cell receptor beta gene prevents expression of endogenous beta genes. Cell 52, 831-841 (1988).
27. Vasseur, F., Le Campion, A. & Penit, C. Scheduled kinetics of cell proliferation and phenotypic changes during immature thymocyte generation. European journal of immunology 31, 3038-3047 (2001).
28. Chong, M.M. et al. Suppressor of cytokine signaling-1 is a critical regulator of interleukin-7-dependent CD8+ T cell differentiation. Immunity 18, 475-487 (2003).
29. Starr, T.K., Jameson, S.C. & Hogquist, K.A. Positive and negative selection of T cells. Annual review of immunology 21, 139-176 (2003).
30. Jameson, S.C., Hogquist, K.A. & Bevan, M.J. Positive selection of thymocytes. Annual review of immunology 13, 93-126 (1995).
31. Bousso, P., Bhakta, N.R., Lewis, R.S. & Robey, E. Dynamics of thymocyte-stromal cell interactions visualized by two-photon microscopy. Science 296, 1876-1880 (2002).
32. Gounari, F. et al. Somatic activation of beta-catenin bypasses pre-TCR signaling and TCR selection in thymocyte development. Nature immunology 2, 863-869 (2001).
33. Ioannidis, V., Beermann, F., Clevers, H. & Held, W. The beta-catenin--TCF-1 pathway ensures CD4(+)CD8(+) thymocyte survival. Nature immunology 2, 691-697 (2001).
34. Sun, Z. et al. Requirement for RORgamma in thymocyte survival and lymphoid organ development. Science 288, 2369-2373 (2000).
35. Goldrath, A.W. & Bevan, M.J. Selecting and maintaining a diverse T-cell repertoire. Nature 402, 255-262 (1999).
36. Azzam, H.S. et al. Fine tuning of TCR signaling by CD5. Journal of immunology 166, 5464-5472 (2001).
37. Gallo, E.M. et al. Calcineurin sets the bandwidth for discrimination of signals during thymocyte development. Nature 450, 731-735 (2007).
38. Li, Q.J. et al. miR-181a is an intrinsic modulator of T cell sensitivity and selection. Cell 129, 147-161 (2007).
39. Chan, S.H., Cosgrove, D., Waltzinger, C., Benoist, C. & Mathis, D. Another view of the selective model of thymocyte selection. Cell 73, 225-236 (1993).
40. Leung, R.K. et al. Deletion of the CD4 silencer element supports a stochastic mechanism of thymocyte lineage commitment. Nature immunology 2, 1167-1173 (2001).
41. Itano, A. et al. The cytoplasmic domain of CD4 promotes the development of CD4 lineage T cells. The Journal of experimental medicine 183, 731-741 (1996).
42. Yasutomo, K., Doyle, C., Miele, L., Fuchs, C. & Germain, R.N. The duration of antigen receptor signalling determines CD4+ versus CD8+ T-cell lineage fate. Nature 404, 506-510 (2000).
43. Brugnera, E. et al. Coreceptor reversal in the thymus: signaled CD4+8+ thymocytes initially terminate CD8 transcription even when differentiating into CD8+ T cells. Immunity 13, 59-71 (2000).
44. Lundberg, K., Heath, W., Kontgen, F., Carbone, F.R. & Shortman, K. Intermediate steps in positive selection: differentiation of CD4+8int TCRint thymocytes into CD4-8+TCRhi thymocytes. The Journal of experimental medicine 181, 1643-1651 (1995).

45. Singer, A. New perspectives on a developmental dilemma: the kinetic signaling model and the importance of signal duration for the CD4/CD8 lineage decision. Current opinion in immunology 14, 207-215 (2002).
46. Yu, Q., Erman, B., Bhandoola, A., Sharrow, S.O. & Singer, A. In vitro evidence that cytokine receptor signals are required for differentiation of double positive thymocytes into functionally mature CD8+ T cells. The Journal of experimental medicine 197, 475-487 (2003).
47. He, X. et al. CD4-CD8 lineage commitment is regulated by a silencer element at the ThPOK transcription-factor locus. Immunity 28, 346-358 (2008).
48. He, X. et al. The zinc finger transcription factor Th-POK regulates CD4 versus CD8 T-cell lineage commitment. Nature 433, 826-833 (2005).
49. Sato, T. et al. Dual functions of Runx proteins for reactivating CD8 and silencing CD4 at the commitment process into CD8 thymocytes. Immunity 22, 317-328 (2005).
50. Wilkinson, B. et al. TOX: an HMG box protein implicated in the regulation of thymocyte selection. Nature immunology 3, 272-280 (2002).
51. Hernandez-Hoyos, G., Anderson, M.K., Wang, C., Rothenberg, E.V. & Alberola-Ila, J. GATA-3 expression is controlled by TCR signals and regulates CD4/CD8 differentiation. Immunity 19, 83-94 (2003).
52. Aliahmad, P. & Kaye, J. Development of all CD4 T lineages requires nuclear factor TOX. The Journal of experimental medicine 205, 245-256 (2008).
53. Sun, G. et al. The zinc finger protein cKrox directs CD4 lineage differentiation during intrathymic T cell positive selection. Nature immunology 6, 373-381 (2005).
54. Nawijn, M.C. et al. Enforced expression of GATA-3 during T cell development inhibits maturation of CD8 single-positive cells and induces thymic lymphoma in transgenic mice. Journal of immunology 167, 715-723 (2001).
55. Wang, L. et al. Distinct functions for the transcription factors GATA-3 and ThPOK during intrathymic differentiation of CD4(+) T cells. Nature immunology 9, 1122-1130 (2008).
56. Taniuchi, I. et al. Differential requirements for Runx proteins in CD4 repression and epigenetic silencing during T lymphocyte development. Cell 111, 621-633 (2002).
57. Burnet, M. Auto-immune disease. II. Pathology of the immune response. British medical journal 2, 720-725 (1959).
58. Kappler, J.W., Roehm, N. & Marrack, P. T cell tolerance by clonal elimination in the thymus. Cell 49, 273-280 (1987).
59. Ohki, H., Martin, C., Coltey, M. & Le Douarin, N.M. Implants of quail thymic epithelium generate permanent tolerance in embryonically constructed quail/chick chimeras. Development 104, 619-630 (1988).
60. Ohki, H., Martin, C., Corbel, C., Coltey, M. & Le Douarin, N.M. Tolerance induced by thymic epithelial grafts in birds. Science 237, 1032-1035 (1987).
61. Fowell, D. & Mason, D. Evidence that the T cell repertoire of normal rats contains cells with the potential to cause diabetes. Characterization of the CD4+ T cell subset that inhibits this autoimmune potential. The Journal of experimental medicine 177, 627-636 (1993).
62. Modigliani, Y. et al. Lymphocytes selected in allogeneic thymic epithelium mediate dominant tolerance toward tissue grafts of the thymic epithelium haplotype. Proceedings of the National Academy of Sciences of the United States of America 92, 7555-7559 (1995).
63. Sakaguchi, S., Sakaguchi, N., Asano, M., Itoh, M. & Toda, M. Immunologic self-tolerance maintained by activated T cells expressing IL-2 receptor alpha-chains (CD25). Breakdown of a single mechanism of self-tolerance causes various autoimmune diseases. Journal of immunology 155, 1151-1164 (1995).

64. Hori, S., Nomura, T. & Sakaguchi, S. Control of regulatory T cell development by the transcription factor Foxp3. Science 299, 1057-1061 (2003).
65. Khattri, R., Cox, T., Yasayko, S.A. & Ramsdell, F. An essential role for Scurfin in CD4+CD25+ T regulatory cells. Nature immunology 4, 337-342 (2003).
66. Brunkow, M.E. et al. Disruption of a new forkhead/winged-helix protein, scurfin, results in the fatal lymphoproliferative disorder of the scurfy mouse. Nature genetics 27, 68-73 (2001).
67. Bennett, C.L. et al. The immune dysregulation, polyendocrinopathy, enteropathy, X-linked syndrome (IPEX) is caused by mutations of FOXP3. Nature genetics 27, 20-21 (2001).
68. Wildin, R.S. et al. X-linked neonatal diabetes mellitus, enteropathy and endocrinopathy syndrome is the human equivalent of mouse scurfy. Nature genetics 27, 18-20 (2001).
69. Ueno, T. et al. CCR7 signals are essential for cortex-medulla migration of developing thymocytes. The Journal of experimental medicine 200, 493-505 (2004).
70. Kwan, J. & Killeen, N. CCR7 directs the migration of thymocytes into the thymic medulla. Journal of immunology 172, 3999-4007 (2004).
71. Atibalentja, D.F., Byersdorfer, C.A. & Unanue, E.R. Thymus-blood protein interactions are highly effective in negative selection and regulatory T cell induction. Journal of immunology 183, 7909-7918 (2009).
72. Derbinski, J. et al. Promiscuous gene expression in thymic epithelial cells is regulated at multiple levels. The Journal of experimental medicine 202, 33-45 (2005).
73. Derbinski, J., Schulte, A., Kyewski, B. & Klein, L. Promiscuous gene expression in medullary thymic epithelial cells mirrors the peripheral self. Nature immunology 2, 1032-1039 (2001).
74. Gotter, J., Brors, B., Hergenhahn, M. & Kyewski, B. Medullary epithelial cells of the human thymus express a highly diverse selection of tissue-specific genes colocalized in chromosomal clusters. The Journal of experimental medicine 199, 155-166 (2004).
75. Klein, L., Roettinger, B. & Kyewski, B. Sampling of complementing self-antigen pools by thymic stromal cells maximizes the scope of central T cell tolerance. European journal of immunology 31, 2476-2486 (2001).
76. Gray, D., Abramson, J., Benoist, C. & Mathis, D. Proliferative arrest and rapid turnover of thymic epithelial cells expressing Aire. The Journal of experimental medicine 204, 2521-2528 (2007).
77. Gabler, J., Arnold, J. & Kyewski, B. Promiscuous gene expression and the developmental dynamics of medullary thymic epithelial cells. European journal of immunology 37, 3363-3372 (2007).
78. Kishimoto, H. & Sprent, J. Negative selection in the thymus includes semimature T cells. The Journal of experimental medicine 185, 263-271 (1997).
79. McCaughtry, T.M., Wilken, M.S. & Hogquist, K.A. Thymic emigration revisited. The Journal of experimental medicine 204, 2513-2520 (2007).
80. Ramsdell, F., Jenkins, M., Dinh, Q. & Fowlkes, B.J. The majority of CD4+8- thymocytes are functionally immature. Journal of immunology 147, 1779-1785 (1991).
81. Bendelac, A., Matzinger, P., Seder, R.A., Paul, W.E. & Schwartz, R.H. Activation events during thymic selection. The Journal of experimental medicine 175, 731-742 (1992).
82. Finnish-German, A.C. An autoimmune disease, APECED, caused by mutations in a novel gene featuring two PHD-type zinc-finger domains. Nature genetics 17, 399-403 (1997).
83. Nagamine, K. et al. Positional cloning of the APECED gene. Nature genetics 17, 393-398 (1997).
84. Anderson, M.S. et al. Projection of an immunological self shadow within the thymus by the aire protein. Science 298, 1395-1401 (2002).
85. Ramsey, C., Bukrinsky, A. & Peltonen, L. Systematic mutagenesis of the functional domains of AIRE reveals their role in intracellular targeting. Human molecular genetics 11, 3299-3308 (2002).
86. Ilmarinen, T. et al. Functional interaction of AIRE with PIAS1 in transcriptional regulation. Molecular immunology 45, 1847-1862 (2008).

87. Liiv, I. et al. DNA-PK contributes to the phosphorylation of AIRE: importance in transcriptional activity. Biochimica et biophysica acta 1783, 74-83 (2008).
88. Org, T. et al. The autoimmune regulator PHD finger binds to non-methylated histone H3K4 to activate gene expression. EMBO reports 9, 370-376 (2008).
89. Pitkanen, J. et al. The autoimmune regulator protein has transcriptional transactivating properties and interacts with the common coactivator CREB-binding protein. The Journal of biological chemistry 275, 16802-16809 (2000).
90. Oven, I. et al. AIRE recruits P-TEFb for transcriptional elongation of target genes in medullary thymic epithelial cells. Molecular and cellular biology 27, 8815-8823 (2007).
91. Abramson, J., Giraud, M., Benoist, C. & Mathis, D. Aire's partners in the molecular control of immunological tolerance. Cell 140, 123-135 (2010).
92. Thien, C.B. et al. Loss of c-Cbl RING finger function results in high-intensity TCR signaling and thymic deletion. The EMBO journal 24, 3807-3819 (2005).
93. McCarty, N. et al. Signaling by the kinase MINK is essential in the negative selection of autoreactive thymocytes. Nature immunology 6, 65-72 (2005).
94. McCarty, N., Shinohara, M.L., Lu, L. & Cantor, H. Detailed analysis of gene expression during development of T cell lineages in the thymus. Proceedings of the National Academy of Sciences of the United States of America 101, 9339-9344 (2004).
95. Pinon, J.D., Labi, V., Egle, A. & Villunger, A. Bim and Bmf in tissue homeostasis and malignant disease. Oncogene 27 Suppl 1, S41-52 (2008).
96. Bouillet, P. et al. BH3-only Bcl-2 family member Bim is required for apoptosis of autoreactive thymocytes. Nature 415, 922-926 (2002).
97. Rathmell, J.C., Lindsten, T., Zong, W.X., Cinalli, R.M. & Thompson, C.B. Deficiency in Bak and Bax perturbs thymic selection and lymphoid homeostasis. Nature immunology 3, 932-939 (2002).
98. Jorgensen, T.N. et al. Bim and Bcl-2 mutually affect the expression of the other in T cells. Journal of immunology 179, 3417-3424 (2007).
99. Hu, Q., Sader, A., Parkman, J.C. & Baldwin, T.A. Bim-mediated apoptosis is not necessary for thymic negative selection to ubiquitous self-antigens. Journal of immunology 183, 7761-7767 (2009).
100. Liston, A. et al. Generalized resistance to thymic deletion in the NOD mouse; a polygenic trait characterized by defective induction of Bim. Immunity 21, 817-830 (2004).
101. Thompson, J. & Winoto, A. During negative selection, Nur77 family proteins translocate to mitochondria where they associate with Bcl-2 and expose its proapoptotic BH3 domain. The Journal of experimental medicine 205, 1029-1036 (2008).
102. Lee, H.M. & Hsieh, C.S. Rare development of Foxp3+ thymocytes in the CD4+CD8+ subset. Journal of immunology 183, 2261-2266 (2009).
103. Jordan, M.S. et al. Thymic selection of CD4+CD25+ regulatory T cells induced by an agonist self-peptide. Nature immunology 2, 301-306 (2001).
104. Lerman, M.A., Larkin, J., 3rd, Cozzo, C., Jordan, M.S. & Caton, A.J. CD4+ CD25+ regulatory T cell repertoire formation in response to varying expression of a neo-self-antigen. Journal of immunology 173, 236-244 (2004).
105. Aschenbrenner, K. et al. Selection of Foxp3+ regulatory T cells specific for self antigen expressed and presented by Aire+ medullary thymic epithelial cells. Nature immunology 8, 351-358 (2007).
106. Peterson, D.A., DiPaolo, R.J., Kanagawa, O. & Unanue, E.R. Cutting edge: negative selection of immature thymocytes by a few peptide-MHC complexes: differential sensitivity of immature and mature T cells. Journal of immunology 162, 3117-3120 (1999).
107. van Santen, H.M., Benoist, C. & Mathis, D. Number of T reg cells that differentiate does not increase upon encounter of agonist ligand on thymic epithelial cells. The Journal of experimental medicine 200, 1221-1230 (2004).

108. Lohr, J., Knoechel, B., Kahn, E.C. & Abbas, A.K. Role of B7 in T cell tolerance. Journal of immunology 173, 5028-5035 (2004).
109. Tang, Q. et al. Cutting edge: CD28 controls peripheral homeostasis of CD4+CD25+ regulatory T cells. Journal of immunology 171, 3348-3352 (2003).
110. Salomon, B. et al. B7/CD28 costimulation is essential for the homeostasis of the CD4+CD25+ immunoregulatory T cells that control autoimmune diabetes. Immunity 12, 431-440 (2000).
111. Takahashi, S. et al. In vivo overexpression of CTLA-4 suppresses lymphoproliferative diseases and thymic negative selection. European journal of immunology 35, 399-407 (2005).
112. Lio, C.W. & Hsieh, C.S. A two-step process for thymic regulatory T cell development. Immunity 28, 100-111 (2008).
113. Wirnsberger, G., Mair, F. & Klein, L. Regulatory T cell differentiation of thymocytes does not require a dedicated antigen-presenting cell but is under T cell-intrinsic developmental control. Proceedings of the National Academy of Sciences of the United States of America 106, 10278-10283 (2009).
114. Yao, Z. et al. Nonredundant roles for Stat5a/b in directly regulating Foxp3. Blood 109, 4368-4375 (2007).
115. Vang, K.B. et al. IL-2, -7, and -15, but not thymic stromal lymphopoeitin, redundantly govern CD4+Foxp3+ regulatory T cell development. Journal of immunology 181, 3285-3290 (2008).
116. Fontenot, J.D., Rasmussen, J.P., Gavin, M.A. & Rudensky, A.Y. A function for interleukin 2 in Foxp3-expressing regulatory T cells. Nature immunology 6, 1142-1151 (2005).
117. Ouyang, W., Beckett, O., Ma, Q. & Li, M.O. Transforming growth factor-beta signaling curbs thymic negative selection promoting regulatory T cell development. Immunity 32, 642-653 (2010).
118. Liu, Y. et al. A critical function for TGF-beta signaling in the development of natural CD4+CD25+Foxp3+ regulatory T cells. Nature immunology 9, 632-640 (2008).
119. Chen, Z., Benoist, C. & Mathis, D. How defects in central tolerance impinge on a deficiency in regulatory T cells. Proceedings of the National Academy of Sciences of the United States of America 102, 14735-14740 (2005).
120. Le Borgne, M. et al. The impact of negative selection on thymocyte migration in the medulla. Nature immunology 10, 823-830 (2009).
121. Millet, V., Naquet, P. & Guinamard, R.R. Intercellular MHC transfer between thymic epithelial and dendritic cells. European journal of immunology 38, 1257-1263 (2008).
122. Koble, C. & Kyewski, B. The thymic medulla: a unique microenvironment for intercellular self-antigen transfer. The Journal of experimental medicine 206, 1505-1513 (2009).
123. Boehm, T., Scheu, S., Pfeffer, K. & Bleul, C.C. Thymic medullary epithelial cell differentiation, thymocyte emigration, and the control of autoimmunity require lympho-epithelial cross talk via LTbetaR. The Journal of experimental medicine 198, 757-769 (2003).
124. Anderson, G. & Jenkinson, E.J. Lymphostromal interactions in thymic development and function. Nature reviews. Immunology 1, 31-40 (2001).
125. Rossi, S.W. et al. RANK signals from CD4(+)3(-) inducer cells regulate development of Aire-expressing epithelial cells in the thymic medulla. The Journal of experimental medicine 204, 1267-1272 (2007).
126. Hikosaka, Y. et al. The cytokine RANKL produced by positively selected thymocytes fosters medullary thymic epithelial cells that express autoimmune regulator. Immunity 29, 438-450 (2008).
127. Akiyama, T. et al. The tumor necrosis factor family receptors RANK and CD40 cooperatively establish the thymic medullary microenvironment and self-tolerance. Immunity 29, 423-437 (2008).
128. Irla, M. et al. Autoantigen-specific interactions with CD4+ thymocytes control mature medullary thymic epithelial cell cellularity. Immunity 29, 451-463 (2008).

129. Park, B. et al. Redox regulation facilitates optimal peptide selection by MHC class I during antigen processing. Cell 127, 369-382 (2006).
130. Wearsch, P.A., Peaper, D.R. & Cresswell, P. Essential glycan-dependent interactions optimize MHC class I peptide loading. Proceedings of the National Academy of Sciences of the United States of America 108, 4950-4955 (2011).
131. Sauer, R.T. & Baker, T.A. AAA+ proteases: ATP-fueled machines of protein destruction. Annual review of biochemistry 80, 587-612 (2011).
132. Kloetzel, P.M. & Ossendorp, F. Proteasome and peptidase function in MHC-class-I-mediated antigen presentation. Current opinion in immunology 16, 76-81 (2004).
133. Tanaka, K. & Kasahara, M. The MHC class I ligand-generating system: roles of immunoproteasomes and the interferon-gamma-inducible proteasome activator PA28. Immunological reviews 163, 161-176 (1998).
134. Murata, S. et al. Regulation of CD8+ T cell development by thymus-specific proteasomes. Science 316, 1349-1353 (2007).
135. Murata, S., Takahama, Y. & Tanaka, K. Thymoproteasome: probable role in generating positively selecting peptides. Current opinion in immunology 20, 192-196 (2008).
136. Nitta, T. et al. Thymoproteasome shapes immunocompetent repertoire of CD8+ T cells. Immunity 32, 29-40 (2010).
137. Parcej, D. & Tampe, R. ABC proteins in antigen translocation and viral inhibition. Nature chemical biology 6, 572-580 (2010).
138. Blanchard, N. et al. Endoplasmic reticulum aminopeptidase associated with antigen processing defines the composition and structure of MHC class I peptide repertoire in normal and virus-infected cells. Journal of immunology 184, 3033-3042 (2010).
139. York, I.A. et al. The ER aminopeptidase ERAP1 enhances or limits antigen presentation by trimming epitopes to 8-9 residues. Nature immunology 3, 1177-1184 (2002).
140. Serwold, T., Gonzalez, F., Kim, J., Jacob, R. & Shastri, N. ERAAP customizes peptides for MHC class I molecules in the endoplasmic reticulum. Nature 419, 480-483 (2002).
141. Saveanu, L. et al. Concerted peptide trimming by human ERAP1 and ERAP2 aminopeptidase complexes in the endoplasmic reticulum. Nature immunology 6, 689-697 (2005).
142. Koopmann, J.O. et al. Export of antigenic peptides from the endoplasmic reticulum intersects with retrograde protein translocation through the Sec61p channel. Immunity 13, 117-127 (2000).
143. Roelse, J., Gromme, M., Momburg, F., Hammerling, G. & Neefjes, J. Trimming of TAP-translocated peptides in the endoplasmic reticulum and in the cytosol during recycling. The Journal of experimental medicine 180, 1591-1597 (1994).
144. Romieu-Mourez, R., Francois, M., Boivin, M.N., Stagg, J. & Galipeau, J. Regulation of MHC class II expression and antigen processing in murine and human mesenchymal stromal cells by IFN-gamma, TGF-beta, and cell density. Journal of immunology 179, 1549-1558 (2007).
145. Geppert, T.D. & Lipsky, P.E. Antigen presentation by interferon-gamma-treated endothelial cells and fibroblasts: differential ability to function as antigen-presenting cells despite comparable Ia expression. Journal of immunology 135, 3750-3762 (1985).
146. Busch, R., Doebele, R.C., Patil, N.S., Pashine, A. & Mellins, E.D. Accessory molecules for MHC class II peptide loading. Current opinion in immunology 12, 99-106 (2000).
147. Bodmer, H., Viville, S., Benoist, C. & Mathis, D. Diversity of endogenous epitopes bound to MHC class II molecules limited by invariant chain. Science 263, 1284-1286 (1994).
148. Viville, S. et al. Mice lacking the MHC class II-associated invariant chain. Cell 72, 635-648 (1993).
149. Bikoff, E.K. et al. Defective major histocompatibility complex class II assembly, transport, peptide acquisition, and CD4+ T cell selection in mice lacking invariant chain expression. The Journal of experimental medicine 177, 1699-1712 (1993).

150. Landsverk, O.J., Bakke, O. & Gregers, T.F. MHC II and the endocytic pathway: regulation by invariant chain. Scandinavian journal of immunology 70, 184-193 (2009).
151. Hartman, I.Z. et al. A reductionist cell-free major histocompatibility complex class II antigen processing system identifies immunodominant epitopes. Nature medicine 16, 1333-1340 (2010).
152. Hsing, L.C. & Rudensky, A.Y. The lysosomal cysteine proteases in MHC class II antigen presentation. Immunological reviews 207, 229-241 (2005).
153. Nakagawa, T. et al. Cathepsin L: critical role in Ii degradation and CD4 T cell selection in the thymus. Science 280, 450-453 (1998).
154. Hsing, L.C. et al. Roles for cathepsins S, L, and B in insulitis and diabetes in the NOD mouse. Journal of autoimmunity 34, 96-104 (2010).
155. Maehr, R. et al. Cathepsin L is essential for onset of autoimmune diabetes in NOD mice. The Journal of clinical investigation 115, 2934-2943 (2005).
156. Honey, K., Nakagawa, T., Peters, C. & Rudensky, A. Cathepsin L regulates CD4+ T cell selection independently of its effect on invariant chain: a role in the generation of positively selecting peptide ligands. The Journal of experimental medicine 195, 1349-1358 (2002).
157. Klein, L., Hinterberger, M., Wirnsberger, G. & Kyewski, B. Antigen presentation in the thymus for positive selection and central tolerance induction. Nature reviews. Immunology 9, 833-844 (2009).
158. Carrier, A. et al. Differential gene expression in CD3epsilon- and RAG1-deficient thymuses: definition of a set of genes potentially involved in thymocyte maturation. Immunogenetics 50, 255-270 (1999).
159. Viken, M.K. et al. Reproducible association with type 1 diabetes in the extended class I region of the major histocompatibility complex. Genes and immunity 10, 323-333 (2009).
160. Cheunsuk, S. et al. Prss16 is not required for T-cell development. Molecular and cellular biology 25, 789-796 (2005).
161. Gommeaux, J. et al. Thymus-specific serine protease regulates positive selection of a subset of CD4+ thymocytes. European journal of immunology 39, 956-964 (2009).
162. Viret, C. et al. Thymus-specific serine protease controls autoreactive CD4 T cell development and autoimmune diabetes in mice. The Journal of clinical investigation 121, 1810-1821 (2011).
163. Boes, M. et al. T-cell engagement of dendritic cells rapidly rearranges MHC class II transport. Nature 418, 983-988 (2002).
164. Kleijmeer, M. et al. Reorganization of multivesicular bodies regulates MHC class II antigen presentation by dendritic cells. The Journal of cell biology 155, 53-63 (2001).
165. Rudensky, A., Preston-Hurlburt, P., Hong, S.C., Barlow, A. & Janeway, C.A., Jr. Sequence analysis of peptides bound to MHC class II molecules. Nature 353, 622-627 (1991).
166. Chicz, R.M. et al. Specificity and promiscuity among naturally processed peptides bound to HLA-DR alleles. The Journal of experimental medicine 178, 27-47 (1993).
167. Dengjel, J. et al. Autophagy promotes MHC class II presentation of peptides from intracellular source proteins. Proceedings of the National Academy of Sciences of the United States of America 102, 7922-7927 (2005).
168. Gueguen, M. & Long, E.O. Presentation of a cytosolic antigen by major histocompatibility complex class II molecules requires a long-lived form of the antigen. Proceedings of the National Academy of Sciences of the United States of America 93, 14692-14697 (1996).
169. Brazil, M.I., Weiss, S. & Stockinger, B. Excessive degradation of intracellular protein in macrophages prevents presentation in the context of major histocompatibility complex class II molecules. European journal of immunology 27, 1506-1514 (1997).
170. Dorfel, D. et al. Processing and presentation of HLA class I and II epitopes by dendritic cells after transfection with in vitro-transcribed MUC1 RNA. Blood 105, 3199-3205 (2005).

171. Qi, L., Rojas, J.M. & Ostrand-Rosenberg, S. Tumor cells present MHC class II-restricted nuclear and mitochondrial antigens and are the predominant antigen presenting cells in vivo. Journal of immunology 165, 5451-5461 (2000).
172. Jaraquemada, D., Marti, M. & Long, E.O. An endogenous processing pathway in vaccinia virus-infected cells for presentation of cytoplasmic antigens to class II-restricted T cells. The Journal of experimental medicine 172, 947-954 (1990).
173. Tewari, M.K., Sinnathamby, G., Rajagopal, D. & Eisenlohr, L.C. A cytosolic pathway for MHC class II-restricted antigen processing that is proteasome and TAP dependent. Nature immunology 6, 287-294 (2005).
174. Taylor, G.S. et al. A role for intercellular antigen transfer in the recognition of EBV-transformed B cell lines by EBV nuclear antigen-specific CD4+ T cells. Journal of immunology 177, 3746-3756 (2006).
175. Nimmerjahn, F. et al. Major histocompatibility complex class II-restricted presentation of a cytosolic antigen by autophagy. European journal of immunology 33, 1250-1259 (2003).
176. Munz, C. et al. Human CD4(+) T lymphocytes consistently respond to the latent Epstein-Barr virus nuclear antigen EBNA1. The Journal of experimental medicine 191, 1649-1660 (2000).
177. Zhou, D. et al. Lamp-2a facilitates MHC class II presentation of cytoplasmic antigens. Immunity 22, 571-581 (2005).
178. Yorimitsu, T. & Klionsky, D.J. Autophagy: molecular machinery for self-eating. Cell death and differentiation 12 Suppl 2, 1542-1552 (2005).
179. Mizushima, N., Levine, B., Cuervo, A.M. & Klionsky, D.J. Autophagy fights disease through cellular self-digestion. Nature 451, 1069-1075 (2008).
180. Ahlberg, J. & Glaumann, H. Uptake--microautophagy--and degradation of exogenous proteins by isolated rat liver lysosomes. Effects of pH, ATP, and inhibitors of proteolysis. Experimental and molecular pathology 42, 78-88 (1985).
181. Roberts, P. et al. Piecemeal microautophagy of nucleus in Saccharomyces cerevisiae. Molecular biology of the cell 14, 129-141 (2003).
182. Sattler, T. & Mayer, A. Cell-free reconstitution of microautophagic vacuole invagination and vesicle formation. The Journal of cell biology 151, 529-538 (2000).
183. Cuervo, A.M. & Dice, J.F. A receptor for the selective uptake and degradation of proteins by lysosomes. Science 273, 501-503 (1996).
184. Bandyopadhyay, U., Kaushik, S., Varticovski, L. & Cuervo, A.M. The chaperone-mediated autophagy receptor organizes in dynamic protein complexes at the lysosomal membrane. Molecular and cellular biology 28, 5747-5763 (2008).
185. Salvador, N., Aguado, C., Horst, M. & Knecht, E. Import of a cytosolic protein into lysosomes by chaperone-mediated autophagy depends on its folding state. The Journal of biological chemistry 275, 27447-27456 (2000).
186. Dice, J.F. Peptide sequences that target cytosolic proteins for lysosomal proteolysis. Trends in biochemical sciences 15, 305-309 (1990).
187. Cuervo, A.M. & Dice, J.F. Regulation of lamp2a levels in the lysosomal membrane. Traffic 1, 570-583 (2000).
188. Kim, I., Rodriguez-Enriquez, S. & Lemasters, J.J. Selective degradation of mitochondria by mitophagy. Archives of biochemistry and biophysics 462, 245-253 (2007).
189. Schmid, D., Pypaert, M. & Munz, C. Antigen-loading compartments for major histocompatibility complex class II molecules continuously receive input from autophagosomes. Immunity 26, 79-92 (2007).
190. Ohsumi, Y. & Mizushima, N. Two ubiquitin-like conjugation systems essential for autophagy. Seminars in cell & developmental biology 15, 231-236 (2004).
191. Ashford, T.P. & Porter, K.R. Cytoplasmic components in hepatic cell lysosomes. The Journal of cell biology 12, 198-202 (1962).

192. Mortimore, G.E. & Poso, A.R. Intracellular protein catabolism and its control during nutrient deprivation and supply. Annual review of nutrition 7, 539-564 (1987).
193. Mizushima, N., Yamamoto, A., Matsui, M., Yoshimori, T. & Ohsumi, Y. In vivo analysis of autophagy in response to nutrient starvation using transgenic mice expressing a fluorescent autophagosome marker. Molecular biology of the cell 15, 1101-1111 (2004).
194. Kroemer, G., Marino, G. & Levine, B. Autophagy and the integrated stress response. Molecular cell 40, 280-293 (2010).
195. Nobukuni, T. et al. Amino acids mediate mTOR/raptor signaling through activation of class 3 phosphatidylinositol 3OH-kinase. Proceedings of the National Academy of Sciences of the United States of America 102, 14238-14243 (2005).
196. Yu, L. et al. Termination of autophagy and reformation of lysosomes regulated by mTOR. Nature 465, 942-946 (2010).
197. Nakatogawa, H., Suzuki, K., Kamada, Y. & Ohsumi, Y. Dynamics and diversity in autophagy mechanisms: lessons from yeast. Nature reviews. Molecular cell biology 10, 458-467 (2009).
198. Mizushima, N. et al. Mouse Apg16L, a novel WD-repeat protein, targets to the autophagic isolation membrane with the Apg12-Apg5 conjugate. Journal of cell science 116, 1679-1688 (2003).
199. Kabeya, Y. et al. LC3, GABARAP and GATE16 localize to autophagosomal membrane depending on form-II formation. Journal of cell science 117, 2805-2812 (2004).
200. Tanida, I., Ueno, T. & Kominami, E. Human light chain 3/MAP1LC3B is cleaved at its carboxyl-terminal Met121 to expose Gly120 for lipidation and targeting to autophagosomal membranes. The Journal of biological chemistry 279, 47704-47710 (2004).
201. Kabeya, Y. et al. LC3, a mammalian homologue of yeast Apg8p, is localized in autophagosome membranes after processing. The EMBO journal 19, 5720-5728 (2000).
202. Kirisako, T. et al. The reversible modification regulates the membrane-binding state of Apg8/Aut7 essential for autophagy and the cytoplasm to vacuole targeting pathway. The Journal of cell biology 151, 263-276 (2000).
203. Levine, B. & Klionsky, D.J. Development by self-digestion: molecular mechanisms and biological functions of autophagy. Developmental cell 6, 463-477 (2004).
204. Levine, B., Mizushima, N. & Virgin, H.W. Autophagy in immunity and inflammation. Nature 469, 323-335 (2011).
205. Lunemann, J.D. & Munz, C. Autophagy in CD4+ T-cell immunity and tolerance. Cell death and differentiation 16, 79-86 (2009).
206. Kuma, A. et al. The role of autophagy during the early neonatal starvation period. Nature 432, 1032-1036 (2004).
207. Komatsu, M. et al. Loss of autophagy in the central nervous system causes neurodegeneration in mice. Nature 441, 880-884 (2006).
208. Lunemann, J.D. et al. Beta-amyloid is a substrate of autophagy in sporadic inclusion body myositis. Annals of neurology 61, 476-483 (2007).
209. Hara, T. et al. Suppression of basal autophagy in neural cells causes neurodegenerative disease in mice. Nature 441, 885-889 (2006).
210. Pua, H.H., Dzhagalov, I., Chuck, M., Mizushima, N. & He, Y.W. A critical role for the autophagy gene Atg5 in T cell survival and proliferation. The Journal of experimental medicine 204, 25-31 (2007).
211. Miller, B.C. et al. The autophagy gene ATG5 plays an essential role in B lymphocyte development. Autophagy 4, 309-314 (2008).
212. Deretic, V. Autophagy as an immune defense mechanism. Current opinion in immunology 18, 375-382 (2006).

213. Ling, Y.M. et al. Vacuolar and plasma membrane stripping and autophagic elimination of Toxoplasma gondii in primed effector macrophages. The Journal of experimental medicine 203, 2063-2071 (2006).
214. Amano, A., Nakagawa, I. & Yoshimori, T. Autophagy in innate immunity against intracellular bacteria. Journal of biochemistry 140, 161-166 (2006).
215. Lee, H.K., Lund, J.M., Ramanathan, B., Mizushima, N. & Iwasaki, A. Autophagy-dependent viral recognition by plasmacytoid dendritic cells. Science 315, 1398-1401 (2007).
216. Gutierrez, M.G. et al. Autophagy is a defense mechanism inhibiting BCG and Mycobacterium tuberculosis survival in infected macrophages. Cell 119, 753-766 (2004).
217. Li, Y. et al. Efficient cross-presentation depends on autophagy in tumor cells. Cancer research 68, 6889-6895 (2008).
218. Takeuchi, H. et al. Synergistic augmentation of rapamycin-induced autophagy in malignant glioma cells by phosphatidylinositol 3-kinase/protein kinase B inhibitors. Cancer research 65, 3336-3346 (2005).
219. Blommaart, E.F., Krause, U., Schellens, J.P., Vreeling-Sindelarova, H. & Meijer, A.J. The phosphatidylinositol 3-kinase inhibitors wortmannin and LY294002 inhibit autophagy in isolated rat hepatocytes. European journal of biochemistry / FEBS 243, 240-246 (1997).
220. Bjorkoy, G. et al. p62/SQSTM1 forms protein aggregates degraded by autophagy and has a protective effect on huntingtin-induced cell death. The Journal of cell biology 171, 603-614 (2005).
221. Kirkin, V., Lamark, T., Johansen, T. & Dikic, I. NBR1 cooperates with p62 in selective autophagy of ubiquitinated targets. Autophagy 5, 732-733 (2009).
222. Simonsen, A. et al. Alfy, a novel FYVE-domain-containing protein associated with protein granules and autophagic membranes. Journal of cell science 117, 4239-4251 (2004).
223. Riley, B.E. et al. Ubiquitin accumulation in autophagy-deficient mice is dependent on the Nrf2-mediated stress response pathway: a potential role for protein aggregation in autophagic substrate selection. The Journal of cell biology 191, 537-552 (2010).
224. Sandoval, H. et al. Essential role for Nix in autophagic maturation of erythroid cells. Nature 454, 232-235 (2008).
225. Schweers, R.L. et al. NIX is required for programmed mitochondrial clearance during reticulocyte maturation. Proceedings of the National Academy of Sciences of the United States of America 104, 19500-19505 (2007).
226. Paludan, C. et al. Endogenous MHC class II processing of a viral nuclear antigen after autophagy. Science 307, 593-596 (2005).
227. Riedel, A. et al. Endogenous presentation of a nuclear antigen on MHC class II by autophagy in the absence of CRM1-mediated nuclear export. European journal of immunology 38, 2090-2095 (2008).
228. Nedjic, J., Aichinger, M., Emmerich, J., Mizushima, N. & Klein, L. Autophagy in thymic epithelium shapes the T-cell repertoire and is essential for tolerance. Nature 455, 396-400 (2008).
229. Kasai, M. et al. Autophagic compartments gain access to the MHC class II compartments in thymic epithelium. Journal of immunology 183, 7278-7285 (2009).
230. Hinterberger, M. et al. Autonomous role of medullary thymic epithelial cells in central CD4(+) T cell tolerance. Nature immunology 11, 512-519 (2010).
231. Hubert, F.X. et al. Aire regulates the transfer of antigen from mTECs to dendritic cells for induction of thymic tolerance. Blood 118, 2462-2472 (2011).
232. Klein, L., Klein, T., Ruther, U. & Kyewski, B. CD4 T cell tolerance to human C-reactive protein, an inducible serum protein, is mediated by medullary thymic epithelium. The Journal of experimental medicine 188, 5-16 (1998).

233. Ohnmacht, C. et al. Constitutive ablation of dendritic cells breaks self-tolerance of CD4 T cells and results in spontaneous fatal autoimmunity. The Journal of experimental medicine 206, 549-559 (2009).
234. Cosgrove, D. et al. Mice lacking MHC class II molecules. Cell 66, 1051-1066 (1991).
235. Klein, L. & Kyewski, B. Self-antigen presentation by thymic stromal cells: a subtle division of labor. Current opinion in immunology 12, 179-186 (2000).
236. Fengsrud, M., Erichsen, E.S., Berg, T.O., Raiborg, C. & Seglen, P.O. Ultrastructural characterization of the delimiting membranes of isolated autophagosomes and amphisomes by freeze-fracture electron microscopy. European journal of cell biology 79, 871-882 (2000).
237. Mizushima, N. & Klionsky, D.J. Protein turnover via autophagy: implications for metabolism. Annual review of nutrition 27, 19-40 (2007).
238. Kraft, C., Peter, M. & Hofmann, K. Selective autophagy: ubiquitin-mediated recognition and beyond. Nature cell biology 12, 836-841 (2010).
239. Baba, M., Osumi, M., Scott, S.V., Klionsky, D.J. & Ohsumi, Y. Two distinct pathways for targeting proteins from the cytoplasm to the vacuole/lysosome. The Journal of cell biology 139, 1687-1695 (1997).
240. Scott, S.V., Baba, M., Ohsumi, Y. & Klionsky, D.J. Aminopeptidase I is targeted to the vacuole by a nonclassical vesicular mechanism. The Journal of cell biology 138, 37-44 (1997).
241. Rubinsztein, D.C. et al. Autophagy and its possible roles in nervous system diseases, damage and repair. Autophagy 1, 11-22 (2005).
242. Nakagawa, I. et al. Autophagy defends cells against invading group A Streptococcus. Science 306, 1037-1040 (2004).
243. Tanida, I., Ueno, T. & Kominami, E. LC3 conjugation system in mammalian autophagy. The international journal of biochemistry & cell biology 36, 2503-2518 (2004).
244. Aichinger, M., Wu, C., Nedjic, J. & Klein, L. Macroautophagy substrates are loaded onto MHC class II of medullary thymic epithelial cells for central tolerance. The Journal of experimental medicine 210, 287-300 (2013).
245. Chang, C.H., Guerder, S., Hong, S.C., van Ewijk, W. & Flavell, R.A. Mice lacking the MHC class II transactivator (CIITA) show tissue-specific impairment of MHC class II expression. Immunity 4, 167-178 (1996).
246. Heino, M. et al. RNA and protein expression of the murine autoimmune regulator gene (Aire) in normal, RelB-deficient and in NOD mouse. European journal of immunology 30, 1884-1893 (2000).
247. Tanaka, Y. et al. Accumulation of autophagic vacuoles and cardiomyopathy in LAMP-2-deficient mice. Nature 406, 902-906 (2000).
248. Massey, A.C., Kaushik, S., Sovak, G., Kiffin, R. & Cuervo, A.M. Consequences of the selective blockage of chaperone-mediated autophagy. Proceedings of the National Academy of Sciences of the United States of America 103, 5805-5810 (2006).
249. Kaushik, S., Massey, A.C., Mizushima, N. & Cuervo, A.M. Constitutive activation of chaperone-mediated autophagy in cells with impaired macroautophagy. Molecular biology of the cell 19, 2179-2192 (2008).
250. Hooijberg, E., Bakker, A.Q., Ruizendaal, J.J. & Spits, H. NFAT-controlled expression of GFP permits visualization and isolation of antigen-stimulated primary human T cells. Blood 96, 459-466 (2000).

Curriculum Vitae of Chunyan Wu

Personal information

Name: Chunyan Wu

Date of birth: 4th February, 1985

Place of birth: Lanzhou, Gansu, P.R. China

Address: Goethestraße.31/R410, Institute for Immunology, University of Munich, 80336, Germany

Email: caiqshow5427@gmail.com

Phone: 49-0176-62359582

Education

09/2009-Present:

Major: Immunology, Institute for Immunology, College of Medicine, University of Munich, Munich, Germany

09/2007-06/2009:

Major: Bioinformatics, College of Life Science & Technology, Northwest A&F University, Yangling, P.R. China

Degree: Master of Science

09/2003-06/2007:

Major: Bioengineering, College of Life Science & Technology, Northwest A&F University, Yangling, P.R. China

Degree: Bachelor of Engineering

Publications

1. **C, Wu.**, M, Aichinger., J, Nedjic. and L, Klein. Thymic epithelial cells use macroautophagy to turn their inside out for CD4 T cell tolerance. *Autophagy.* 2013; 9(6):931-2.

2. M, Aichinger.*, **C, Wu.***, J, Nedjic. and L, Klein. Macroautophagy substrates are loaded onto MHC Class II of medullary thymic epithelial cells for central tolerance. *The journal of Experimental Medicine.* 2013; 210 (2):287-300. **(* Co-first author)**

3. **C. Y, Wu.**, G. H, Zhao., Y. Q, Zhao., H, Liu., P. J, Zhang. And D. K, Chen. A soluble antigen-specific factor from $CD4^+CD25^+$ T cells of OVA tolerant mice inducing OVA-specific peripheral tolerance independently *in vivo*. *The journal of Animal and Veterinary Advances.* 2011; 10 (5):642-650.

Awards

05/2011： Fellowship of ’’6th European Network of Immunology Institutes’’ Summer School, Italy

09/2009-08/2013： PhD scholarship of the China Scholarship Council for studying in Institute for Immunology, University of Munich, Germany

Acknowledgments

I would like to thank all the people working with me on my PhD project. The support from Martin, Sonja, Christine and Steffi really gave me a lot strength and confidence to face all the difficulties during my study. Without you guys, I should be far away from this exciting and celebrated day.

Many thanks also should be given to the whole Klein Lab. You are the best colleagues I have ever met and your friendship means a lot to me. I will never forget the comfortable atmosphere when we are working together. Thanks to Ksenija, your extensive knowledge in our two years Journal Club spent together and super kindly personality during the working time really impressed me a lot, and your countless help made me easily overcoming those difficulties in my study. Also, thank you for reading my thesis.

Ludger, thanks to you for being my great supervisor. Thank you for giving me this chance to join your lab. Your patient and inspiring ideas really made me clearly realize the extraordinary characteristics that are needed to become a qualified researcher. It is really an honor to work on such an exciting project, and I have learned much during the last four years.

Especially thanks to Dr. Lindsey Goff for editing the introduction section of my thesis and Yuchen Nan for helping me a lot on the thesis revision.

Finally, I want to thank my family and my friends and especially, my parents. I am thankful for supporting me as always. Yuchen, thanks for supporting me in the last writing days. I really look forward to spend the future days with you; your support is my biggest motivation of my life. Bing, Hui, Yan and Yu thank you for being my good friends, I will always remember the happy days we spent in Munich.